PHYSICOCHEMICAL AND THERMOCHEMICAL PROPERTIES OF SULFONATED POLY(ETHERETHERKETONE) ELECTROLYTE MEMBRANES

by

STEPHEN L. N. H. RHODEN
M.S. University of Central Florida, 2007
B.S. University of the West Indies, 2003

A dissertation submitted in partial fulfillment of the requirements
for the degree of Doctor of Philosophy
in the Department of Chemistry
in the College of Sciences
at the University of Central Florida
Orlando, Florida

Fall Term
2010

Major Professor: Diego J. Diaz

ABSTRACT

Fuel cells have long been seen as an alternative to combustion powered and diesel powered engines and turbines. Production of energy via a fuel cell conversion method can generate up to 60% efficiency in comparison to 30% using a combustion powered engine, with low co-production of harmful side-products. The polymer electrolyte membrane (PEM) adapted for the fuel cell application is one of the main components that determines the overall efficiency. This research project was focused towards novel PEMs, such as sulfonated poly(etheretherketone) or SPEEK, which are cost-efficient and robust with high proton conductivities under hydrated conditions. The degree of sulfonation (DS) of a particular SPEEK polymer determines the proton conducting ability, as well as the long term durability. For SPEEK with high DS, the proton conduction is facile, but the mechanical stability of the polymer decreases almost proportionally. While low DS SPEEK does not have sufficient sulfonic acid density for fast proton conduction in the membrane, the membrane keeps its mechanical integrity under fully saturated conditions. The main purpose of this work was to address both issues encountered with SPEEK sulfonated to low and high DS. The addition of both solid acids and synthetic cross-links were studied to address the main downfalls of the respective SPEEK polymers. Optimization of these techniques led to increased understanding of PEMs and notably better electrochemical performance of these fuel cell materials.

Oxo-acids such as tungsten (VI) oxide (WO_3) and phosphotungstic acid (PTA) have been identified as candidate materials for creating SPEEK composite membranes. The chemistry of these oxo-acids is well known, with their use as highly acidic catalyst

centers adopted for countless homogeneous and heterogeneous, organic and inorganic reactions. Uniform dispersion of WO_3 hydrate in SPEEK solution was done by a sol-gel process in which the filler particles were grown in an ionomer solution, cast and allowed to dry. PTA composites were made by adding the solid acid directly to a solution of the ionomer and casting. The latter casting was allowed to dry and Cs^+- exchanged to stabilize the PTA from dissolution and leaching from the membrane. The chemical and physical properties of these membranes were characterized and evaluated using mainly conductometric and X-ray photoelectron spectroscopic methods. Composite SPEEK/ PTA membranes showed a 50% decrease in PEM resistance under hydrogen fuel cell testing conditions, while SPEEK/ WO_3 composites demonstrated a ten-fold increase in the membrane's in-plane proton conductivity. The chemical and physical properties of these composites changed with respect to their synthesis and fabrication procedures. This study will expound upon their relations.

for mommy and daddy.

ACKNOWLEDGMENTS

I would like to thank my advisor Dr. Diego J. Diaz for his support and understanding, it has been new horizons for both of us. To my distinguished group of committee members: Dr. Clovis A. Linkous, your knowledge and understanding of science and life is truly astounding, and is something I definitely aspire towards; Dr. Nahid N. Mohajeri, thank you for taking the time to properly understand and listen to all my thoughts, you have made my experience at the energy center intellectually stimulating; Dr. D. Howard Miles, you are a true stalwart, thanks for all the time, helpful advice in my times of need and facilitating my development as a researcher and a man; To Drs Christian Clausen III and Michael Hampton who have spent many hours with me: whether teaching, office hours, sitting on my committees, and being good role-models for me to take after, thanks a lot.

I would like to thank the U.S. Department of Energy for providing funding under contract number: DE-FC36-06GO16028. Thanks to Kirk Scammon and the Materials Characterization Facility at the Advanced Materials and Processing Center at the University of Central Florida for his expertise on XPS, and also to Dr. Russ Kunz and Len Bonville at the University of Connecticut for their helpful input. Thanks to everyone at the Florida Solar Energy Center, working with them was a pleasure.

I would like to thank my Mom, Norma Doreen Rhoden, without her love and dedication this would not be possible, I love you unconditionally. To my Dad Alvan Douglas Rhoden, thanks for all you gave me before departing, it carries me to this day, rest peacefully and keep watching over me. Thanks to my brothers Alvan, Brian and

Craig Rhoden, for helping me stay level headed, with their wise words of wisdom in times when I needed it. I probably would not have had this scholastic opportunity without becoming a U.S. citizen, my Grand-aunt Phyllis and Grandmother Momma (Zeta) Lee facilitated this, lots of love and thanks. My loving girlfriend Tracey-Ann, it's been great adventure after great adventure being with you, I look forward to our future together. To my good friend Muzzafer and Candace, salud, we're going to make it!! To all my family and friends who understood that I could not be there all the time, but that I still loved them none the less, thanks for understanding, and cheers, this is for you all.

TABLE OF CONTENTS

LIST OF FIGURES

LIST OF TABLES

LIST OF ACRONYMS/ABBREVIATIONS

%T	Percent transmittance
CV	Cyclic Voltammetry
DS	Degree of sulfonation
DMAc	Dimethylacetamide
DMF	Dimethylformamide
DSC	Differential scanning calorimetry
DMFC	Direct methanol fuel cell
equiv.	Equivalent
EW	Equivalent weight
FC	Fuel cell
FTIR	Fourier-Transform infrared spectroscopy
GDL	Gas diffusion layer
HPA	Heteropolyacid
IEC	Ion exchange capacity
IR	Infrared
LSV	Linear sweep voltammetry
MEA	Membrane electrode assembly
MS	Mass spectrometry
NMP	N-methyl-2-pyrrolidone
PEK	Polyetherketone
PEEK	Poly(ether ether ketone)
PEM	Proton exchange membrane

PEMFC	Proton exchange membrane fuel cell
PTA	Phosphotungstic acid
ppm	Parts per million
ppb	Parts per billion
RH	Relative humidity
SPEEK	Sulfonated poly(ether ether ketone)
TGA	Thermogravimetric analysis
TGA-MS	Thermogravimetric/mass spectrometry
Wt%	Weight percent
XRD	X-ray Diffraction

CHAPTER 1. INTRODUCTION

Energy Situation

The energy debate has moved to the top of the agenda, right across the social, political and economic circles. Access to sufficient energy is vital for making our economies work but at the same time one of the main sources of the greenhouse gas emissions that put our climate at risk. Compounded over the past few years oil prices have gone up and down like a rollercoaster, jumping to a record high in July 2008 of $147.27/ barrel and then falling back again to $33.87 in December 2009.[1] Market value for fossil fuels are creating more uncertainty for the global economy while at the same time giving an indirect incentive for investing in renewable energy technologies, which are now booming.

Fuel Cells for Energy Production

Current energy production relying heavily on the combustion of fossil fuels is forecast to have a harsh future impact on world ecology and economics. Electrochemical technology is an ongoing area of research which has shown significant promise in the production of stationary and mobile energy reserves, while maintaining sustainability and its environmental friendliness. With the increasing threat by the fast depletion of petroleum, coal and natural gas and the green house effect caused by burning fossil fuels, world leaders are forced to seek and develop more efficient energy conversion devices as regenerative power sources to save the valuable natural resources. In fact, since 1894,

a pioneering researcher by the name of Ostwald, pointed out the profligacy of the steam engine and expressed the hope that the 20th century would become the "Age of Electrochemical Combustion".[2] This still visionary paper also highlighted the reduction of emissions with the elimination of the burning of fuels: ‘‘kein rauch, kein russ’’, roughly translated to "no smoke, no soot". Electrochemical devices, such as batteries, fuel cells and super capacitors are soon set to replace current thermal-based technologies as alternative power systems. These relatively novel systems share common features with each other, with: the chemical processes taking place at the phase boundary of the electrode/ electrolyte and both ion and electron transport being separated.

Fuel cells have shown particular promise due to: fuel flexibility, low noise and emission pollution, high energy efficiency, and finally, application to stationary, small mobile and vehicular tasks. This is in stark contrast to conventional combustion based engines. These thermally-driven power sources are limited by their Carnot efficiency. Fuel cells however, are not limited by Carnot's maximum, and near theoretical efficiencies can be achieved by using intelligently engineered electrochemical devices. Single fuel cells can be combined in series to create a stack with cumulative power output. Stacks can thus be sized according to power demands of the end-user. High energy efficiency and power density in fuel cells are a direct function of the thermodynamics, porous electrode kinetics, materials for fuel cell assembly and reactant mass transfer. Current research and development of new fuel cell materials will help to address these and other challenges to developing commercial fuel cells.

Fuel Cells

A fuel cell is an electrochemical conversion device which utilizes a constant supply of fuel such as hydrogen, hydrazine or methanol and an oxidant such as oxygen, or air. There are many types of fuel cells. These are generally classified by the type of electrolyte used for electrode compartment separation (excluding direct methanol fuel cells, which are named after the fuel used). Over many years, the scope of research on fuel cells has broadened extensively, leading to many different variations in fuel cell technology. Perry and Fuller have summarized the history of the fuel cell recently.[2] There are six major types of fuel cells based on different electrolytes. They all operate at different temperature ranges, use different materials, differ in fuel tolerance and still share the same underlying electrochemical principle.

1. Proton exchange or polymer electrolyte membrane fuel cell (PEMFC).
2. Direct methanol fuel cell (DMFC).
3. Alkaline fuel cell (AFC).
4. Phosphoric acid fuel cell (PAFC)
5. Molten carbonate fuel cell (MCFC)
6. Solid oxide fuel cell (SOFC)

The various types currently used are described in Tables 1 and 2.

Table 1. Various types of fuel cells, their attributes and applications. Reproduced from DOE hydrogen program fact sheet (October 2006).

Fuel cell type	Operating Temperature	System Output	Efficiency	Applications
AFC	90-100 °C	10 kW-100 kW	60-70% electric	Military and space
PAFC	150-200 °C	50 kW-1 MW	80-85% overall with CHP (37-42% electric)	Distributed generation
PEMFC	50-100 °C	<250 kW	50-60% electric	Back-up power, portable power, vehicular and small distributed generation
DMFC	60-90 °C	1-100W	Same as PEMFC	
MCFC	600-700 °C	<1 MW	85% overall with CHP (60% electric)	Electric utility and large distributed generation
SOFC	650-1000 °C	5 kW-3 MW	85% overall with CHP (60% electric)	Auxiliary power, electric utility and large distributed generation

*Combined heat and power (CHP)

The requirement of fuel purity to avoid poisoning the anode and carbonization of the electrode, has limited the practical use of fuel cell to commercial or residential purposes. Increased research efforts in the1960s led to the development of electrolytes which use fuels alternative to pure hydrogen. However, typical acid electrolytes such as phosphoric acid ((H_3PO_4) PAFC) and sulfuric acid (H_2SO_4) begin to lose proton conductivity below 100 °C and the corrosive nature of these electrolytes puts further limitations on cell hardware choice.

In spite of all the recent activity in fuel cells over the last decade, the PAFC technology is still the only one utilized commercially, with over 300 field units currently

deployed worldwide. Their application however, like AFCs, MCFCs and SOFCs, is mainly limited to stationary power generation due to large system sizes.

Table 2 outlines the oxidation/ reduction reactions occurring at the electrodes for each fuel cell type.

Table 2. Differentiating between the various types of fuel cells, the electrolytes utilized and the redox chemistry.

Fuel cell	Electrolyte	Electrode Reactions
AFC	A porous matrix saturated with aqueous lithium, sodium or potassium hydroxide solution	$Anode: H_2 + 2(OH)^- \rightarrow 2H_2O + 2e^-$ $Cathode: \frac{1}{2}O_2 + H_2O + 2e^- \rightarrow 2(OH)^-$ $Overall: H_2 + \frac{1}{2}O_2 \rightarrow H_2O$
PAFC	Liquid phosphoric acid matrix	$Anode: H_2 \rightarrow 2H^+ + 2e^-$ $Cathode: \frac{1}{2}O_2 + 2H^+ + 2e^- \rightarrow H_2O$ $Overall: H_2 + \frac{1}{2}O_2 \rightarrow H_2O$
PEMFC	Sulfonated polymer capable of proton exchange	$Anode: H_2 \rightarrow 2H^+ + 2e^-$ $Cathode: \frac{1}{2}O_2 + 2H^+ + 2e^- \rightarrow H_2O$ $Overall: H_2 + \frac{1}{2}O_2 \rightarrow H_2O$
DMFC	Sulfonated polymer capable of proton exchange	$Anode: CH_3OH + H_2O \rightarrow CO_2 + 6H^+ + 6e^-$ $Cathode: \frac{3}{2}O_2 + 6H^+ + 6e^- \rightarrow 3H_2O$ $Overall: CH_3OH + \frac{3}{2}O_2 \rightarrow 2H_2O + CO_2$
MCFC	Beta-alumina ceramic matrix saturated with aqueous lithium, sodium or potassium carbonate solution	$Anode1: H_2 + {CO_3}^{2-} \rightarrow H_2O + CO_2 + 2e^-$ $Anode2: CO + {CO_3}^{2-} \rightarrow 2CO_2 + 2e^-$ $Cathode: \frac{1}{2}O_2 + CO_2 + 2e^- \rightarrow {CO_3}^{2-}$ $Overall: H_2 + \frac{1}{2}O_2 \rightarrow H_2O$
SOFC	Yttria-stabilized zirconium oxide	$Anode1: H_2 + O^{2-} \rightarrow H_2O + 2e^-$ $Anode2: CO + O^{2-} \rightarrow CO_2 + 2e^-$ $Anode3: CH_4 + 4O^{2-} \rightarrow 2H_2O + CO_2 + 8e^-$ $Cathode: \frac{1}{2}O_2 + 2e^- \rightarrow O^{2-}$ $Overall: H_2 + \frac{1}{2}O_2 \rightarrow H_2O$

PEMFC is advantageous over the PAFC, AFC and MCFC due to use of a solid electrolyte, which shows reduced corrosion and removes the difficulty of sealing and circulation of the liquid electrolyte. Quick startup and low temperatures of operation also

make PEMFCs advantageous over other types of fuel cells. However, the main disadvantages are the requirement of expensive catalysts to carry out the electrocatalytic reactions. The necessary noble metal catalysts have high sensitivity to carbon monoxide and other impurities in the fuel stream at low temperatures (less than 100 $^{\circ}$C). Therefore, operating a PEMFC at higher temperatures (100 $^{\circ}$C and above) improves on these issues, while simultaneously improving the efficiency of both membrane water management and combined heat and power production.

Hydrogen Polymer Electrolyte Membrane Fuel Cells

The proton exchange membrane fuel cell, PEMFC, takes its name from the unique electrolyte used for protonic conduction. A hydrogen PEMFC is simply a water electrolysis cell in reverse ($H_2O \rightarrow H_2 + \frac{1}{2}O_2$). These electrochemical energy conversion devices can be put together in a very compact system consisting of the anode and cathode electrodes and the electrolyte. The electrodes, anode and cathode, are separated by the polymer membrane. The PEM acts as the separator, preventing gas cross-over and mixing, as the primary proton conducting medium and as means for water transport. Proton conduction depends heavily on membrane water content, thus the membrane has to be sufficiently humidified. These layers are put together as a catalyst coated membrane (CCM), and with gas diffusion layers, are called a membrane electrode assembly (MEA), the heart of a PEMFC. The application of a fuel such as hydrogen and oxygen as oxidant performs the two half-cell electrochemical reactions:

Anode half reaction: $H_2 \longrightarrow 2H^+ + 2e^-$ $E^o = 0$ V (1)

Cathode half reaction: $\frac{1}{2}O_2 + 2H^+ + 2e^- \longrightarrow H_2O$ $E^o = 1.23$ V (2)

Overall reaction: $H_2 + \frac{1}{2}O_2 \longrightarrow H_2O$ $E_{cell}=1.23$ V (3)

These reactions take place at the anode and cathode catalyst layers, respectively. Immediately following the reaction, protons are conducted through the PEM, while electrons are transported to the electrical load terminals of the fuel cell stack. Figure 1 shows the main components of an H_2/O_2 PEM fuel cell.

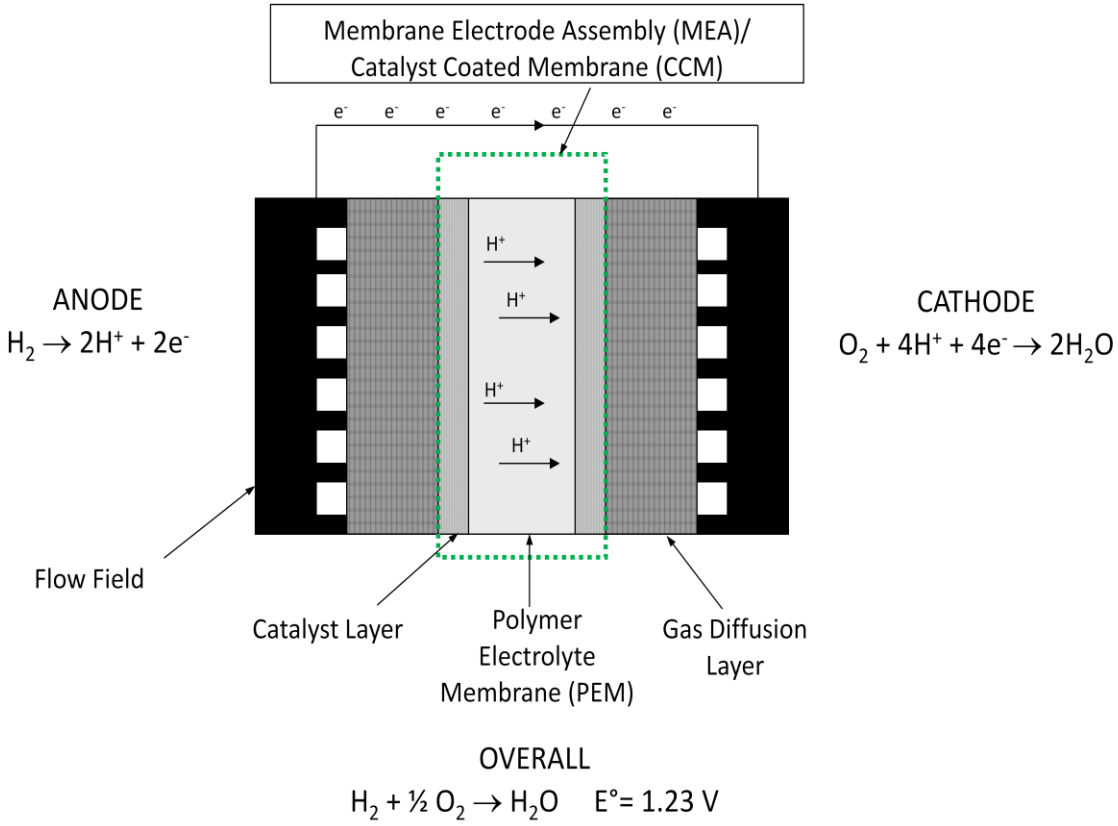

Figure 1. Schematic of a fuel cell.

The electrons cannot be conducted through the PEM, and are forced around the circuit to do electrical work, effectively completing the circuit by supplying electrons to the cathode compartment for reduction of oxygen to water. A small amount of heat is also produced during the reaction.

As mentioned before, hydrogen PEMFCs operate with zero environmentally harmful emissions, and water being the only byproduct. In contrast to combustion engines, fuel cells can produce electricity with a much higher efficiency. Fuel cells operate with no moving parts, which if durable components are used, can lead to a reliable and long-lasting system which runs at a whisper's noise level. Fuel cell stack size and capacity can be scaled to accommodate power demands and capacity respectively, which is difficult to do with batteries. Fuel cells can accommodate higher energy densities than batteries and can also be reenergized much faster, by simply filling the fuel or oxidant reservoir.

The current produced by a fuel cell is in direct relation to the electron transfer rate, whereas the potential (voltage) is related to the overall reaction's Gibbs free energy.

$$I = {}^{E}/_{R} \tag{4}$$

$$\Delta G = -nFE \tag{5}$$

Where I is current produced, E is the cell voltage, R is the cell resistance, ΔG is the Gibbs free energy, and n is the number of electrons per mole of product.

Fuel cells cannot reach their theoretical potential of 1.23 V, due to irreversible losses during operation. Current diagnostic tools allow the current density/ potential

curve to be broken down to address the corresponding performance losses of activation, ohmic and transport contributions (Figure 2).

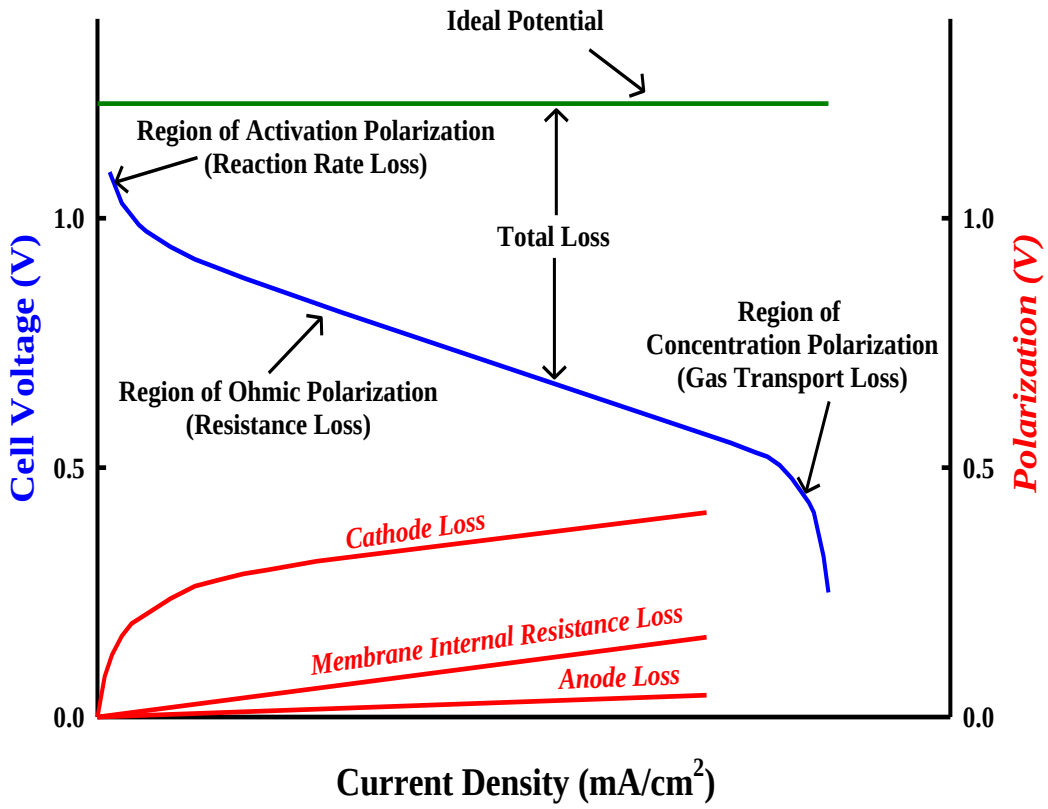

Figure 2. Current-voltage curve for a typical hydrogen PEMFC, showing the ideal/ theoretical potential, and the polarization losses which cause deviation from this ideal voltage. In red: polarization present in various FC components.

At the open circuit voltage (OCV), no current is produced. When steady-state current is drawn from the cell, the primary electrochemical reactions increase, producing a steady-state reversible voltage. This voltage is determined mainly by the design and quality of the membrane electrode assembly employed. In the low current density region, activation polarization due to kinetic limitations of the cathode reactions dominate other

sources of polarization. A large deviation in this activation region is mainly due to one or a mixture of the following sources: low reaction rates, oxidation of hydrogen fuel cross-over and/ or electrical shorting.

Kinetic performance is directly related to the electrodes being used, usually an ionomer blend with noble metal catalyst. Numerous researchers have adopted a blend of Nafion® and platinum on carbon (Pt/C) as the standard for hydrogen PEM fuel cell testing.[3,4,5]. When operating on pure hydrogen, the anode contribution to the cell potential is often overlooked on the assumption that it stays close to the theoretical reversible potential of a hydrogen electrode, i.e., $E^o = 0$ V; that is, it is assumed that the anode reaction has a low to negligible overpotential, due to the facile anode hydrogen oxidation reaction (HOR). In contrast with the "theoretically" reversible voltage generated at the anode, the cathode oxygen reduction reaction (ORR) is an activated process that produces a much higher overpotential. Losses in the ORR are dominant at low current densities where electrode kinetics are considerable slower, with the activation polarization being directly proportional to the rate of chemical and/ electrochemical reactions occurring on the catalyst surface. The activation energy barrier of these reactions should be minimized to increase the electrode's electron transfer kinetics.

At current densities above 100 mA/ cm^2, a larger ohmic-related voltage drop intrinsic to a particular fuel cell occurs. This ohmic resistance is the sum across all the internal resistances. And it is the resistance which controls the slope of the pseudo-linear portion of the current-voltage curve. These ohmic losses are related to a combination of electronic resistances in the porous carbon electrode substrates or gas diffusion layers (GDL), and also in electron transport in the two catalyst layers, but are mainly due to

protonic resistances within the polymer electrolyte membrane and ionomer in the catalyst layers.

At high current densities, losses in the reversible voltage of the fuel cell are dominated by mass-transport kinetics and thermodynamics. The mass-transport limitations are mainly due to: partial pressure of oxygen in air, limited diffusion of oxygen into the electrode, and blocking of catalytic reaction sites with liquid water throughout the electrode compartments. An initial comprehension of the two-phase fluid dynamics of gas entering and water leaving the porous electrodes is a basic model. Establishing a water balance inside a cell can provide information on the water-transport from anode to PEM to cathode. The net water diffusion rate is determinate on the sum of a Fick's-law based back-diffusion of water along a concentration gradient, and the electro-osmotic drag associated with proton mobility (Figure 3). How protons and water molecules diffuse through a particular MEA is dependent on the structural interactions of the FC components, but is mainly dependent on the membrane employed.

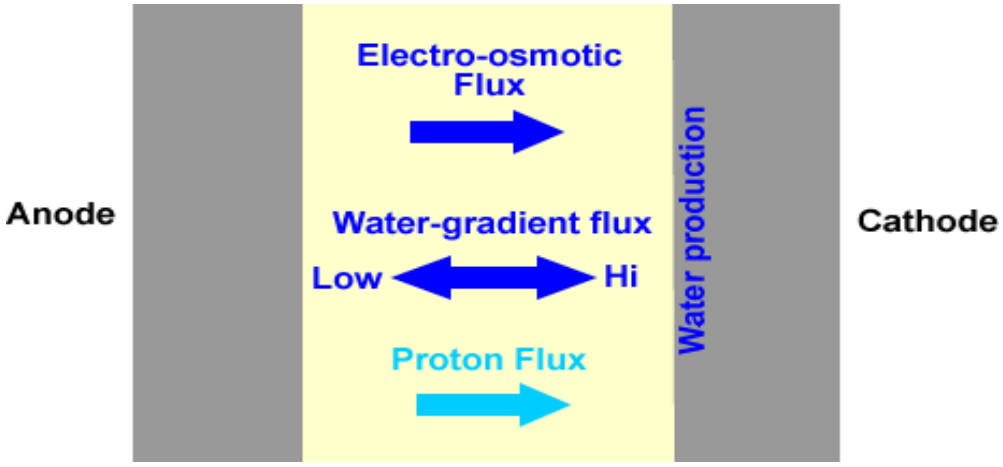

Figure 3. Fluxes through the catalyst coated membrane.

Recent review articles have discussed the complex structure-property relationships, which occur throughout the MEA.[6,7,8,9,10]. The performance of PEMs generally depends on its proton conductivity, a property that is mostly attributed to the level of hydration. Usually high levels of hydration are better able to support high proton conductivities. When the water content of the membrane becomes too high, the cathode compartment may become flooded, greatly reducing the ability of reactants to diffuse into/ out of the cathode electrocatalyst layer efficiently, hence reducing the ORR kinetics. Kunz et al have discussed this phenomenon as it pertains to various membrane materials.[11,12] The electro-osmotic drag is a quantitative measure of membrane hydration, and as said before, has been used to describe the properties of membranes, especially protonic conductivity. If electro-osmotic drag, water uptake and proton conductivity of PEMs are to be better understood, how and why proton exchange membranes operate on a micro-structural level needs to be further investigated.

Polymer Electrolyte Membranes

As the "heart" or main component of a fuel cell, the proton exchange or polymer electrolyte membrane used in a fuel cell has to meet certain criteria. The PEM must form a thin gas barrier which is electronically insulated, shows high mechanical strength and stability, while demonstrating and maintaining good proton conduction with minimal ohmic losses at high current densities. Development of a membrane which meets these criteria, mainly the "good proton conduction" has attracted much attention in recent research. Understanding the basic principles which govern proton transport has given insight into novel materials for fuel cell applications.

Proton mobility was studied as early as communications by Grotthus in 1806.[13] In this memoir, proton transfer has been trivialized by deeming it to occur from one binding site to another (such as a sulfonic acid or interstitial oxygen sites) via hydrogen bonding, with the path of least resistance created by small structural reorientation of the proton conductor matrix. This has been referred to as the Grotthus mechanism or "proton hopping". The structural reorganization is said to involve reorientation of solvent or carrier dipoles (H_3O^+ or $H_5O_2^+$) as the natural pathway for proton diffusion to occur.[14] In the so called vehicle-mechanism, the proton diffuses through the conducting matrix together with the solvent/ vehicle, for example H_2O becoming an H_3O^+ ion.[15] The author concluded that bulk H_2O is a necessity for structural reorganization and obtaining increased proton transfer rates.

Many research efforts have been to improve overall fuel cell performance at elevated temperatures using dry gases.[16,17,18,19] Reducing membrane thickness decreases ohmic resistance, enhances membrane conductivity, cuts material cost and accelerates hydration speed. On the other hand, because of difficulties with fuel cross-over, compounded with thin-film durability and mechanical stability, there is a limit to the extent to which membrane thickness can be reduced. To fully realize their potential, it is desirable that the PEM fuel cells be operated without external humidification and still achieve proton conductivities of 0.1 S/cm.

An appropriate avenue to achieve a balance between conductivity and mechanical properties would be to control the acidic site distribution in the membrane. The resulting polymer, in theory, will be highly conductive; with other properties of the membrane varying based on how the acid sites are incorporated. Two main themes generalize how

the aforementioned is currently being studied: acidifying, usually sulfonation, of known polymeric materials with high thermochemical stability, or synthesizing new block or random copolymers; fabricating composite PEMs by mixing inorganic proton conductors or potential proton conductors either in an ionomer matrix or with a potential strongly inert polymer species.

These two themes also encompass the current thrust of the study to be detailed herein. High proton conductivity is only a small part of the PEM fuel cell performance puzzle. Commercialization of a robust PEM for hydrogen fuel cell technology requires easy manufacturing, and to have the ability to be processed into thin low resistance sheets. It must also be compatible with current electrode materials to avoid interfacial resistance losses. This is important as the electrocatalyst layer may or may not have an altered HOR or ORR based on additives introduced to the PEM. The PEM should have a structure which makes it be an electron insulator, be impervious to fuel and oxidant gases, and exhibit chemical, thermal and dimensional stability under PEM fuel cell conditions. Understanding the chemistry of these property-structure relationships and how they change with the composite membrane structure will develop this novel area of research and development.

Nafion® and its Composites

Two major improvements have been made in PEMFC technology since the advent of NASA's space exploration programs. The first was the development of perfluorosulfonic acid membranes that are more stable than the hydrocarbon-based membranes used in the early PEMFCs.[20] Most notably, DuPont developed Nafion®, which consists of a poly(tetrafluoroethylene) (PTFE) backbone with perfluorinated-vinyl-

polyether side chains terminated with a sulfonic acid group (Figure 5).[21] The second is the discovery of supported catalysts, which have decreased electrocatalyst loading considerably.[22] DuPont originally developed these perfluorosulfonic acid (PFSA) type membranes in the early 1960s, for use in the chloro-alkali industry. It was readily recognized that the membranes were well suited for PEFCs, and so the first Nafion-based PEMFC was tested in 1966. Similar PFSA membranes have been developed recently by the Asahi Chemical Company (commercially Aciplex) and Asahi Glass Company (commercially Flemion) also. Nafion® and similar derivatives are essentially fully fluorinated and therefore do not suffer from rapid degradation in a fuel cell since C-F bonds are more stable than C-H bonds.

Early concepts of a Nafion® morphology-property study were reviewed by Gierke et al.[23] Nafion® membranes have since been understood to have approximately 40 Å-in diameter clusters of sulfonate-ended perfluoroalkyl ether groups of inverted micelles connected by small ionomeric channels, which are well separated from the perfluorinated polymer backbone. As compared with the model put forth by Gierke, Yeager and Steck have proposed a structural model which does not have a set geometrical definition. Most importantly from both these models, is the widely accepted fact that there exists several distinct transitional inter-phases between hydrophobic and hydrophilic regions.[24] In the presence of water the hydrophilic part is hydrated, with proton conductivities approaching 0.2 S/cm at fuel cell running conditions; with the absorbed water helping in further phase separation. The hydrophobic backbone provides Nafion® with superior mechanical stability in both oxidative and reductive environments.

Nafion® films properties have shown to vary widely, depending on solvent used for casting, solvent evaporation rate, film thickness and thermal history.[25,26,27]. The performance of Nafion® has been related to its water management, i.e. electro-osmotic drag and subsequent proton conductivity by Zawodzinski et al.[28] High humidification and hydration requirements for good Nafion® (fuel cell) performance have been correlated. A Nafion® membrane equilibrated with 25 °C liquid water becomes hydrated by about 2.5 times as much compared to a similar membrane equilibrated in saturated water vapor at 25 °C. This increased membrane water content leads to improved proton conductivity, as explained earlier by Kreuer.[14]

Improving PEM performance at low humidity and high temperature conditions are current targets of Nafion® research groups. They have studied the addition of metal oxide proton conductors such as silica (SiO_2), tungsten trioxide (WO_3), zirconia (ZrO_2) and titania.[29,30,31,32] Blending hygroscopic oxides into the membranes showed increased water uptakes compared to that of the pristine polymer. Composite membranes also showed improved mechanical and thermal stability when compared to pure Nafion® membrane, with some composites showed reduced hydrogen or methanol cross-over, due to narrowing of water channels allowing low water permeation and electro-osmotic drag. However, the chemical blending of the inorganic oxides in Nafion® had limited mechanical stability, becoming too brittle when oxide content came to a critical level. The loss in mechanical stability leads to large performance losses of these PEMs. Improving chemical and mechanical stability, and to increase PEM proton conductivity has recently been investigated using a novel class of superconducting fillers, such as heteropolyacids (HPAs).

Fast proton-conducting inorganic compounds, like HPAs, exhibit outstandingly high proton conductivities when 29 waters of hydration are bound to the molecule, approximately 0.17 S/cm at room temperature.[33] Others showing the fully hydrated inorganic material with 25 °C proton conductivities as high as 0.19 S/cm.[34] Heteropolyacids are known as the highest proton conducting inorganic solid electrolytes at near ambient conditions.[35] The strong acidity and labile protons of HPAs, are attributable to the large polyanion structure having low delocalized surface charge density. Simply said, there are weak interactions between the polyanion and protons on a its surface. The heteropolyacid phosphotungstic acid, $H_3PW_{12}O_{40}$ (PTA), has shown higher thermal stability and acidity than silicotungstic ($H_3SiW_{12}O_{40}$) and phosphomolybdic ($H_3PMo_{12}O_{40}$) acids.[36]

The Keggin structure, named after J. F. Keggin, who deduced the structure using X-ray diffraction, has overall tetrahedral symmetry and is composed of a central XO_4 (X=P, Si…) tetrahedron surrounded by 12 MO_3 (M=W, Mo….) octahedra.[37] The primary Keggin structure of $H_3PW_{12}O_{40}$ is well-established. A central P atom in tetrahedral coordination (PO_4) is surrounded by 12 WO_6 octahedra.[38] The position of the three protons are heavily debated.[39,40] The Keggin anionic unit has negative three charge, which is balanced by three super acidic protons. It is accepted that PTA is a purely Brönstead acid, with a Hammett acidity exceeding that of sulfuric acid and Nafion®.[36] There exist four types of oxygen atoms in a Keggin ion (Figure 4): 4 central oxygen atoms, 12 oxygen atoms that bridge two tungsten atoms sharing a central oxygen atom (edge-sharing), 12 oxygen atoms that bridge tungsten atoms not sharing a central oxygen atom, and 12 terminal oxygen atoms bound singularly to a tungsten atom. PTA

crystallizes with a secondary lattice structure inter-connected by water molecules ($H_5O_2^+$). The hydration state of PTA is dependent on temperature and relative humidity. The hexahydrate form of PTA is the most stable at ambient conditions, but crystallized forms containing 13 and 29 waters of hydration are known to exist.

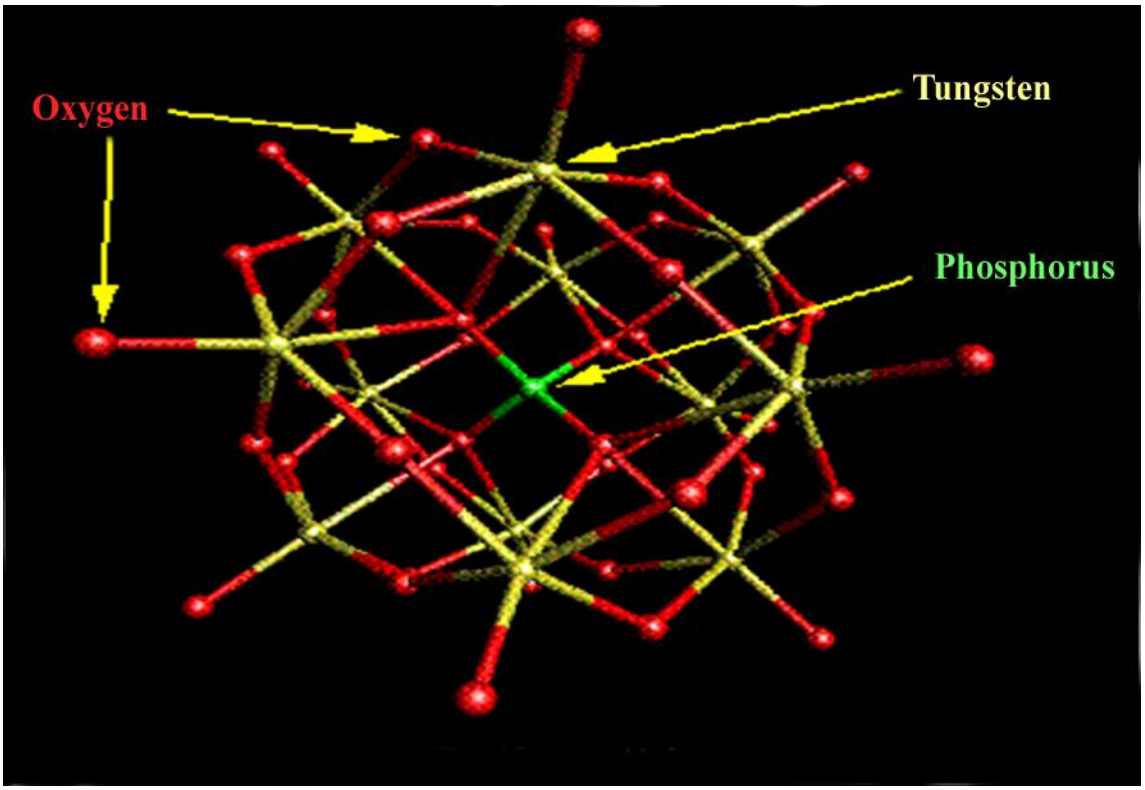

Figure 4. Showing the structure of a Keggin molecule such as phosphotungstic acid, $H_3PW_{12}O_{40}$.

HPAs with Keggin type structures are very stable in solid and solution states. Although PTA is soluble in most polar solvents, minimally soluble salts can be made by partial substitution for H^+ by alkaline cations. The salts of PTA made with large mono-valent cations such as Cs^+ are insoluble and possess high surface areas.[41,42] Blending of Nafion® solutions and casting membranes with fast proton conductors, such

as PTA and its alkaline cation-stabilized salts, have been done previously with improvements in both the proton conductivity and the fuel cell performance of the membranes.[43,44,45] The effect of water on the proton conductivity of HPAs is pertinent to their use in PEMFCs.

The leading choice of solid PEMs, the perfluorinated membranes, are not suitable for prolonged use in steam at elevated temperatures, and severe reducing or oxidizing environments. Suitable high temperature polymers and their preparation methods have garnered much attention recently.[6,8,10,16,46] Polyesters, aromatic polyesters and polybenzimidazoles are prospective polymers with moderate thermal stability up to 300 $^{\circ}$C, while polyphenylene sulfides, polysulfones, poly(arylether sulfones), various polyetherketones (PEKs) and some polyimides have shown to be stable up to 300 $^{\circ}$C.

It is clear that tuning of these materials for optimum performance requires a detailed knowledge of chemical microstructure and nano-scale morphology. In particular, proton conductivity, water management, relative affinity of methanol and water in direct methanol fuel cells, hydration stability at high temperatures, electro-osmotic drag and mechanical, thermal and oxidative stability are important properties that must be controlled in the rational design of these PEM fuel cell membranes.[47]

Alternative Hydrocarbons Based PEM Fuel Cell Membranes

Over the course of membrane development, major research developments have been performed with the purpose of producing an alternative option to the dominant Nafion®, perfluorinated-type membranes. The main reasons being:

1. reduced cost
2. reduced fuel cross-over
3. improved performance at high temperatures (above 100 $^{\circ}$C)
4. fluoride emissions
5. low humidity dependence

The cost of Nafion® is roughly between \$500 to \$1000 U.S./ m^2, which is substantially too high for current commercialization requirements.[48] Also, the micro-structure of Nafion® allows hydrogen or related fuel diffusion through the membrane matrix into the cathode compartment where direct mixing with the oxidant occurs, greatly reducing the electrochemical conversion efficiency. Operating at high temperature and low relative humidity conditions allows easier membrane and fuel cell water management, as well as non-dependence on an engineered humidification system. These will bring down the costs related to the cell from an engineering standpoint. Remediation of any effluent materials during synthesis and/or electrochemical operation will become a larger problem upon commercialization of the novel PEM material. From a synthetic chemist's standpoint, design of a "green" PEM without the dangerous solvents, expensive monomer starting reactants, low-toxicity, with enhanced attributes is of much interest.

Sulfonated hydrocarbon based membranes, particularly poly(etheretherketone), are known good alternatives.[49,50,51] The hydrophobic/ hydrophilic balance as well as the physicochemical properties of a membrane, can be changed based on preparation from multi-component composites, similar to Nafion®.[52,53] Kreuer et al have deconvoluted the macroscopic and microscopic structure/ property relations which exist in both perfluorinated Nafion-type and polyetherketone (PEK)-type polymers using small angle X-ray scattering (SAXS) experiments.[54] The experiments gave insight into channel separation, channel diameter, number of dead-end channels and degree of branching, for both types of polymers. The microstructure can be visualized from the schematic in Figure 5. The water-filled channels in Nafion-type membranes are wider compared to those in SPEKs, and well separated, showing less branching and have fewer dead-end channels compared to that of the hydrocarbon variety. The various differences between these two types of polymers is qualitatively explained based on the microstructures and the acidity of the sulfonic acid functional groups.[54,55,56]

Increasing the number of sulfonic acid groups, that is the degree of sulfonation (DS) groups in SPEEK, makes it highly hydrophilic, with other properties altered such as reduced crystallinity and subsequently increased solubility. More generally, when PEEK DS is lower than 30%, the SPEEK is soluble only in concentrated sulfuric acid (H_2SO_4); above 30% DS, SPEEK is soluble in hot *N*,*N*-dimethylformamide (DMF), dimethylacetamide (DMAc), *N*-Methyl-2-pyrrolidone (NMP) and dimethylsulfoxide (DMSO), at 40% DS the polymer is room temperature soluble in the same solvents. Above 70 and 80 % DS, the polymer is soluble in hot methanol and water, respectively.[57] Controlling the DS of the polymer can allow a synthetic chemist to tailor the polymer to

specific chemical and physical properties. Membrane conductivity increases with DS also, but a trade-off of decreased thermal stability becomes evident.[58]

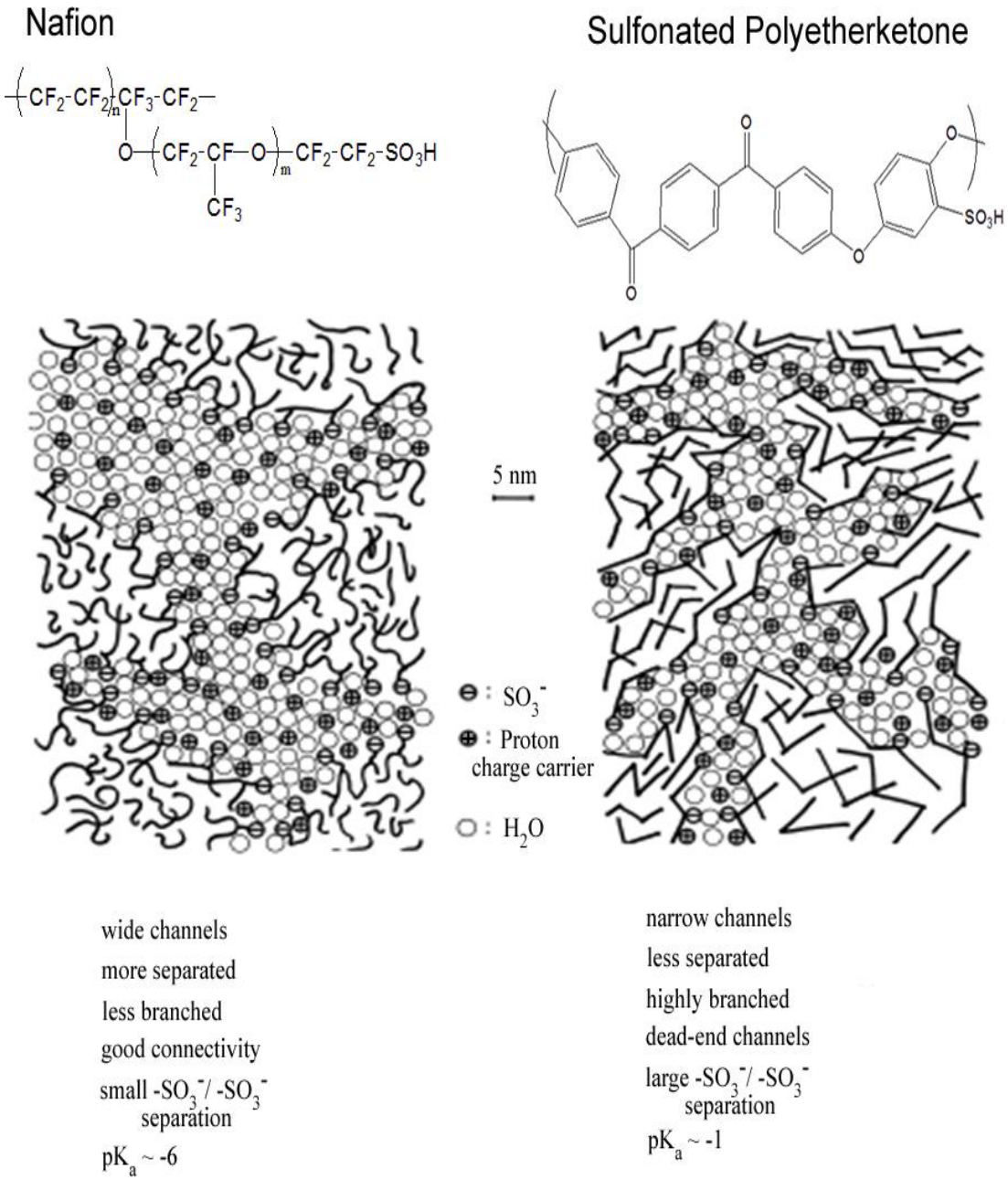

Figure 5. Used with the permission of the Journal of Membrane Science (Elsevier). Picture taken from Kreuer (59) of the nano-scopic hydrated microstructures that make up Nafion® and SPEK-type polymers

Chemical modification of SPEK-type membranes by blending with other polymers and inorganic solid acids, as well as cross-linking, may provide the wide variation in features necessary to adapt polymer's properties for specific fuel cell applications.[8]

In PEM membrane synthesis, addition of the solid acid improved swelling characteristics, proton conductivity and thermal resistance of Nafion® and SPEEK polymers. The 29 hydrate form of PTA was shown to have proton conductivities as high as 0.19 S/cm by Miyake.[60] As with most hydrated proton conductors, there is a sharp decrease the in the conductivity when the bound waters of hydration are removed. This removal can be caused by prolonged exposure to dry atmospheres and/or elevated temperatures. However, Fenton has studied the addition of phosphotungstic acid and its cesium salt form (Cs-PTA) to Nafion® and sulfonated poly(etherketoneketone) (SPEKK) membranes.[43,44,45,53] Improved conductivities were observed for the solid acid-containing membranes relative to their pristine parent materials. However, these compounds become poor proton conductors in dry atmospheres. Current studies on compounds which conduct protons are based on the "Grotthus" mechanism, i.e., bulk mechanism. High and stable proton conductivity is to be expected from proton conductors of this type.

Tungsten oxides are intrinsic semiconducting metal oxides capable of withstanding high temperatures making them an outstanding choice for robust, nano-structured, inorganic frameworks. Preparation of WO_3 and tungsten oxide hydrates ($WO_3 \cdot xH_2O$) has been previously achieved by several experimental routes, such as: anodization, pulsed laser deposition, electrodeposition, electro-spinning, acid

precipitation, chemical etching, sol-gel synthesis, thermal evaporation, R-F sputtering and chemical vapor deposition.[61] Properties of these materials vary widely based on the structure formed from each experimental technique employed. Previously it was shown that tungsten oxide hydrates, $WO_3 \cdot xH_2O$, had relatively high proton conductivities.[62] Mecheri et al. have since explained how blending of 25 and 50 wt% of $WO_3 \cdot 2H_2O$, in a SPEEK membrane of 80% DS utilizing DMAc as solvent was accomplished.[63] It was discovered that composite membranes showed higher proton conductivity compared to the pure 80% DS PEEK membrane. While providing improved conductivity, the 50 wt% $WO_3 \cdot 2H_2O$ membrane had decreased water uptake and improved heat resistance as well. It would seem that some interactions between the waters of hydration in the tungstic acid and the sulfonic acid groups occur, giving rise to a synergistic, highly stable and conductive composite blend. X-ray diffraction patterns indicated that the hydration grade of the oxide in the membrane decreased with increasing WO_3 content. Tungstates are known to be easily protonated in solution, with the protonated material showing a strong tendency to condense into polyoxoanions.[64,65] Studying the effects of colloidal WO_3 within a sulfonic acid matrix may give the high proton conductivity and low gas permeation necessary for good membrane performance.

Other methods of increasing thermal and chemical stability of hydrocarbon polymers have been investigated widely.[66,67,68,69] The main disadvantage to adopting low DS PEEK as a PEMFC material is its poorly conductive randomly distributed sulfonic acid groups on an inflexible, slightly hydrophilic PEEK backbone, which is an unfavorable feature, when compared to a Nafion-based structure (Figure 5). The

microstructure of PEMs have been related to their electrochemical properties, especially the spatial distribution of the ionic sites within the membrane.[70]

Use of high DS SPEEK polymers in electrolysis or fuel cell-based applications is limited due to the high swelling of the polymer matrix. To overcome these problems, cross-linking of sulfonated hydrocarbon-type membranes is seen as a reasonable approach for mitigating the excessive water uptake of the highly sulfonated polymers, while maintaining their intrinsically high proton conductivities.[71] It is therefore pertinent to the proton conductivity that a synthetic process be developed which does not remove the sulfonic acid functionalities, and/or produces a hydrophilic network with a low activation energy barrier for proton translation, in and through the PEM.

Work done so far in this vein include, but are not limited to, sulfonic acid polymers based on: polystyrene[72], poly(arylene ether sulfone)[73], polysulfone[74], poly(phthalazinoneethersulfoneketone)[75], poly(vinyl alcohol)[76] and PEEK.[70,71,77,78,79] SPEEK has been studied widespread for use in PEMFCs, ion exchange resins, and water electrolysis operations, due to its good film-forming properties, low fuel and/or solvent permeation and highly acidic sulfonic groups. In most cases, the cross-linking performed increases mechanical and chemical stability, but removing the functionality of ionic sulfonic acid groups severely decreases observed proton transfer rates.

Kerres et al. has explored cross-linking a sulfinated-sulfochlorinated PEEK with α,ω-dihalogenoalkanes, with the resulting membranes showing good properties towards DMFC applications.[80] However, for DS 70% cross-linked PEMS, the polymer swells excessively and the ability to use these PEMs in high temperature electrochemical cells was limited. Mikhailenko has studied the direct cross-linking of SPEEK utilizing poly-

functional alcohols such as ethylene glycol and glycerine.[78] The main factors controlling the SPEEK cross-linking reactions were: the solvent choice, the amount of cross-linker, and the temperature used for membrane casting and subsequent thermal treatment. The highly sulfonated polymer's mechanical strength increased significantly, while showing greatly reduced swelling. Fully hydrated membrane conductivities at 25 $^{\circ}$C remained relatively stable, between 2.7 x 10^{-2} to 1.4 x 10^{-2} S/cm and remained within this range. The cross-linkages were later found to be through the sulfonic acid groups, with the ethylene glycol cross-linker also reacting with itself, forming ether and carbonyl-linked dimers and trimers into an elaborate interpenetrating network.[81] Loss of sulfonic acid groups will definitely reduce fuel cell performance. Neither the DS nor performance results were reported however.

More recently, Patri and coworkers developed cross-linking of SPEEK with the bis(hydroxymethyl) aromatic compounds 1,4-benzenedimethanol and 2,6-bis(hydroxymethyl)-4-methyl phenol.[79] Similar results to Mikhailenko were noted, in that cross-linking to form stable membranes occurred through sulfonate-ester group formation, greatly decreasing DS but somehow maintaining sufficient proton conductivities of 5 x 10^{-2} to 2.5 x 10^{-2} S/cm. It was then concluded that the unreacted free hydroxyl groups of the cross-linkers may be assisting in the proton conductivity of these PEMS.

The work currently proposed is to cross-link SPEEK using previous methods for increasing polystyrene thermal charring properties, as done mainly by Wilkie and others.[66,67,68] Obtaining selective acylation of SPEEK aromatic hydrogens, while leaving the sulfonic acid groups unreacted, will most likely facilitate high proton conductivities.

A thorough study on the thermal, chemical and mechanical properties of membranes will be adopted for SPEEK membranes cross-linked in this manner.

As mentioned earlier in this document, the addition of solid acids has a considerable effect on Nafion® and SPEK-type polymers as well.[8] Incorporation of the super acid PTA in a stabilized form, and colloidal $WO_3 \cdot xH_2O$ type SPEEK membranes will also be investigated, and their physical and mechanical properties studied and reported.

References

1. Teske, S., Zervos, A., Lins, C., Muth, J., *Energy [R]evolution: A sustainable world energy outlook*, 3rd Ed. Aubrey, C., Editor, p. 1-260, Published by Greenpeace International and European Renewable Energy Council (2010).
2. Perry, M. L.; Fuller, T. F., A Historical Perspective of Fuel Cell Technology in the 20th Century, *J. Electrochem. Soc.* 149, (2002), S59.
3. Astill, T. Zhong, X. Shi, Z. Titichai, N. Holdcroft, S., Factors influencing electrochemical properties and performance of hydrocarbon-based electrolyte PEMFC catalyst layers, *J. Electrochem Soc.* 156 ,4, (2009), B499.
4. Sambandam, S. Ramani, V., Effect of cathode binder IEC on kinetic and transport losses in all-SPEEK MEAs, *Electrochimica Acta*, 53, (2008), 6328-6336.
5. Zhang, J., PEM fuel cell electrocatalyst and catalyst layers: fundamentals and applications, 1st Ed, Published by Springer, pp. 631-654, (2008).
6. Rikukawa, M., Sanui, K., Proton-conducting polymer electrolyte membranes based on hydrocarbon polymers, *Prog. Polym. Sci.*, 25, (2000), 1463-1502.
7. Hickner, M. A., Ghassemi, H., Kim, Y. S., Einsla, B. R., McGrath, J. E., Alternative polymer systems for proton exchange membranes (PEMs), *Chem. Rev.* 104, (2004), 4587-4612.
8. Kerres, J. A., Development of ionomer membranes for fuel cells, *J. Membr. Sci.*, 185, (2001), 3-27.

9. Kreuer, K. D., Paddison, S. J., Spohr, E., Schuster, M., Transport in proton conductors for fuel cell applications: Simulations, elementary reactions, and phenomenology, *Chem. Rev.*, 104, (2004), 4637-4676.

10. Rozière, J., Jones, D. L., Non-perfluorinated polymer materials for proton exchange membrane fuel cells. *Annu. Rev. Mater. Res.* 33, (2003), 503-555.

11. Williams, M. V., Kunz, H. R., Fenton, J. M., Analysis of polarization curves to evaluate polarization sources in hydrogen/air PEM fuel cells, *J. Electrochem. Soc.*, 152, (2005), A635-A644.

12. Jiang, R., Kunz, H. R., Fenton, J. M., Investigation of membrane property and fuel cell behavior with sulfonated poly(etheretherketone) electrolyte: temperature and relative humidity effects, *J. Power Sources,* 150, (2005), 120-128.

13. Grotthus, T., Sur la décomposition de l'eau et des corps qu'elle tient en dissolution à l'aide de l'éctricité galvanique, *Ann. Chim.* LVIII, (1806), 54-74.

14. Kreuer, K. D. Weppner, W., Rabaneau, A., Investigation of proton conducting solids, *Solid State Ionics*, 3/4, (1981), 353-358.

15. Kreuer, K. D., On the complexity of proton conduction phenomena, *Solid State Ionics*, 136-137, (2000), 149-160.

16. Herring, A. M., Inorganic-polymer composite membranes for proton exchange membrane fuel cells, J. *Macromol. Sci., Part C: Polym. Rev.*, 46, (2006), 245-296.

17. Herring, A. M., Fuel cell membranes, In Encyclopedia of Chemical Processing; Lee, S., Ed.; Marcel Dekker: New York, Vol. 2, p.1085-1097, (2005).

18. Costamanga, P., Srinivasan, S., Quantum jumps in the PEMFC science and technology from the 1960s to the year 2000 part I, Fundamental scientific aspects, *J. Power Sources*, 102, (2001), 242-252.

19. Li, Q., He, R., Jensen, J. O., Bjerrum, N. J., Approaches and recent development of polymer electrolyte membranes for fuel cell operating above 100 ˚C, *Chem. Mater.*, 15, (2003), 4896-4915.

20. Kordesch, K. and Simader, G., *Fuel Cells and Their Applications*, Wienheim, Germany, VCH, (1996), 72.

21. Linkous, C. A. Proceedings 9th Int. Hydr. Energy Conf. (1992), 1.

22. Raistrick, I. D. in *Diaphragms, Separators, and Ion-Exchange Membranes*, J. W. Van Zee, J. W., White, R. E., Kinoshita, K. and Burney, H. S., Editors, p. 172, The Electrochemical Society Proceedings Series, Pennington, NJ (1986).

23. Gierke, T. D., Hsu, W. Y., *In perfluorinated ionomer membranes*, Eisenberg, A. Yeager, Y. H. L., Editors, ACS symposium series No. 180, American Chemical Society: Washington DC, (1982), chapter 13 p. 283.

24. Yeager, H. L., Steck, A., Cation and water diffusion in Nafion ion exchange membranes: Influence of polymer structure, *J. Electrochem. Soc*., 128, 9, (1981), 1880-1884.

25. Grot, W. G., Chadds, F. European Patent 0 066 369, 1982.

26. Martin, C. R.., Rhoades, T. A., Fergusson, J. A., Dissolution of perfluorinated ion-containing polymers, *Anal. Chem.*, 54, (1982), 1639-1641.

27. Gebel, G., Aldebert, P., Pineri, M., Structure and related properties of solution-cast perfluorinated ionomer films. *Macromolecules*, 20, (1987), 1428-1430.

28. Zadowzinski, T., Davey, J., Valerio, J., Gottesfeld, S., The water content dependence of electro-osmotic drag in proton conducting polymer electrolytes, *Electrochim. Acta*, 40, (1995), 297–302.

29. Baglio, V., Aricò, A. S., Antonucci, V., Nicotera, I., Oliviero, C., Coppola, L., Antonucci, P. L., An NMR spectroscopic study of water and methanol transport properties in DMFC composite membranes: Influence on the electrochemical behaviour, *J. Power Sources*, 163, (2006), 52-55.

30. Shao, Z. G., Xu, H., Li, M., Hsing, I. M., Hybrid Nafion–inorganic oxides membrane doped with heteropolyacids for high temperature operation of proton exchange membrane fuel cell, *Solid State Ionics*, 177, (2006), 779-783.

31. Saccà, A., Gatto, I., Carbone, A., Pedicini, R., Passalacqua, E., ZrO_2–Nafion composite membranes for polymer electrolyte fuel cells (PEFCs) at intermediate temperature, *J. Power Sources*, 163, (2006), 47-51.

32. Rhee, C. H., Kim, Y., Lee, J. S., Kim, H. K., Chang, H., Nanocomposite membranes of surface-sulfonated titanate and Nafion® for direct methanol fuel cells, *J. Power Sources*, 159, (2006), 1015.

33. England, W. A., Cross, M. G., Hamnett, A., Wiseman, P. J., Goodenough, J. B., Fast proton conduction in inorganic ion-exchange compounds, *Solid State Ionics*, 1, (1980), 231.

34. Nakamura, O., Kodama, T., Ogino, I., Miyake, Y., High-conductivity solid proton conductors dodecamolybdophosphoric acid and dodecatungstophosphoric acid crystals, *Chemistry Letters*, 1, (1979), 17-18.

35. Kreuer, K. D., Proton conductivity : Materials and applications, *Chem. Mater*, 8, (1996), 610-641.

36. Okuhara, T., Misono, M.,Solid superacid catalysts: consider them as potential alternatives to other strong acids that have been targeted as environmentally usound, *ChemTech*, 23, (1993), 23-29.

37. Keggin, J. F., The structure and formula of 12-phosphotungstic acid, *Proc. R. Soc. Lond. A*., 144, (1934), 75-100.

38. Pope, M. T., Muler, A., Polyoxometalate chemistry: An old field with new dimensions in several disciplines, *Angew Chem. Int. Ed. Engl.*, 30, (1991), 34-48.

39. Bekkum, H. Van., Sinnema, A., Koheznikov, I. V., Proton sites in Keggin heteropolyacids from ^{17}O NMR, *Catalysis Lett.*, 34, (1995), 213-221.

40. Yang, J., Janik, M. J., Ma, D., Zheng, A., Zhang, M., Neurock, M., Davis, R. J., Ye, C., Deng, F., Location, acid strength, and mobility of the acidic protons in Keggin 12-$H_3PW_{12}O_{40}$: A combined solid state NMR spectroscopy and DFT quantum chemical calculation study, J. Am. Chem. Soc., 127, (2005), 18274-18280.

41. Okuhara, T., Watanabe, H., Nishimura, T., Inumaru K., Misono, M., Microstructure of cesium hydrogen salts of 12-tungstophosphoric acid relevant to novel acid catalysis, *Chem. Mater*. 12, (2000), 2230-2238.

42. Koheznikov, I. V., Catalysis by heteropoly acids and multicomponent polyoxometalates in liquid-phase reactions, *Chem. Rev*., 98, (1998), 171-198.

43. Ramani, V., Kunz, H. R., Fenton, J. M., Stabilized heteropolyacid/Nafion composite membranes for elevated temperature/low relative humidity PEFC operation, *Electrochimica Acta*, 50, (2005), 1181-1187.

44. Ramani, V., Kunz, H. R., Fenton, J. M., Stabilized composite membranes and membrane electrode assemblies for elevated temperature/ low relative humidity PEFC operation, *J. Power Sources*, 152, (2005), 182-188.

45. Ramani, V., Kunz, H. R., Fenton, J. M., Investigation of Nafion/HPA composite membranes for high/ low temperature humidity PEMFC operation, *J. Membr. Sci*., 232, (2004), 31-44.

46. Savadogo, O., Emerging membranes for electrochemical systems: (I) solid polymer electrolyte membranes for fuel cell systems, *J. New Mater. Electrochem. Syst.*, 1, (1998), 47-66.

47. Mauritz, K. A., Moore, R. B., State of understanding of Nafion, Chem. Rev., 104, (2004), 4635-4585.

48. Appleby, A. J., Recent developments and applications of the polymer fuel cell, *Phil. Trans. R. Soc. Lond. A*, 354, (1996), 1681-1693.

49. Alberti, G. and Casciola, M., Composite membranes for medium temperature PEM fuel cells, *Annu. Rev. Mater. Res.* 33, (2003), 129-154.

50. Rozière, J. Jones, D. L. Non-fluorinated polymer materials for proton exchange membrane fuel cells, *Annu. Rev. Mater. Res.* 33, (2003), 503.

51. Kopitzke, R. Investigation of sulfonated high temperature polymers as proton exchange membrane electrolytes, PhD. Dissertation, Florida Institute of Technology, (1999).

52. Silva, V. S., Ruffman, B., Silva, H., Silva, V. B., Mendes, A., Madeira, L. M., Nunes, S. Zirconium oxide hybrid membranes for direct methanol fuel cells-Evaluation of transport properties, *J. Membr. Sci.* 284, (2006), 137.

53. Ramani, V., Swier, S., Shaw, M. T., Weiss, R. A., Kunz, H. R., Fenton, J. M. Membranes and MEAs based on sulfonated poly(ether ketone ketone) and heteropolyacids for polymer electrolyte fuel cells, *J. Electrochem. Soc.* 155, 6, (2008), B352.

54. Ise, M., Polyer Elektrolyt Membranen: Untersuchungen zur microstuktur und zu den transpotegenschaften fiur protonen und wasser, PhD. Thesis, University of Stuttgart, (2000).

55. Kreuer, K. D., On the development of proton conducting materials for technological applications, *Solid State Ionics*, 97, (1997), 1.

56. Kreuer, K. D., Dippel, Th., Maier, J., Membrane materials for PEM fuel cells: a microstructural approach, *Proc. Electrochem. Soc.*, 95-23, (1995), 241-246.

57. Othman, M. D. H., Ismail, A. F., Mustafa, A., Physico-chemical study of sulfonated poly(etheretherketone) membranes for direct methanol fuel cell application, *Malaysian Polym. J.* 2, (2007), 10-28.

58. Luo, Y., Ruizhen, H., Jin, X., Karasz, F. E., Thermal degradation of sulfonated poly(aryl ether ether ketone), *J. Anal. and Appl. Pyr.* 34, (1995), 229-242.

59. Kreuer, K. D., On the development of proton conducting membranes for hydrogen and methanol fuel cells, *J. Membr. Sci.*, 185, (2001), 29-39.

60. Nakamura, O., Kodama, T., Ogino I., Miyake, Y., High-conductivity solid proton conductors: Dodecamolybdophosphate acid and dodecatungstophosphoric acid crystals, *Chemistry Letters*, (1979), 17-18.

61. Breendon, M., Spizziri, P., Taylor, M., Plessis, J. D., McCulloch, D., Zhu, J., Yu, L., Hu, Z., Rix, C., Wlodarski, W., Kalantar-zadeh, K., Synthesis of nano-structured tundgsten oxide thin films: A simple controllable, inexpensive, aqueous sol-gel method, *Cryst. Growth Des*., 10, (2010), 430-439.

62. Hibino, M., Nakajima, H., Kudo, T., Mizuno, N., Proton conductive amoprphous films of tungsten oxide clusters, *Solid State Ionics*, 100, (1997), 211-216.

63. Mecheri, B., D'Epifiano, A., Di Vona, M. L., Traversa, E., Licoccia, S., Miyayama, M., Sufonated Poly ether ether ketone-based composite membranes doped with a tungsten-based inorganic proton conductor for fuel cell applications, *J. Electrochem. Soc*., 153, (2006), A463-A467.

64. Cotton, F. A., Wilkinson, G., *Advanced Inorganic Chemistry*, 3rd ed. Interscience Publishers, NY, (1972).

65. Hastings, J. J., Howarth, O. W., ^{183}W, ^{1}H and ^{17}O nuclear magnetic resonance study of aqueous isopolytungstates, *J. Chem. Soc. Dalton Trans.*, (1992), 209-215.

66. Grassie, S., Gilks, J., Thermal analysis of polystyrenes cross-linked by p-(dichloromethyl)benzene, *J. Polym. Sci: Polym. Chem. Ed.*, 11, (1973), 1985-1994.

67. Brauman, S. K., Friedel-Crafts reagents as charring agents in impact polystyrene, *J. Polym. Sci.: Polym. Chem. Ed.*, 17, (1979), 1129-1144.

68. Wang, Z., Jiang, D. D., Wilkie, C. A., Gilman, J. W., Further studies on fire retardant polystyrene by Friedel-Crafts chemistry, *Polym. Degr. Stab.* 66, (1999), 373-378.

69. Yao, H., Zhu, J., Mckinney, M. A., Wilkie, C. A., Cross-linking of polystyrene by Friedel-Crafts Chemistry: Multifunctional additives. *J. Vinyl Add. Techn*., 6, (2000), 205-210.

70. Ye, Y., Yen, Y., Cheng, C., Chen, W., Tsai, L., Chang, F., Sulfonated poly (ether ether ketone) membranes cross-linked with sulfonic acid containing benzoxazine monomer as proton exchange membranes, *Polymer*, 50, (2009), 3196-3203.

71. Chen, J., Maekwa, Y., Asano, M., Yoshida, M., Double cross-linked polyethetherketone-based polymer electrolyte membranes prepared by radiation and thermal cross-linking techniques, *Polymer*, 48, (2007), 6002-6009.

72. Xu, J., Yu, J., Guan, R., Li, C., Sun, L., Fang, J., A new crosslinked sulfonated polystyrene for proton exchange fuel cell membrane, *High Perf. Polym.* 22, (2009), 395-417.

73. Feng, S., Shang, Y., Xie, X., Wang, Y., Xu, J., Synthesis and characterization of cross-linked sulfonated poly(arylene ether sulfone) membranes for DMFC applications, *J. Membr. Sci.* 335, (2009), 13-20.

74. Kerres, J., Ullrich, A., Meier, F., Hä ring, T., Synthesis of novel acid based polymer blends for applications in membrane fuel cells, *Solid State Ionics*, 125, (1999), 243-249.

75. Gu, S., He, G., Wu, X., Guo, Y., Liu, H., Peng, L., Xiao, G., Preparation and characteristics of crosslinked sulfonated poly(phthalazinone ether sulfone ketone)

with poly(vinyl alcohol) for proton exchange membrane, *J. Membr. Sci.* 312, (2008), 45-58.

76. Rhim, J., Park, H., Lee, C., Jun, J., Kim, D., Lee, Y., Crosslinked poly(vinyl alcohol) membranes containing sulfonic acid group: proton and methanol transport through membranes, *J. Membr. Sci.* 238, (2004), 143-151.

77. Cai, H., Shao, K., Zhong, S., Zhao, C., Zhang, G., Li., X., Na, H., Properties of composite membranes based on sulfonated poly(ether ether ketone)s (SPEEK)/phenoxy resin (PHR) for direct methanol fuel cells usages, *J. Membr. Sci.* 297, (2007), 162-173.

78. Mikhailenko, S. D., Robertson, G. P., Guiver, M. D., Kaliaguine, S., Properties of PEMs based on cross-linked sulfonated poly(ether ether ketone), *J. Membr. Sci.* 285, (2006), 306-316.

79. Hande, V. R., Rao, S., Rath, S. K., Thakur, A., Patri, M., Crosslinking of sulfonated poly(ether ether ketone) using aromatic bis(hydroxymethyl) compound, *J. Membr. Sci.* 322, (2008), 67-73.

80. Zhang, W., Gogel, V., Friedrich, K. A., Kerres, J., Novel covalently cross-linked poly(etheretherketone) ionomer membranes, *J. Power Sources*, 155, (2006), 3-12.

81. Mikhailenko, S. D., Robertson, G. P.. Guiver, M. D., Kaliaguine, S., Properties of PEM based on cross-linked sulfonated poly(etheretherketone), *J. Membr. Sci.* 285, (2006), 300-316.

CHAPTER 2. EXPERIMENTAL

Chemicals and Materials

Poly(etheretherketone) of type 450 pf (PEEK) was obtained from Victrex, UK. *N*, *N*-dimethylformamide (DMF), 1,4-benzenedimethanol (BDM), phosphotungstic acid (PTA) and cesium carbonate (Cs_2CO_3) were obtained from Sigma-Aldrich. Sulfuric acid (H_2SO_4) (95%), 99.9% sodium hydroxide (NaOH), reagent grade ethanol (EtOH), sodium tungstate dihydrate ($Na_2WO_4 \cdot 2H_2O$), tungsten trioxide (WO_3), cesium tungstate and its hydrate (Cs_2WO_4 and $Cs_2WO_4 \cdot 2H_2O$), zinc chloride ($ZnCl_2$), hydrochloric acid (HCl), dimethylformamide (DMF), dimethylacetamide (DMAc), N-methyl-2-pyrrolidone (NMP)), sodium chloride (NaCl), acetone, hexane, and Rexyn 101 (H) ion exchange resin were obtained from Fisher. Alcohol-based 5% 1100 equivalent weight Nafion® was purchased from Solution Technologies Inc. Fuel cell electrocatalysts platinum on carbon (45.7% Pt on carbon, referred to as Pt-C) and platinum-cobalt on carbon (46% Pt, 4.6% Co on carbon, henceforth referred to as Pt-Co) was purchased from Tanaka Kikinzoku Kogyo, Japan. All polymer synthesis and subsequent handling was nominally exposed to 760 mmHg pressures, at 23 °C and 70% relative humidity (RH), unless otherwise stated.

General Procedures

Preparation of Rexyn 101H Ion Exchange Resin

80 g of Rexyn 101H ion exchange resin was packed into a 100 mL burette using water as the initial mobile phase. Prior to sodium SPEEK or Na_2WO_4 ion exchange, the column was protonated by eluting five bed volumes of 1.6 M HCl, followed by twelve bed volumes of DI H_2O. Only when the pH of solvent eluent was deemed neutral potentiometrically ($5 < pH < 7$), was the column utilized.

Sulfonation of PEEK

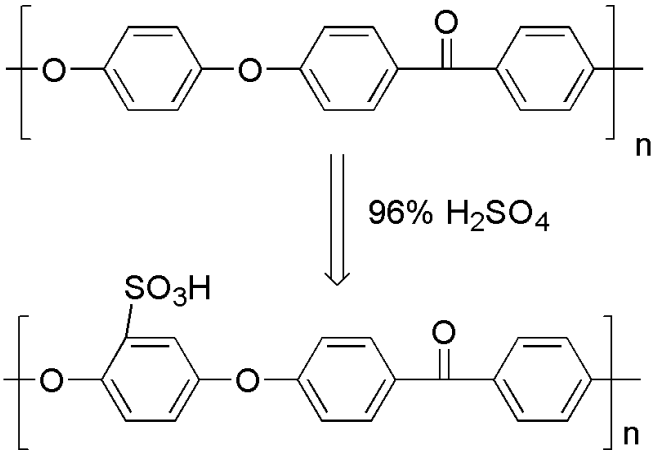

Figure 6. Electrophillic aromatic sulfonation of Victrex PEEK powder

Sulfonation of PEEK was performed as previously described in the literature.[1] PEEK powder was first dried in an oven at 120 $^{\circ}$C for a week to remove surface water. Sulfonation of PEEK (Figure 6) was done using concentrated H_2SO_4, without degradation or cross-linking the polymer.[2] In a typical reaction, 350 mL of 18 M H_2SO_4 was poured

into a three-necked round bottom flask and heated to the desired temperature. A total of 20 g dried PEEK powder was added slowly to the round bottom flask while stirring mechanically. The flask was immediately sealed with the inclusion of air, and allowed to stir isothermally for various reaction times. Table 3 shows some SPEEK polymers of varying DS prepared by varying reaction times and temperatures. Terminating the sulfonation reaction was achieved by decanting the reaction solution slowly with stirring into 4000 mL of a deionized (DI) water/ ice bath. Excess H_2O was removed by filtration, followed by five rinses with 2000 mL volumes of DI H_2O. Non water-soluble low DS SPEEK polymers produced by this method were washed with DI water until a neutral pH was obtained and then dried for 3 days under vacuum at 100 $^{\circ}$C. The low DS non-water soluble SPEEK of 58% DS, polymer ID SPEEK IX (Table 3) were named SPEEK-58.

For water soluble high DS SPEEK polymers, the following procedure was followed. Slow dissolution was effected while stirring in 800 mL H_2O at 60 $^{\circ}$C.

Table 3. Variation in sulfonation of Victrex PEEK properties based on reaction time and temperature

Polymer ID	Temp (°C)	PEEK/ H_2SO_4(g/L)	Time (Hour)	Degree of sulfonation (%)	Ion exchange capacity (meq/g)	EW (g/eq)
SPEEK IX	40	102	25.5	58	1.73	577
SPEEK X	50	102	122.5	85	2.35	418
SPEEK XII	40	102	9	24	0.77	1303
SPEEK XIII	50	68	8	60	1.79	557
SPEEK XIV	45	102	7	37	1.17	858
SPEEK XV	45	102	8	41	1.28	781
SPEEK XVI	50	102	120	76	2.18	458
SPEEK XVII	50	79	120	93	2.54	390
SPEEK XVIII	50	102	120	87	2.43	410
SPEEK XIX	50	102	8	30	0.94	1068
SPEEK XX	50	108	120	73	2.10	475
SPEEK XXII	50	105	144	96	2.62	382
SPEEK XXIII	60	104	121.5	100	2.79	358

This solution was allowed to cool, and finally titrated to neutrality with NaOH. Spectra/Por dialysis tubing (1000 Dalton pore size) was utilized to remove the Na_2SO_4 salt from the sodium SPEEK/H_2O solution. The sodium-exchanged, SPEEK/H_2O-filled tubing was immersed in a reverse osmosis water bath. The water in the bath was changed continuously while recording the conductivity. When the difference between the initial and final conductivities of the surrounding solution remained within a ±2 mS/cm range, the dialysis bag was removed, and the neutral SPEEK/H_2O solution isolated. Obtaining the SPEEK polymer in its acid form was done by passing the sodium SPEEK/H_2O solution through a protonated Rexyn 101-H ion exchange column. The SPEEK/H_2O acid

solution was evaporated to near dryness. Finally, the polymer was dried at 100 °C for 3 days under vacuum. The polymer ID of the water soluble SPEEK product utilized for all experiments was SPEEK XXII, and from hereon will be denoted SPEEK-96.

Membrane Casting

SPEEK-58/PTA membranes

SPEEK with equivalent weight of 577 grams per equivalent was dissolved in a 10:90 ethanol/DMF mixture to make a 5 weight percent (wt%) solution. PTA was added to the SPEEK-58 solution as required to achieve 0, 5, 15, 30 or 40 wt% solid acid content. Each polymer/solid acid solution was cast on a glass plate, and allowed to air dry for 2 days at 23 °C and 70% RH, followed by drying under vacuum at 110 °C overnight. Ramani et al. have described stabilizing Nafion® membranes containing PTA using Cs_2CO_3.[3] Their method was adapted for the SPEEK-58/PTA membranes prepared. Each membrane was immersed in 200 mL of 0.1 M Cs_2CO_3 solution overnight, washed and soaked twice in 400 mL DI water, and then soaked in 200 mL 0.5 M H_2SO_4 for 3 hours. The membranes were removed and rinsed until a pH 6 or greater was obtained from the washings. Membranes were allowed to air dry over a period of five days, followed by drying them at 70 °C for 12 hours

The SPEEK-58/PTA membranes will be referred to as S-0, S-5, S-15, S-30 and S-40 for the membranes containing 0 to 40 wt% PTA respectively. Membranes treated with cesium carbonate and sulfuric acid will be named by adding Cs^+/H^+ respectively to the abbreviation. Membranes S-0 to S-40 Cs^+/H^+ were dissolved in ethanol/DMF and

recast on respective glass plates and dried as above in order to determine if PTA has leached from the center of the membrane. Naming of these re-cast membranes was abbreviated by adding Re- at the beginning of the abbreviation; for example, Re-S-40/Cs^+/H^+ describes a re-cast 58% sulfonated PEEK membrane containing 40 wt% PTA that was previously treated with Cs^+ and H^+.

Preparation of $WO_3 \cdot xH_2O$ and SPEEK-96/ $WO_3 \cdot xH_2O$ membranes

The appropriate amount of tungstic acid hydrate ($WO_3 \cdot xH_2O$) was made by initially weighing and dissolving the molar equivalent of $Na_2WO_4 \cdot 2H_2O$ into 5 mL of DI H_2O. The aqueous solution was then passed through an acid exchanged Rexyn 101H column to form the $WO_3 \cdot xH_2O$ acid collected as a clear solution. If the solution was left to stand, yellow crystals of the acid hydrate began to crystallize from solution. These yellow crystals of $WO_3 \cdot xH_2O$ were separated from solution by vacuum filtration using a fine pore filter paper.

For membrane preparation, the eluting clear $WO_3 \cdot xH_2O$ (15 and 30 wt%) solution was also collected into a 5 wt% SPEEK-96/ H_2O polymer solution. The beginning and ending of elution was followed using a pH meter. The mixture was stirred for ten minutes while warming at 60 $^{\circ}$C and then cast on a glass plate and allowed to air dry.

Cross-linked SPEEK-96

SPEEK-96 was dissolved in DI water producing a 5 wt% solution. Membrane casting was done by spreading the solution onto a glass plate. The cast polymer was allowed to air dry for 5 days at 23 $^{\circ}$C and 70% RH, followed by drying at 100 $^{\circ}$C for 2

hours. Cross-linked membranes were produced by adding BDM cross-linker and metal oxide or transition metal catalysts, in various amounts, to respective aqueous SPEEK solutions. Total reactant dissolution was quickly achieved by warming and stirring continuously with a magnetic stirrer for 10 minutes. Membranes containing 6, 12 and 24 wt% BDM were solution cast and air dried for 5 days at before-mentioned conditions.

To effect thermal cross-linking, each membrane was subjected to a 200 $^{\circ}$C isothermal treatment for 15 minutes, followed by immediate cooling to room temperature. Heat treated membranes were then placed in a 60 $^{\circ}$C, 400 mL DI water bath for 45 minutes, removed and transferred to a beaker containing 200 mL of 23 $^{\circ}$C, 0.5 M NaOH for 30 minutes, and then rinsed thoroughly with DI water until a neutral wash was obtained. The procedure was followed by submersion of the polymer in 0.5 M H_2SO_4 for 30 minutes, rinsing the acid soaked membranes with DI H_2O, and then soaking the solid product in a room temperature DI water bath while monitoring the pH. A neutral pH wash indicated the removal of H_2SO_4 from the polymer. The wash water was also evaluated for chloride and sulfate using a Dionex ion chromatograph, utilizing a 1.0 mL/min flow rate of 90 mmol/ L Na_2CO_3 solvent. When the concentration of both ions was in the ppb range, the polymer was then removed and dried at 23 $^{\circ}$C and 70% RH overnight.

Determination of appropriate cross-linking catalyst

Various transition metal chlorides, as well as PTA and $WO_3 \cdot xH_2O$ were thought to be good candidates for effectively catalyzing the BDM cross-linking of the SPEEK polymer network. Table 4 below shows the properties of membranes which were cross-

linked (as described in the previous section) using various catalysts tested with SPEEK-96 polymer and 12 wt% benzenedimethanol cross-linker.

Table 4. Overview of attempted 96% DS SPEEK and 90% DS SPEEK cross-linking reactions using various catalysts

Catalyst used	Catalyst amount(g)	Cross-linker amount (wt%)	Final degree of sulfonation (%)	Mechanical/ solubility properties
Control	0	12	93	ductile/ dissolved
$CoCl_2$	1	12	-	very brittle/ DND
$SnCl_2$	1	12	-	ductile/ DND
$ZnCl_2$	1	12	89	ductile/ DND
$FeCl_2$	1	12	-	brittle/ became swollen
$WO_3 \cdot xH_2O$	15	12	59	Ductile/ DND
PTA	12	12	-	Ductile/ dissolved

DND – did not dissolve in warm water

Polymers synthesized with $ZnCl_2$, $SnCl_2$ and $WO_3 \cdot xH_2O$ catalysts showed the best properties based on their mechanical and solubility properties. These membranes were resistant to solvation in most common solvents (H_2O, acetone, hexane, DMF, DMAc and NMP at room and at their respective boiling temperatures.

Naming of the $ZnCl_2$ cross-linked membranes was done based on the percent BDM used, for example, X-12-SPEEK-96 represents a SPEEK-96 membrane containing 12 wt% BDM, X-24-SPEEK-96 was 24 wt% BDM...etc. The cross-linked SPEEK/ $WO_3 \cdot xH_2O$ membranes all contained the same 12 wt% BDM, but were named based on their solid acid catalyst loading, for example were named X-SPEEK-90/15-WO_3 stands for a 90% sulfonated PEEK membrane cross-linked with 15 wt% $WO_3 \cdot xH_2O$. The latter-mentioned membranes will be characterized further in Chapter 5.

Formulations and Analysis of Phosphotungstic Acids

Different formulations and treatments of phosphotungstic acid, $H_3PW_{12}O_{40}$ samples were prepared for thermogravimetric and differential thermal analysis (TG/DTA) and X-ray photoelectron spectroscopy (XPS) (Table 5).

Table 5. Nomenclature and methods of preparation for PTA samples.

Sample Abbreviation	**Sample Preparation Method**
PTA-EtOH/DMF	PTA crystallized from a solution of ethanol and dimethylformamide (EtOH/DMF), followed by drying under vacuum at 110 °C overnight
PTA/Cs^+	PTA-EtOH/DMF and treated with a solution of 0.2 M Cs_2CO_3.
PTA/Cs^+/H^+	PTA treated as above, and then followed by 1 hour immersion in 0.1 M H_2SO_4 at room temperature, rinsed with DI water to neutrality.
PTA + CsCl	PTA-EtOH/DMF and treated with 0.2 M CsCl.
Na_3PTA	PTA dissolved in water, neutralized with NaOH, and evaporated down until a precipitate was obtained.
PTA anhydrous	PTA heated to 210 °C for 1 hour.
PTA-6H_2O	PTA heated overnight at 40 °C and 20% relative humidity.
PTA recrystallized	PTA dissolved in water and evaporated down until recrystallization occurred.
PTA.13H_2O	PTA as obtained from vendor (Sigma-Aldrich).
PTA/Cs^+/H^+-80% RH	A sample chamber was fused to the end of a Fuel Cell Technology test cell. Equilibrium was achieved at 80% relative humidity then the chamber was opened and the sample vial was quickly capped.

Titrations

The DS was determined by a back titration technique. First, the SPEEK was dried and weighed, and then it was immersed in a 2-3 M sodium chloride solution for 3 days. The displaced H^+ ions were back titrated to neutrality with a 0.01 M NaOH solution using phenolphthalein as indicator. The DS, or number of milliequivalents of H^+ per gram of ionomer was determined by using Equation 6.

$$DS = \left(\frac{(moles_{titrant} \times Mw_{PEEK})}{W_{SPEEK} - (Mw_{SO_3H} \times moles_{titrant})} \right) \quad (6)$$

Here, $moles_{titrant}$ are the moles of base used to achieve the equivalence point, $Mw_{\text{-PEEK}}$ is the molecular weight of the PEEK monomer repeat unit, W_{SPEEK} is the dry weight of the sulfonated PEEK and Mw_{SO3H} is the molecular weight of the sulfonic acid group. The values for Mw_{PEEK} and Mw_{SO3H} are 288 and 81 g/mol, respectively.[4]

The equivalent weight (EW) and the ion exchange capacity (IEC) of SPEEK are used to quantify the number of moles of sulfonic acid groups present as a function of the polymer mass. The equivalent weight and the ion exchange capacity are described in Equations 7 and 8, respectively.

$$EW = \left(\frac{Mw_{PEEK}}{DS} \right) + Mw_{SO_3H} \quad (7)$$

$$IEC = \left(\frac{1000}{EW} \right) \tag{8}$$

Membrane Electrode Assembly Fabrication

SPEEK/PTA membranes

Catalyst ink was prepared by homogenizing 1100 EW Nafion®, water, methanol and Tanaka 46% Pt-Co mixture for 6 hours. A SPEEK and a SPEEK/Cs-PTA membrane named S-0 Cs^+/H^+ and S-15 Cs^+/H^+, respectively, were dried at 60 °C for 1 hour prior to catalyst spray application. The homogeneous electrocatalyst ink slurry prepared previously was sprayed on the anode and cathode sides of the dried S-0/Cs^+/H^+ and S-15/Cs^+/H^+ membranes. The respective catalyst coated membranes produced had total catalyst metal loadings of 0.55 mg Pt-Co/cm^2 and 0.54 mg Pt-Co/cm^2. A 50 μm, 1100 g/eq Nafion® membrane was also sprayed with 0.44 mg Pt-Co/cm^2. Each CCM fabricated was placed between two 50 μm Teflon sheets; this was then placed between two graphite plates covered with two rubber sheets. Hot pressing of the aforementioned CCM was achieved by placing the entire rubber-graphite-Teflon-membrane-Teflon-graphite-rubber assembly between 130 °C heated stainless steel plates at a pressure of 400 psi for 15 minutes. The commercial gas diffusion layers purchased from SGL were of type carbon 10BC. MEAs were sealed between two Fuel Cell Energy 25 cm^2 single serpentine flow fields using 25 μm thick Teflon gaskets on each side. The bolts on the cell were tightened by applying increasing torque of 20, 30 and finally 40 in-lbs.

$ZnCl_2$ and $WO_3 \cdot xH_2O$ Cross-linked SPEEK-90 membranes

Tanaka Pt/C (45.7% Pt) electrocatalyst ink was added to a vial containing 5 wt% 1100 EW Nafion®, methanol and H_2O. The vial was then placed into a constant flow H_2O bath while the catalyst and solvent slurry (Pt/C) was homogenized for 6 hours. The ink prepared by this method was sprayed onto both anode and cathode sides of the membrane. All membranes were oven dried at 60 ºC for an hour, before and after ink application to determine catalyst loading. CCMs had catalyst loadings of minimally 0.4 mg Pt/cm^2, with a maximum of 0.45 mg Pt/cm^2. Each CCM fabricated was placed between two 50 μm Teflon sheets; these were then placed between two graphite plates covered with two rubber sheets. Hot pressing of the aforementioned MEA was achieved by placing the entire rubber-graphite-Teflon-membrane-Teflon-graphite-rubber assembly at 150 °C for 15 minutes, under 400 psi pressure producing CCMs which were uniform in thickness about the Pt/C catalyst layer. These CCMs were determined to be crack and pinhole free before building the cell. Commercial gas diffusion layers purchased from SGL were of type carbon 10BC, these were cut to fit over the catalyst coated area on the membrane to fabricate the MEA. MEAs were sealed between two Fuel Cell Energy 5 cm^2 single serpentine flow fields using approximately 25 μm thick Teflon gaskets on each side. The bolts on the cell were tightened by applying increasing torque of 20, 30 and finally 40 in-lbs.

Techniques

Molecular Weight Determinations

Molecular weight determinations were done as previously described by Deveaux.[5] The solution viscosities were measured in a Canon-Fenske type viscometer at 25 $^{\circ}$C in sulfuric acid. The intrinsic viscosity [η] was taken as the inherent viscosity extrapolated to zero concentration. The procedures were carried out with ASTM international standard D 2857-95 standard practice for dilute solution viscosity of polymers.

Infrared Spectroscopy

Infrared spectra of the samples were recorded on a Perkin Elmer Spectrum 100 FTIR using the attenuated total reflectance mode (ATR-FTIR). ATR-FTIR was achieved by placing the membranes on the diamond window while clamping the membrane in the path of the beam. A minimum of 64 scans between 4000 and 650 cm^{-1} were done for elucidation of each membrane structure.

Water Uptake of Membranes

The amount of water absorbed in SPEEK-58 and the SPEEK-58/PTA composite membranes was measured by drying the membranes at 90 $^{\circ}$C overnight. Their dry weight was recorded and the membranes were submerged in DI H_2O for 2 days. Fully hydrated membranes were blotted dry with absorbent paper before being weighed again. Water

uptake measurements were done in triplicate. The weight gain of the absorbed water was calculated with reference to the initial dry weight of the membrane. This is shown in Equation 9.

$$WU = \left(\frac{W_{wet} - W_{dry}}{W_{dry}} \right) \times 100 \quad (9)$$

The WU of cross-linked SPEEK-96 membranes equilibrated in DI H_2O at 25, 80 and 100 °C was also determined by the difference in mass of H_2O-soaked membranes to dried ones. To obtain the dry membrane weight (W_{dry}), a 2 × 2 cm square of the polymer was cut and dried under vacuum at 110 °C overnight. Each membrane was subsequently submerged in DI H_2O at 25, 80 and 100 °C for 24, 2 and 2 hours respectively before taking measurements. At the specific temperatures, longer soaking times did not cause a significant increase in the WU measurements. After this time had elapsed, individual membranes were removed from the H_2O bath. Any remaining surface H_2O was removed using absorbent paper, and the membrane was reweighed to give the wet weight (W_{wet}). Equation 9 was used for the cross-linked SPEEK-96 WU determination.

The maximum H_2O molecules per sulfonic acid group, λ_{max} was calculated from Equation 10. This value was calculated based on the 100 ºC WU of the polymers:

$$\lambda_{\max} = \frac{WU_{100} \times 10}{Mw_{H_2O} \times IEC} \quad (10)$$

where Mw_{H2O} is the molecular weight of water, or 18.015 g/mol.

In-plane Proton Conductivity

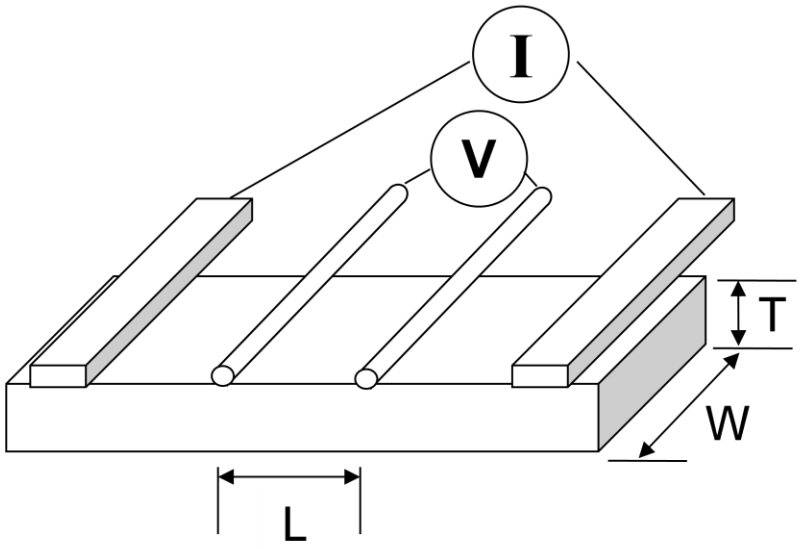

Figure 7. Bekktech Teflon conductivity test cell setup

Proton conductivity of the membranes was measured in-plane using the four point probe method. A Scribner Associates Incorporated 850c Fuel Cell Test Station was used to control the inlet hydrogen gas flow. A 2.5 cm by 0.5 cm width (W) membrane of known thickness T, was placed in a Bekktech Teflon test cell under the four Pt-electrodes (Figure 7). The test cell was then placed between two graphite compression plates with serpentine gas flow channels. The membrane was initially allowed to condition for 2 hours at 80% RH and 80 $^{\circ}$C cell temperature. The proton resistance was measured while sweeping and holding each RH for an hour; from steady state at 80% RH, to 20, 50, 80 and finally 100%. The in-plane PEM proton resistivity, ρ, was calculated using Equation 11, where R and A are the proton resistance measured and the cross-sectional area (T x W) of the membrane respectively, and L = 0.425 mm is the distance between the voltage

sense electrodes. The reciprocal of ρ gives the absolute protonic conductivity, σ, of the membrane.

$$\sigma = \frac{1}{\rho} = \frac{\mathrm{L}}{RA} \tag{11}$$

Thermal Studies

Differential scanning calorimetry (DSC) measurement was performed using a Perkin-Elmer, Diamond DSC under flowing N_2 with about 5 ± 2 mg of polymer for each thermogram determination. Samples were initially heated from 0 to 140 °C and held isothermally for 15 minutes, cooled to 0 °C and finally increased from 0 °C to 260 °C at a heating rate of 10 °C/min.

Thermogravimetric analysis (TGA) of SPEEK polymers was carried out by loading between 5 – 10 mg of a sample into a platinum sample pan and placing into a Perkin-Elmer Diamond TG/DTA instrument. Under helium atmosphere, the TGA sample chamber temperature was ramped from 30 °C to 600 °C at a rate of 10 °C/min. The decomposition gas stream under the flowing helium gas experiments was evaluated using a Pfeiffer Thermostar GSD-301T mass spectrometer (MS), complete with electron impact ionizer controlled with Quadstar 32-bit software. A similar experiment was performed on synthesized polymers under an air atmosphere; however, the MS could not be used to evaluate the gas stream, as high air concentration damages the filament used for detection.

For phosphotungstic acid and tungstic acid determinations, between 5 to 10 mg of each sample was placed in an aluminum sample pan and inserted into a Perkin-Elmer, Diamond TG/DTA. Under a helium atmosphere, the sample chamber temperature was ramped up from 30 $^{\circ}$C to 210 $^{\circ}$C at a rate of 10 $^{\circ}$C/min.

Uniaxial Tensile Testing

Mechanical strength has been compared to structure and properties of polymeric systems. Prior to stress-strain curve determinations, all membranes were allowed to equilibrate at 70% RH and 23 $^{\circ}$C overnight. SPEEK-96 as-cast, X-12-SPEEK-96 and X-24-SPEEK-96 samples were each cut into quad rectangular strips measuring approximately 5 mm wide and 65 mm long in dimensions; with membrane thickness varying between 30 to 60 mm. Each strip was mounted between two clamps and tested with an in-house-built mechanical testing system. This consisted of a data acquisition instrument, a linear actuator and a load cell controlled using LabView software. The uniaxial stress–strain curve for each strip was obtained at a 254 mm/min pulling rate, open to ambient conditions. The stress was calculated based on the cross-sectional area from the measured width of the strip and the nominal membrane thickness utilized.

X-Ray Diffraction

A Rigaku D/Max Beta X-ray diffractometer using Cu Kα radiation, was employed to characterize SPEEK-96 and various composite $WO_3 \cdot xH_2O$ samples. Analysis was done over a 2θ range of 10° to 60°. A 1° diversion slit, 1° scattering slit, and 0.6° receiving

slit (on detector) were used, with a scanning rate of 3 degrees/ minute. The X-ray generator voltage and current were set to 40 kV and 30 mA, respectively. Samples were supported on a metal sample holder, either affixed uniformly by tape or by placing putty above it. Analysis of data was done using Jade 7.0 analysis software and JCPDS reference files.

X-ray Photoelectron Spectroscopy

XPS data were acquired on a Physical Electronics model 5400 XPS system using a magnesium anode. The W4*f* peak position (appearing as a doublet) was obtained by using a pass energy of 44.75 eV with a step size of 0.5 eV. The time per step was 50 ms. High resolution XPS spectra were acquired with a pass energy of 35.75 eV and step size of 0.1 eV. The time between steps was 50 ms. In low resolution mode, elemental analysis was conducted on the samples. All samples were ground with a mortar and pestle till a fine powder was achieved. The samples were frozen with liquid nitrogen to ensure that the hydration state was constant during the high vacuum technique.

Electrochemical Performance

SPEEK/PTA membranes

SPEEK and SPEEK/PTA MEA performance was evaluated by obtaining polarization curves at 80 $^{\circ}$C, with cathode and anode gases being humidified to 73 $^{\circ}$C (75% RH) and 80 $^{\circ}$C (100% RH) respectively. Performance was then tested at 100 $^{\circ}$C

with anode and cathode gases being humidified to 69% RH. A Teledyne Medusa RD was used to control the inlet gas flows and temperatures while a Scribner Associates Inc. 890C Fuel Cell Test Station was utilized to apply/ monitor voltages, current and resistances during cell performance. Pure hydrogen was used at the anode and air or oxygen was utilized at the cathode. The voltage was initially held at 0.55 V till an equilibrated current was obtained under humidified gases. The current was then swept and held from 20 mA/cm^2 to open circuit voltage (0 A) and finally to 2000 mA/cm^2 while measuring the voltage. The loads were tested in the following order: 20, 0, 10, 20, 40, 60, 80, 100, 200, 300, 400, 500, 600, 700, 800, 900, 1000, 1100, 1200, 1300, 1400, 1500, 1600, 1700, 1800, 1900 and 2000 mA/cm^2, holding each current for 5 minutes. The experiment was stopped when the cell voltage dropped below 0.3 V. The membrane resistance was measured during performance testing using the current-interruption technique. The technique produces an IR-free cell voltage that removes any polarization produced by the cell, allowing for direct measurement of the hydrogen PEM fuel cell performance.

Cross-linked SPEEK-96/ X-15-WO_3 membranes

Fuel cell testing was accomplished using a Scribner 850C test stand to flow the oxidant (air/O_2) and fuel (H_2) gases to a 25 cm^2 Fuel Cell Technologies test cell. The protocol for electrochemical performance testing was exactly the same as the SPEEK/PTA membranes.

Electrochemical Characterization

Electrochemical characterization of the cell was also performed before and after each performance test. Linear sweep voltammetry (LSV) and cyclic voltammetry (CV) were used to estimate the hydrogen cross-over rate and the electrochemical surface area (ECA) respectively. For the cyclic voltammetry experiments, the anode compartment (both reference and counter electrode) was humidified with 25 $^{\circ}$C hydrogen gas, while 25 $^{\circ}$C humidity nitrogen gas was passed through the cathode compartment. The potential was cycled five times between 0.035 to 0.8 V versus RHE at a rate of 30 mV/s. Linear sweep voltammetry using the limiting current method was used to determine the hydrogen cross-over. With hydrogen gas flowing at the anode and nitrogen flowing at the cathode, the cell voltage was scanned from 0.01 to 0.8 V at 4 mV/s with the temperature being held at 25 $^{\circ}$C. The potential was controlled using a Princeton Applied Research 263 Potentiostat/ Galvanostat (AMETEK Princeton Applied Research, Oak Ridge, TN).

References

1. Ramani, V. and Sambandam, S., SPEEK/functionalized silica composite membranes for polymer electrolyte fuel cells, *J. Power Sources*, 170, (2007), 259.
2. Liler, M., Reaction mechanisms in sulphuric acid and other strong acid solutions, Academic Press Inc., London and New York (1971).
3. Ramani, V., Kunz, H. R. and Fenton, J. M., Stabilized heteropolyacid/Nafion composite membranes for elevated temperature/ low relative humidity PEFC operation, *Electrochim. Acta*, 50, (2005), 1181.
4. Huang, R. Y. M., Shao, P., Burns, C. M., Feng, X., Sulfonation of poly(ether ether ketone)(PEEK): Kinetic study and characterization, *J. Appl. Polym. Sci.* 82, (2001), 2651-2660.
5. Deveaux, J., Delimoy, D., Daoust, D., Legras, R., Mercier, P., Strazielle, C. and Nield, E., On the molecular weight determination of a poly(aryl-ether-ether-ketone) (PEEK) *Polymer*, 26, (1985), 1994-2000.

CHAPTER 3. LOW SULFONATION PEEK AND PHOSPHOTUNGSTIC ACID COMPOSITES

As stated in the introduction, one of the goals of this work is to synthesize new formulations of SPEEK by adding PTA to low DS SPEEK, and then stabilizing to make robust composites. The work presented herein gives an efficient way to synthesize SPEEK/ PEMs, based on the addition of solid acids.

Sulfonation of PEEK

SPEEK was prepared with a low DS by controlling the reaction temperature and time. The sulfonated hydrocarbon polymer was achieved in a 95% yield. The final product was kept in a dessicator prior to use in membrane fabrication or testing. The sulfonated polymer showed solubility in warm DMF, dimethylacetamide and *N*-methylpyrrolidinone. However, the sulfonated polymer did not show solubility in water, regardless of water temperature. The polymer's insolubility at high temperatures in water is ideal for hydrogen PEM fuel cell applications. The equivalent weight was determined by titration to be 577 g/eq, which relates to a degree of sulfonation of 58% in PEEK. The purity of the SPEEK-58 polymer was tested by thin layer chromatography, and was shown to be homogeneous. Losses in the calculated yield were thought to be due to product solvation and purification during processing. Pure and composite

membranes ranging from 40 to 50 microns were cast using 58% sulfonated PEEK and PTA. As-cast membranes were orange in color and with opacity ranging from transparent at low PTA content to opaque for high PTA content. The membrane mechanical properties degraded with the higher PTA content, as the membranes became brittle and difficult to handle, while the non-PTA SPEEK membrane (S-0) was ductile and pliable.

Molecular Weight Determinations

Two initial polymer concentrations of 0.2 and 0.5 g/dL, for both 450 pf PEEK, SPEEK-58, and SPEEK-96 were each diluted 4 times to give a large variation on the concentration scale. All viscosity measurements were made at 22 $^{\circ}$C and 70% RH. The intrinsic viscosity [η_a] was determined as reported earlier, using concentrations uncorrected and corrected for sulfonation.[1] The apparent intrinsic viscosity for the unsulfonated material can be related to the molecular weight $[\overline{M}w]_a$ by the following Mark-Houwink relation:

$$[\eta_a] = 6.195\times10^{-5}(\overline{M}w)_a^{0.94} \tag{12}$$

Based on the assumption that PEEK has a 100% DS, the k factor in the Mark-Houwink relation translates by 1.278. The sulfonated polymers' intrinsic viscosities and molecular weights $(\overline{M}w)_s$ are therefore related by Equation 13

$$[\eta_s] = 3.849 \times 10^{-5} (\overline{M}w)_s^{0.94} \quad (13)$$

Plots of natural log of the relative viscosity versus the polymer concentration was done to determine the $(\overline{M}w)_a$ and $(\overline{M}w)_s$ of 450 pf powder SPEEK-58 and SPEEK-96 respectively (Figure 8). Table 6 shows the results of these determinations. It has been reported previously that no chemical degradation and cross-linking take place during PEEK sulfonation while utilizing concentrated sulfuric acid (<100% conc.) at 23 °C. [1,2] Therefore the $[\overline{M}w]$ for 450 pf PEEK, SPEEK-58 and SPEEK-96 should be quite similar, if measurements are made at constant temperatures. However, the $[\overline{M}w]$ for DS 58% PEEK was 77% percent higher than that of the unsulfonated polymer. It follows that for Equation 13 to be valid, the DS value has to be ~100%. The $[\overline{M}w]$ for the 96% sulfonated material showed 10% deviation from the real value.

Table 6. Intrinsic viscosity and molecular weights for PEEK and sulfonated PEEK

Sample	Degree of Sulfonation (%)	[η] (dL/g)	$[\overline{M}w]$ (g/mol)
450pf PEEK	-	1.145	100750 [a]
SPEEK-58	58	1.218	178179 [b]
SPEEK-96	96	0.7849	114570 [b]

[a] Calculated from Equation 12
[b] Calculated from Equation 13

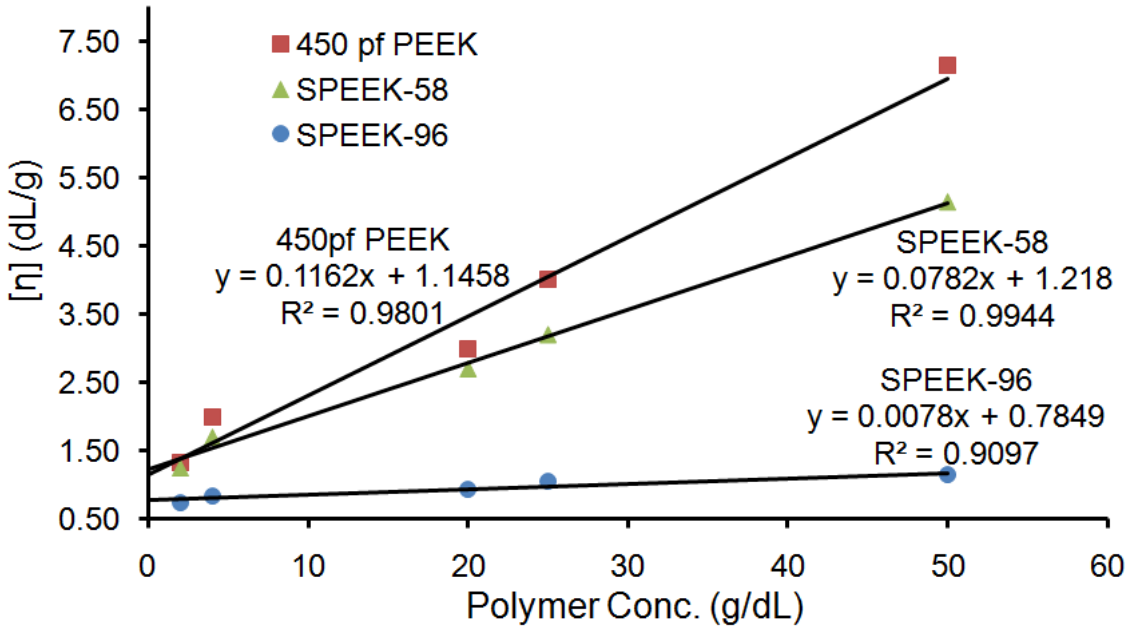

Figure 8. Graphical representation of intrinsic viscosity determinations of Victrex 450 pf PEEK, SPEEK-58 and SPEEK-96, in dilute solutions of sulfuric acid.

From these dilute sulfuric acid [$\overline{M}w$] determinations, it was concluded that no degradation or cross-linking occurred during any PEEK sulfonation reaction using H_2SO_4.

Water Uptake Measurements

The hydration of a PEM fuel cell membrane composite and its ability to retain these waters of hydration is paramount to obtaining the high protonic conductivity necessary for good cell performance under relatively dry conditions. The hydration of the membrane allows the protons to become easily dissociated from the polymer main chain for subsequent transport through polymer channels.[2] The ability to uptake water by the SPEEK/PTA composite membranes was hence evaluated.

Water uptake of the membranes decreased upon increasing the PTA concentration in the stabilized SPEEK/PTA composites, as shown in Table 7. Upon increasing the amount of PTA/Cs^+ in the membranes, a lower water uptake is somewhat expected, since the overall density of -SO_3H acid groups in the composite are diminished. Furthermore, the exchange of the H^+ for Cs^+ ions in the PTA/Cs^+ ostensibly removes water of hydration. Brown et al. showed in their x-ray diffraction studies this latter phenomenon.[3] Treating PTA with Cs^+ ion is commonly done as a method for rendering the PTA ion water-insoluble, a necessary step if the cluster compound is to be used as a proton-conducting solid electrolyte.[3] The PTA resulting from Cs_2CO_3 treatment should not be regarded as having had complete substitution of Cs^+ for H^+. Work on pH shifts resulting from exposure of PTA crystals to Cs^+ solution showed only a 4% exchange. This would imply that only the surface region of the PTA particles is undergoing ion exchange.

Table 7. Water uptake at 25 °C of SPEEK-58 composite membranes.

Sample	% Water Uptake (1st Trial)	% Water Uptake (2nd Trial)
S-0 Cs^+/H^+	49	50
S-5 Cs^+/H^+	47	50
S-15 Cs^+/H^+	44	47
S-30 Cs^+/H^+	40	42
S-40 Cs^+/H^+	42	45

As it has been reported that leaching of the solid acids from the composite membrane matrix occurs, water uptake studies were also carried out.[4] The samples were tested for water uptake, dried, and then retested. The value for the secondary water

uptake measurements increased slightly over primary water uptake for the matching membrane samples. The observed increase can be attributed to the leaching of the stabilized PTA membranes. The stabilized PTA remaining in the membrane matrix is believed to be specifically located underneath the membrane surface. It was interpreted that this leads to a higher volume of sulfonated polymer to uptake water, compared with the composite containing cesium.[4]

ATR- Fourier-Transform Infrared Spectroscopy

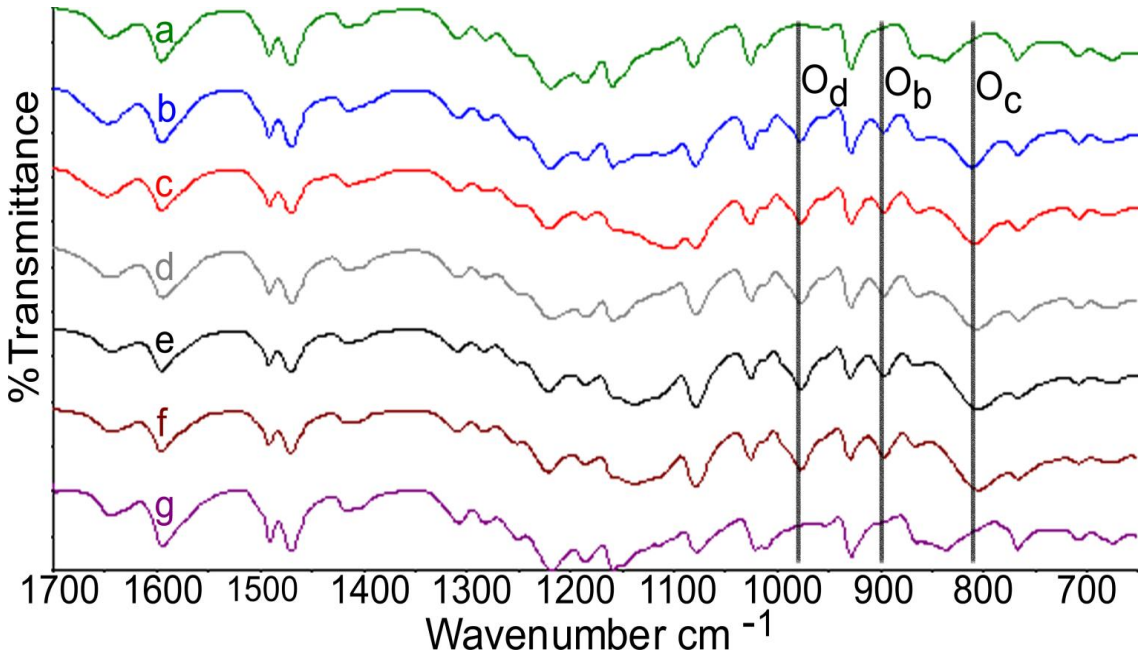

Figure 9. ATR-FTIR of sulfonated PEEK/PTA composite membranes non-stabilized: a) S-0, b) S-5, c) S-15, d) S-30, e) S-40, and stabilized: f) S-40/Cs^+, and g) S-40/Cs^+/H^+ showing an increase in percent transmittance of PTA stretches for the W-O terminal double bonds (O_d) at 980 cm^{-1}, W-O-W inter-linking bridges between corner sharing octahedra (O_b) at 910 cm^{-1}, and W-O-W intra bridges between edge sharing octahedral (O_c) at 810 cm^{-1}.

Figure 9 shows the ATR-FTIR spectra obtained on various SPEEK and SPEEK composite samples. The IR spectrum for SPEEK/PTA membranes closely resembles that of previous work done on similar composites.[5] The labeled lines show the various tungsten-oxygen bond stretches present in the PTA as follows: O_d is for the W-O terminal double bonds at 980 cm^{-1}; O_b is the W-O-W inter-linking bridges between corner sharing octahedra at 910 cm^{-1}; and O_c is the W-O-W intra bridges between edge sharing octahedra, shown at 810 cm^{-1}.[6] On closer inspection of the FTIR spectra of the SPEEK/PTA composite membranes before stabilization, it is observed that the percent transmittance of PTA stretches decreased with increasing solid acid content. Notably, these tungsten-oxygen stretches were still present in the membrane spectrum after cesium treatment (Figure 9-f). The disappearance of PTA stretching bands from the FTIR surface measurements of the composite polymer occurred after the 0.1M H_2SO_4 acid/DI water treatment of the polymer (Figure 9-g). This acid treatment should effectively exchange any Cs^+ cations attached to the sulfonic acid groups of the polymer. Therefore, it can be stated that the sulfuric acid treatment causes leaching of the cesium-stabilized PTA from the surface of SPEEK composite membranes. This phenomenon was also observed for membranes with 5%, 15%, and 30% PTA/Cs^+.

In order to better understand if the loss of PTA/Cs^+ is only a surface effect or a bulk process, the protonated membranes were re-dissolved and re-cast. In this process, a portion of any remaining PTA/Cs^+ in the bulk of the polymer would be transferred to the surface and its existence would be confirmed by ATR-FTIR. Figure 10 shows the spectrum of all re-cast membranes and confirms the reappearance of the W-O stretching bands.

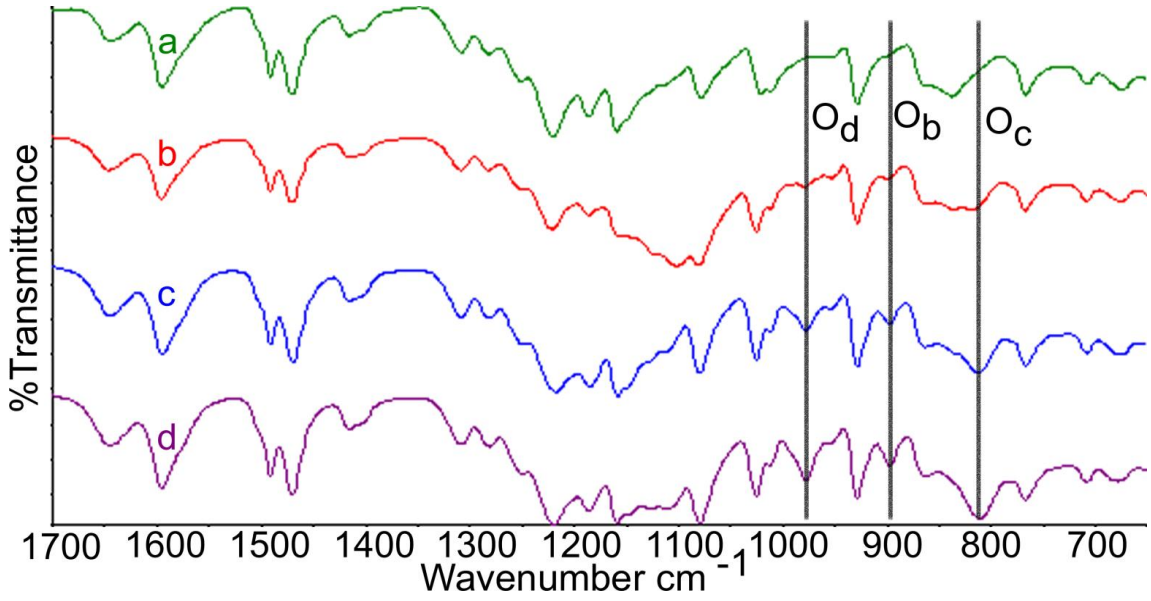

Figure 10. ATR-FTIR of re-cast sulfonated PEEK/PTA stabilized composites : a) Re-S-5/Cs^+/H^+, b) Re-S-15/Cs^+/H^+, c) Re-S-30/Cs^+/H^+, d) Re-S-40/Cs^+/H^+ showing the presence of PTA/Cs^+ in membranes except for Re-S-5/Cs^+/H^+ membrane.

The Re-S-5 membrane did not show any perceptible W-O stretches, however, suggesting that the small initial loading was dispersed below detection limits. The as-cast membranes were compared quantitatively to re-cast composites using FT-IR by calculating the peak ratios of PTA at 910 cm^{-1} to the SPEEK carbonyl at 1650 cm^{-1} (Table 8). The intensities of the stretches are quantitatively comparable with the PTA stretches seen in S-15/Cs^+ membrane before H_2SO_4 treatment. The percent difference between peak ratios for as-cast to re-cast membranes is less than 3% for the composites. Therefore, only the surface of a SPEEK/PTA/Cs^+/H^+ membrane composite loses its solid acid, and it is not representative of the entire membrane matrix.

Table 8. ATR-FTIR peak area ratio of 910 cm^{-1} to 1650 cm^{-1} for PTA/SPEEK

Membrane Studied	Ratio for PTA/SPEEK bands
S-5	0.180894
S-15	0.188347
S-30	0.195603
S-40	0.226348
Re-S-15/Cs+/H+	0.171303
Re-S-30/Cs+/H+	0.192402
Re-S-40/Cs+/H+	0.199806

Proton conductivity, more simply the long-range transport of protons, is a well known phenomenon for many different materials.[7] The two predominant mechanisms used to describe protonic motion are the "vehicle" mechanism, where the proton is bound to and carried by a mobile species, and the Grotthus mechanism, where the proton is transferred between fixed, adjacent binding sites. In many materials, protonic motion can be ascribed to either or both mechanisms, depending on the precise conditions. Proton exchange membrane conductivity is also highly dependent on the number of available acid groups, accompanied by their ease of dissociation while dry or hydrated.

Membrane Proton Conductivity

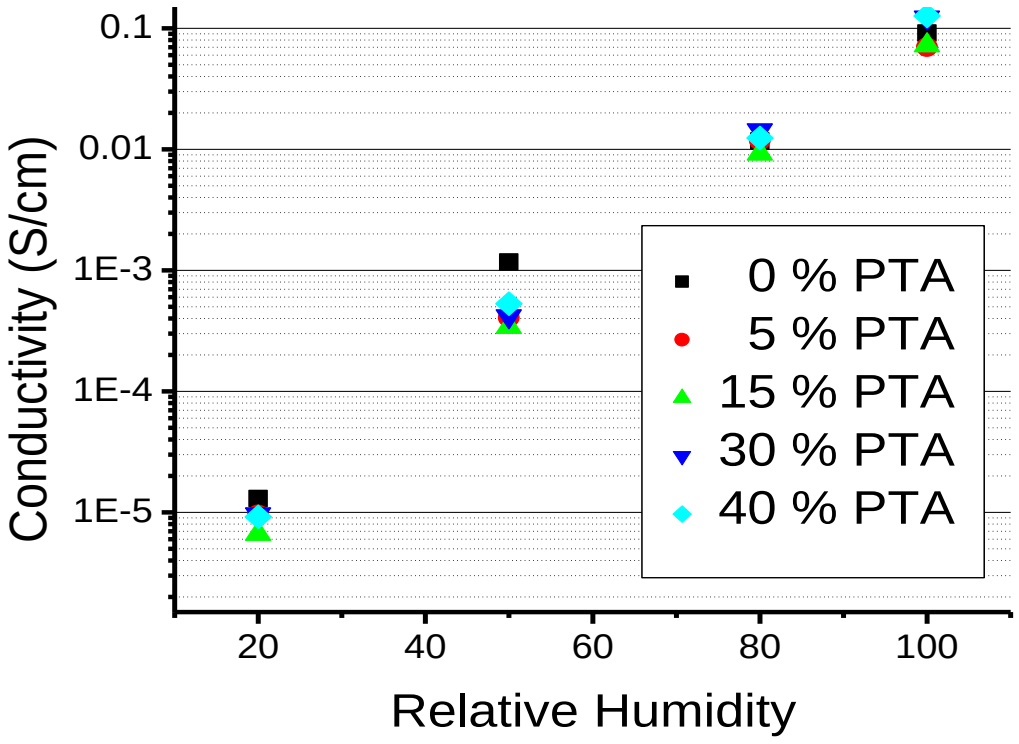

Figure 11. Conductivity measurements of stabilized SPEEK/PTA composite membranes: S-0/Cs^+/H^+, S-15/Cs^+/H^+, S-30/Cs^+/H^+, and S-40/Cs^+/H^+.

Figure 11 shows the four probe-measured conductivity of stabilized SPEEK/PTA composites containing 0%, 5%, 15%, 30% and 40% PTA by weight, represented as S-0, S-5, S-15, S-30 and S-40 respectively. The conductivity, σ, for the stabilized membranes gave nearly identical results. At low relative humidity, the stabilized membranes containing PTA/Cs^+ had the lowest conductivity values. As will be shown by TG/DTA experiments presented later, the hydration state of PTA/Cs^+ in the SPEEK composite membrane is negligible. Hence, the addition of the non-hydrating PTA/Cs^+ material to

pure SPEEK did not lead to increased proton mobility at low relative humidity. It is only at the highest water vapor pressure (100% RH) where it seems that increased PTA (30 and 40 wt%) loading has the effect of increasing the conductivity to 0.12 S/cm, compared to 0.091 S/cm for the pure SPEEK membrane. These findings support the idea that a water-assisted vehicle mechanism (H_3O^+) is dominant across the sulfonic acid/PTA surface at high relative humidities, even though the Grotthus mechanism is generally assumed to hold for proton transport in pure heteropolyacids.[8,9,34] A water-assisted mechanism as a vehicle for transport has a lower activation energy compared to the Grotthus mechanism for proton transfer, so that Grotthus only becomes predominant at lower water vapor pressures. Bardin and Janik showed density functional theory calculations in which the activation energy for the 'hopping' of protons between an anhydrous PTA molecule's surface oxygens is one order of magnitude lower than when the solid acid is in a hydrated state, or 103.3 kJ/mol and 11.2 kJ/mol respectively.[10] Neither Cs-PTA leaching from a swollen polymer surface during protonation, nor the non-hygroscopic nature of the Cs^+ salt of PTA significantly altered the vehicle-mechanism assisted proton conductivity of composite SPEEK/ PTA membranes.

Thermal Analysis Study

Figure 12 shows the weight-loss thermogram and corresponding endotherm for PTA received as partially hydrated solid crystals. Two endotherms relating to two stages of water release by PTA are shown, one occurring at 45 $^{\circ}$C and the other one at 160 $^{\circ}$C. Total mass loss was about 7% of the original weight, equivalent to roughly 13 waters of hydration. The first transition corresponds to conversion of the 13-hydrate to the

hexahydrate, and the second transition to the hexahydrate becoming effectively anhydrous.

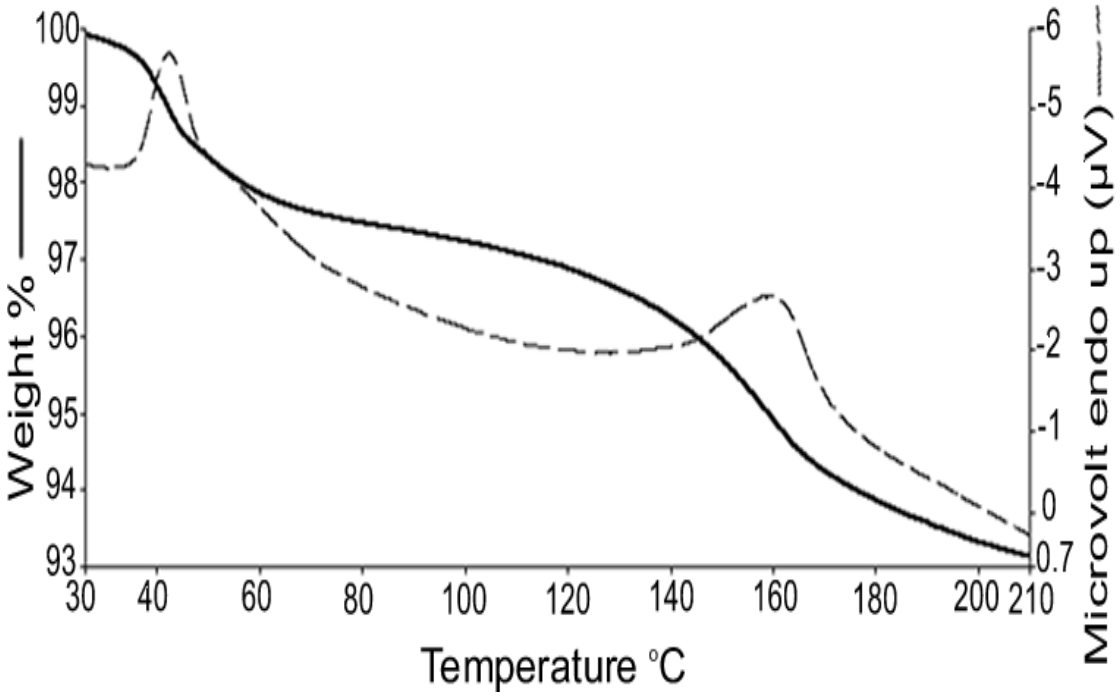

Figure 12. TG/DTA thermogram of PTA as obtained from Aldrich. The first transition corresponds to conversion of the 13-hydrate to the hexahydrate, and the second transition to the hexahydrate becoming effectively anhydrous.

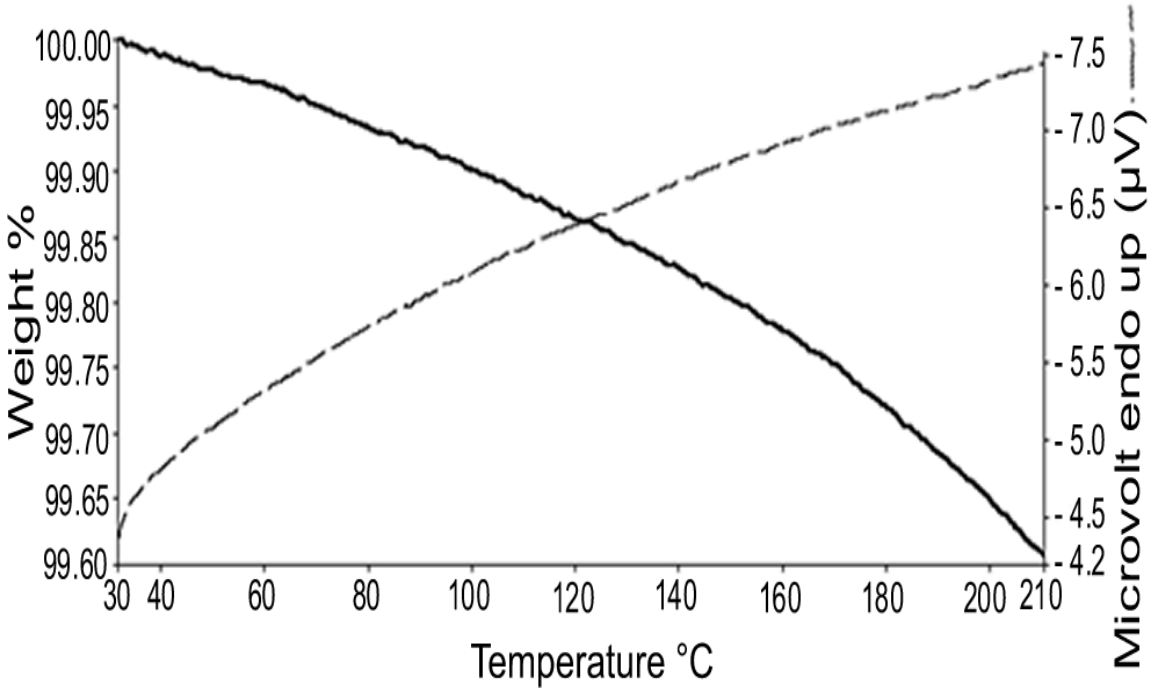

Figure 13. TG/DTA thermogram of PTA stabilized with Cs^+ which shows that PTA/Cs^+/H^+ does not exhibit any significant weight loss and therefore, it was concluded that the PTA cast from DMF-ethanol, stabilized with a Cs^+ treatment is essentially anhydrous.

In contrast, the thermogram for PTA/Cs^+/H^+ as shown in Figure 13 does not exhibit any significant weight loss (approximately 0.39%). Therefore, it was concluded that the PTA cast from DMF-ethanol, stabilized with a Cs^+ treatment is essentially anhydrous. Infrared spectroscopy was also used to determine the hydration state as well as the presence of PTA and SPEEK/PTA in the various samples. The IR stretches for O_d, O_b and O_c in the PTA molecular structure can be identified from the bands between 800 and 1200 cm^{-1}.

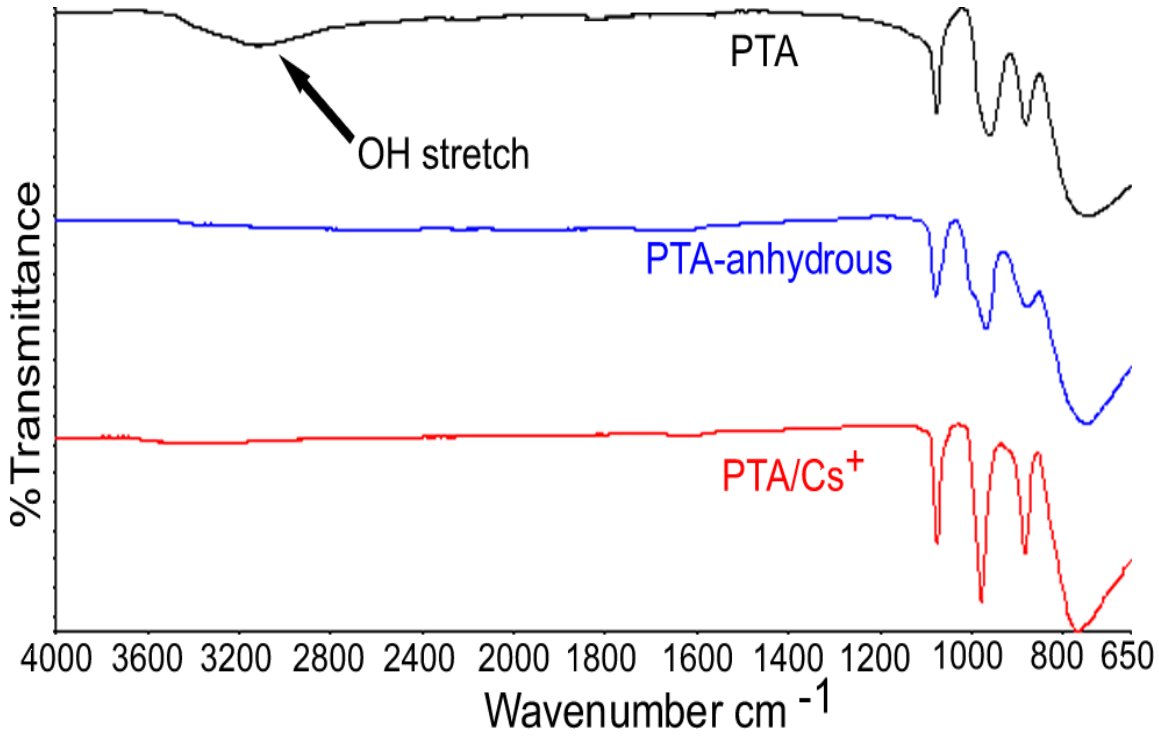

Figure 14. FTIR spectrum of PTA, anhydrous PTA and PTA/Cs^+. The 3000 to 3300 cm^{-1} region, in which the O-H stretch is expected, showed negligible transmittance for PTA/Cs^+.

Figure 14 shows the FTIR spectrum of PTA, anhydrous and hydrous, as well as the Cs^+ salt counterpart. The 3000 to 3300 cm^{-1} region, in which O-H stretch from waters of hydration is expected, showed negligible absorption. Not only is water missing, but also the alkyl C-H stretches that would be present for DMF or ethanol. The FTIR data supports the fact that the PTA/Cs^+/H^+ cast from DMF-ethanol is anhydrous. Similar results were found for PTA treated by Cs_2CO_3 and subsequently by H_2SO_4.

Careful consideration was taken to force water uptake into the solid acid matrix of PTA/Cs^+/H^+. PTA/Cs^+/H^+ was placed in a small vial and was exposed to 80% RH at 80 $^{\circ}$C for 2 hours under a hydrogen atmosphere. The sample was quickly capped to limit its exposure to ambient atmosphere, and a representative sample was run in the TG/DTA

apparatus. It was observed that only a fraction of a percent of mass was eliminated, showing that PTA, subjected to Cs_2CO_3 and H_2SO_4 treatments could not be rehydrated. The results are summarized in Table 9. The PTA/Cs^+ samples did not show any water uptake, so it was concluded that the alkali metal-exchanged solid acid is not capable of binding water to an appreciable extent, and hence does not help with membrane proton conductivity at low relative humidity.

Table 9. Weight loss percentages for PTA samples during TG/DTA study

Sample	**% Weight Loss**
PTA	7.5
PTA-EtOH/DMF	0.11
PTA/Cs^+	0.30
PTA/Cs^+/H^+	0.39
PTA-Cs^+/H^+-80% RH	0.55

X-ray Photoelectron Spectroscopic Study

X-ray photoelectron spectroscopy has been used recently for characterization of organic/inorganic composites.[11,12,13] Representative XPS spectra for the W4$f_{7/2}$ transition in various PTA samples are shown in Figure 15

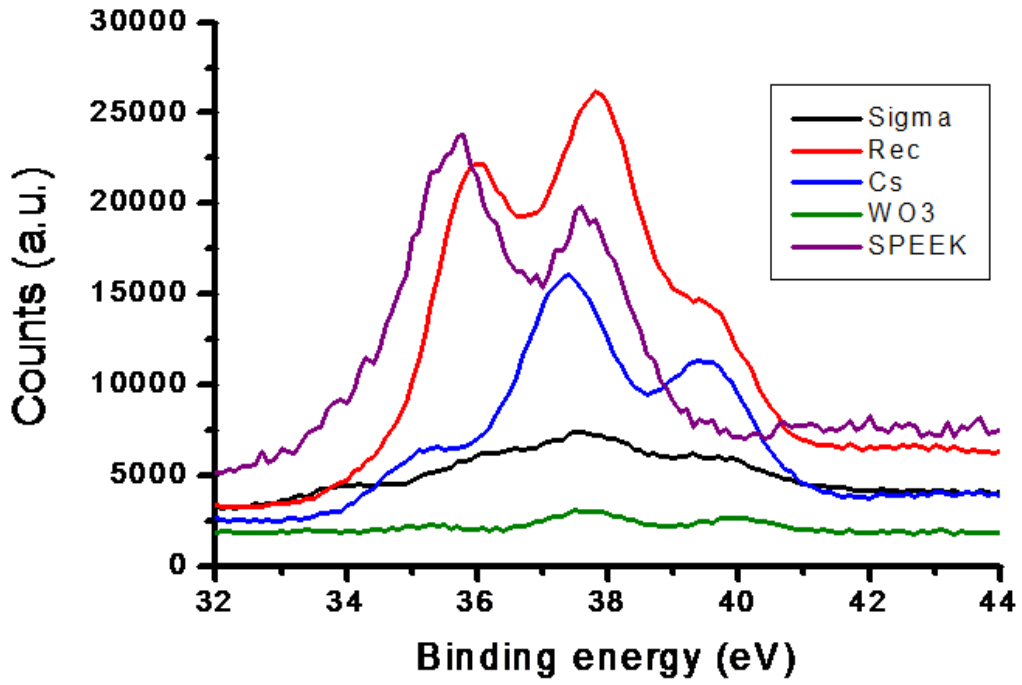

Figure 15. Representative XPS graphs for the W4*f* transition of various solid acid samples. The PTA/Cs^+ sample had the lowest energy at 35.4 eV, while PTA recrystallized from water had the highest value at 37.8 eV.

The W4$f_{7/2}$ binding energies for these PTA compounds described in the experimental section are shown in Table 10, in order of increasing binding energy. A wide spread of W4$f_{7/2}$ transition energies was obtained, spanning a range of 2.4 eV. The PTA/Cs^+ sample had the lowest energy at 35.4 eV, while PTA recrystallized from water had the highest value at 37.8 eV. When chemical shifts of this magnitude are encountered, the first possibility is to consider changes in oxidation state. Although many oxidation states for W have been reported, none of the treatments described above have any significant capability to perform redox chemistry on PTA.[14,15] Furthermore, even the lowest binding energy obtained is well within the range normally attributed to

W^{6+}. Therefore, the chemical shifts must be explained in terms of the chemical environment around the W centers. Several trends among the PTA preparations are observed. Those samples for which some of the protons have been substituted with an alkali metal ion such as Na^+ or Cs^+ have lower binding energy 35.4-35.9 eV); those with high waters of hydration have higher binding energy (>37.5 eV), and those with low hydration (0-6 H_2O/PTA molecule) have intermediate binding energy (36.0-36.2 eV).

Table 10. XPS W4$f_{7/2}$ data for various solid acid compounds

Sample	**Binding Energy (eV)**
WO_3	35.1
PTA/Cs^+ Cs_2CO_3	35.4
PTA/Cs^+/H^+	35.6
S-30 Cs^+/H^+	35.7
PTA + CsCl	35.8
Na_3PTA	35.9
PTA-6H_2O	36.0
PTA·nH_2O, recrystallized from water	36.0, 37.8
PTA-EtOH/DMF	36.2
PTA (anhydrous)	36.2
Na_2WO_4-2H_2O	36.7
Cs_2WO_4 (anhydrous)	37.3, 35.3
Sigma PTA·nH_2O	37.5
Cs_2WO_4·2H_2O	37.7

To help understand the range of binding energy values obtained for PTA, other W-containing compounds were studied via XPS. These results are also shown in Table 10 and they present an even wider range of binding energies. Reference compounds were chosen so as to retain the W^{6+} oxidation state. The octahedrally coordinated WO_3 had the lowest binding energy of all the test samples at 35.1 eV, while the tetrahedral Cs_2WO_4 had among the highest values.

While tetrahedral versus octahedral coordination among all W compounds definitely showed a trend toward higher binding energies, this has little bearing on the PTA samples, which retain octahedral coordination throughout. Even so, the dihydrate of Cs_2WO_4 was shifted to higher binding energy by at least 0.4 eV over the anhydrous material, indicating once again the same trend involving hydration energy. The effect of hydration states on binding energy is apparently related to the amount of hydrogen bonding between the water molecules surrounding the PTA ion and the terminal oxygens of the PTA. This attracts valence electron density away from the W centers, causing the core electrons to be held more strongly.

Treating PTA with a Cs^+ ion solution is a common method for rendering PTA ion water-insoluble, a necessary step if the cluster compound is to be used in a proton-conducting solid electrolyte. The PTA resulting from Cs^+ treatment should not be regarded as having had complete substitution of Cs^+ for H^+. Exposure of PTA crystals to CsCl solution showed only a 4% exchange of cations. On the other hand, the kinetics of ion exchange with the solid particles would suggest that the Cs^+ resides mostly on the outer surface, making them more readily detectable by X-ray photoelectron spectroscopy. Brown et al. concluded that large univalent cations such as Cs^+ tended to make anhydrous

salts, or in other words, alkali metal inclusion is accompanied by water exclusion.[3] Part of the alkali metal trend may be due to changes in the lattice parameter. The lattice parameter for PTA is related to the cationic species separating each molecular ion. For anhydrous PTA, the lattice constant is 10.8 Å, while for $Cs_3PW_{12}O_{40}$ it expands to 13.7 Å.[16] For the hexahydrate, the lattice parameter is intermediate at 12.5 Å.[3] Part of the difficulty in interpretation of the PTA XPS data is uncertainty in the extent of hydration of some of the samples. The commercial samples are typically marked "nH_2O", making no commitment as to its true water content. In this work the number of waters of hydration for the purchased commercial PTA was determined by TGA technique to be 13 (Figure 12).

Nafion® has been the most robust membrane material for PEM fuel cell applications to date, with other polymeric materials playing a less significant role. New membranes for MEA fabrication must show adaptability to endure swelling and shrinking of the membrane-electrode interface while cycling current density. Preliminary cell performance was primarily conducted to determine the suitability of PTA as an additive in SPEEK membranes. A pure SPEEK and a stabilized SPEEK/PTA composite membrane, S-0/Cs^+/H^+ and S-15/Cs^+/H^+ respectively, were incorporated into MEAs having Pt-Co electrodes containing 28 wt% Nafion® binder. A Nafion® membrane MEA was also fabricated for comparison. Before 80 °C or 100 °C cell performance was determined, each cell was conditioned with H_2 and air for three hours at a holding voltage of 0.55 V.

Electrochemical Performance

Figure 16 shows the room temperature cyclic voltammogram before and after cell conditioning of S-0/Cs^+/H^+.

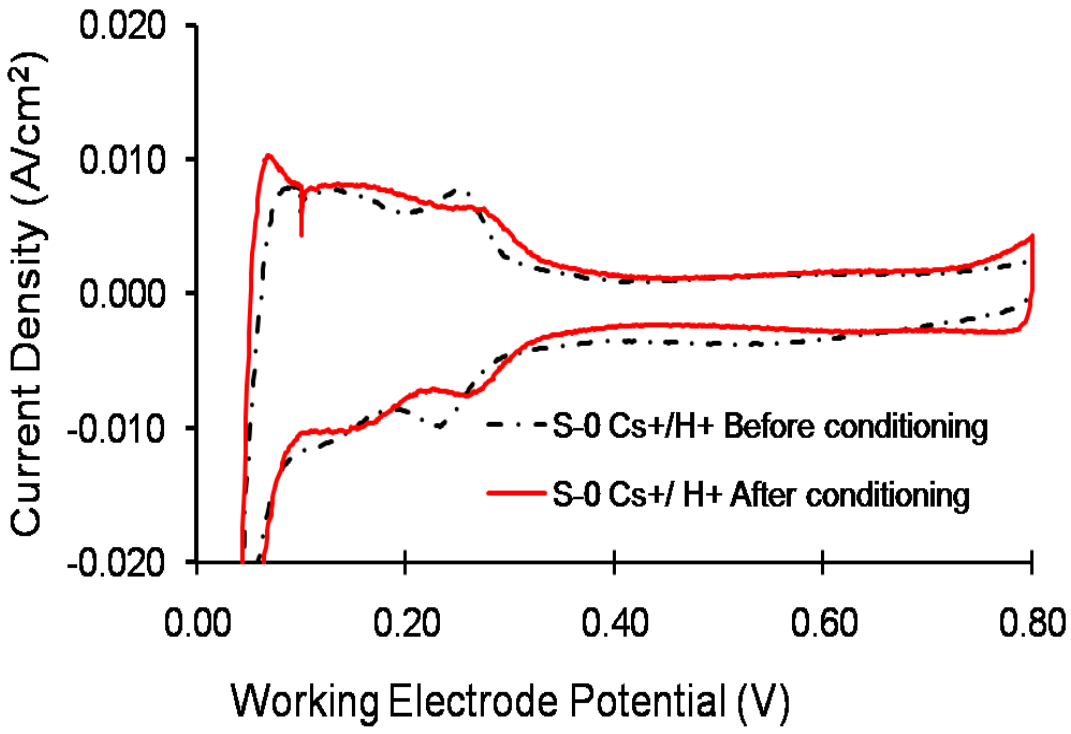

Figure 16. 25 °C cyclic voltammetry of S-0/Cs^+/H^+ membrane before and after cell conditioning.

Peaks recorded in the range of 0.1-0.4 V are associated with H_2 adsorption and desorption on the Pt-Co catalyst's active surface. The ECA of the Pt-Co catalyst layer was estimated using a technique previously described by Jiang et al.[17] The ECA calculated for the S-0/Cs^+/H^+ before cell conditioning showed an increase from 25 to 37 m^2/g Pt after cell conditioning. The increased ECA was understood to be due to higher hydration in the membrane and electrode pores. This allows for increased access

of fuel and oxidant to surface electrocatalytic sites on the Pt-Co alloy. After conditioning, cell performance was then determined at 80 °C with the anode hydrogen gas being humidified to 100% RH and cathode oxygen gas humidified to 75% RH. Figure 17 outlines the current-voltage performance curves obtained for the various PEMs utilizing H_2/O_2 in the fuel/oxidant gas streams.

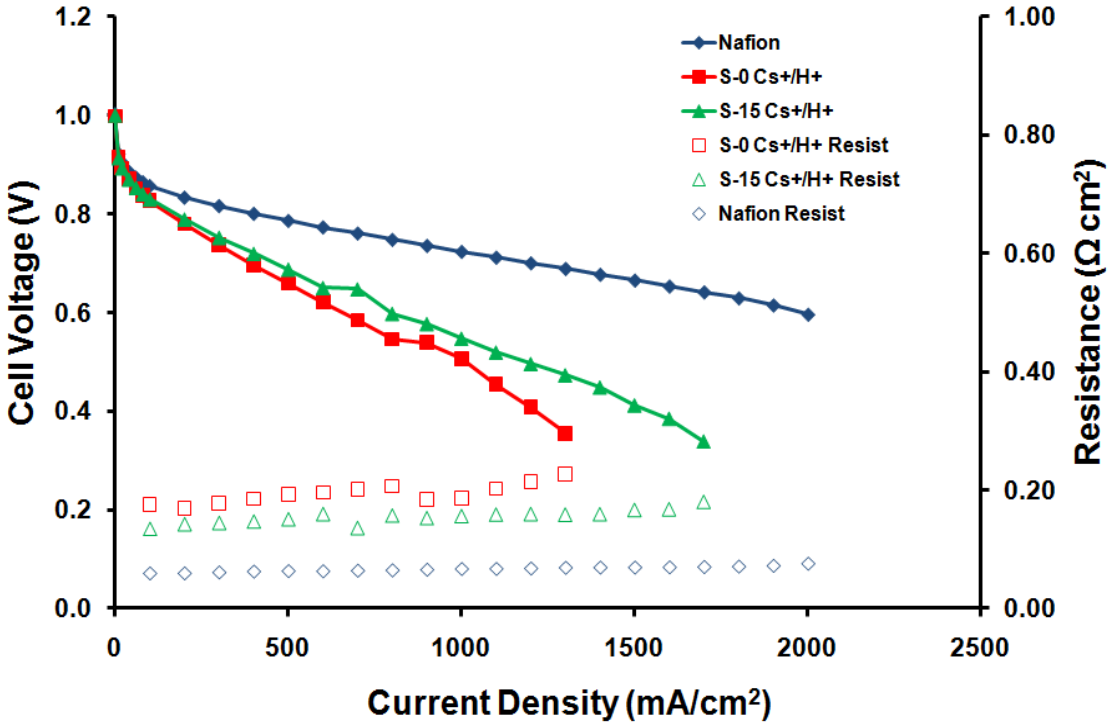

Figure 17. PEM fuel cell performance of various CCMs performed in a H_2/O_2 cell at 80 °C with anode/cathode gases humidified to 100% RH /75% RH respectively.

The Nafion® MEA produced 1.002, 0.856 and 0.800 V respectively while sweeping the current density from OCV (0 mA/cm^2) to 100 and 400 mA/cm^2; whereas the hydrocarbon based membrane S-0/Cs^+/H^+ gave 0.998, 0.826 and 0.697 V and finally the S-15/Cs^+/H^+ cell gave 1.000, 0.830 and 0.720 V for the same respective current

densities. In comparison to performance done earlier by Jiang et al. on a 25 μm, 51% DS SPEEK (SPEEK-51) membrane, voltages of 0.95, 0.77 and 0.72 V were reported for OCV, 200 and 400 mA/cm^2.[17] The SPEEK and SPEEK composite performance at higher current densities was visibly much poorer than the 1100 EW Nafion® membrane. The high resistance of low sulfonation PEEK membranes is well known, due to their narrow dead end channels which restrict proton conductivity.[17] The S-15/Cs^+/H^+ showed a lower average membrane resistance of 0.152 Ω cm^2, compared to 0.193 Ω cm^2 for the non-PTA-containing S-0/Cs^+/H^+ cell. The reported resistance of the SPEEK-51 membrane was 0.084 Ω cm^2, which is in good accordance with its thickness being half that of the S-0/Cs^+/H^+ membrane used in this study.

After testing at 80 °C was complete, cell temperature was increased to 100 °C, while anode and cathode gases were humidified to obtain 69% RH (vapor saturated gases were heated to 90 °C). Figures 18 and 19 were generated based on the polarization data obtained. The lowering of the cell RH at 100 °C increased the average resistance of the hydrocarbon membranes to almost 4 times higher than that measured at 80 °C. Addition of PTA to the SPEEK membrane lowered resistance by almost half, from 0.822 to 0.492 Ω cm^2. The apparent lowering of resistance is not related to the bulk conductivity of the electrolyte, but rather the contact resistance between the electrolyte and the electrodes.

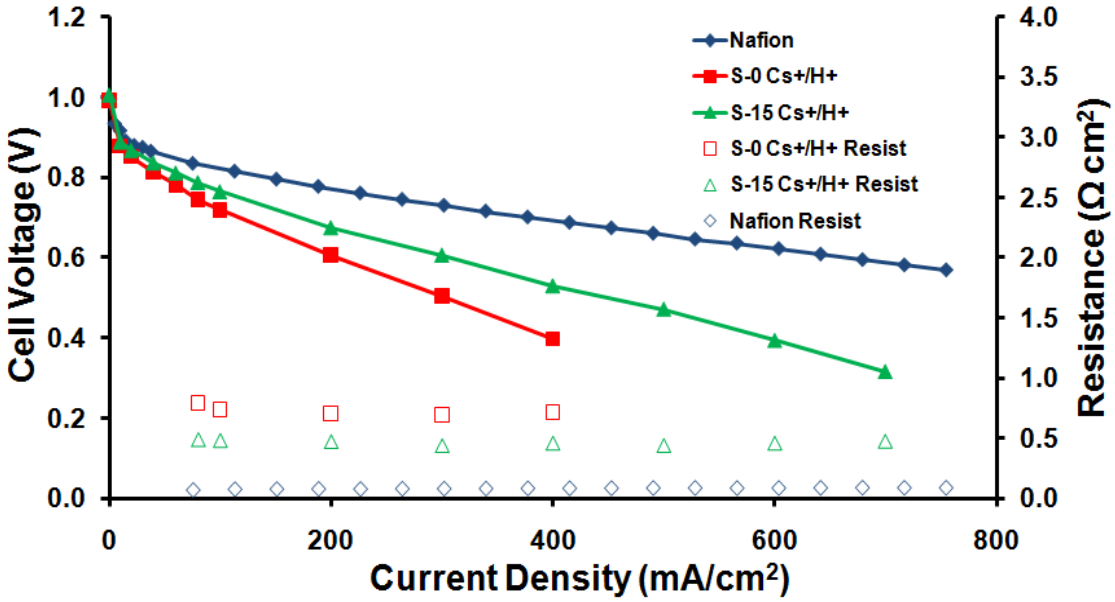

Figure 18. PEM fuel cell performance of various MEAs performed in a H_2/O_2 cell at 100 °C with anode/cathode gases humidified to 69% RH.

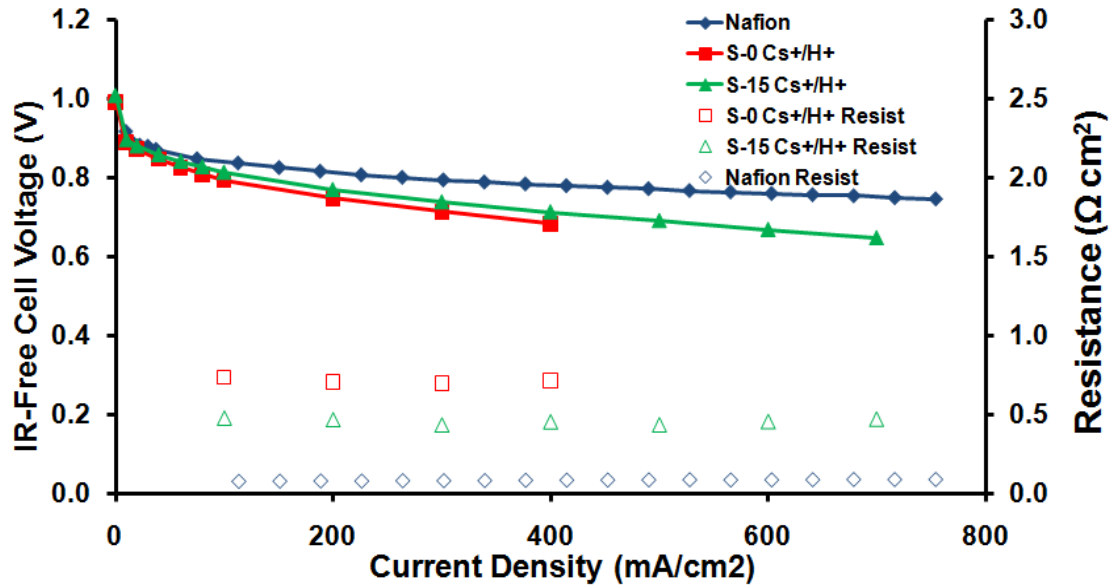

Figure 19. IR-Free voltage PEM fuel cell performance of various MEAs performed in a H_2/O_2 cell at 100 °C with anode/cathode gases humidified to 69% RH.

The current interrupt method measures the total ohmic resistance of the cell and does not differentiate between the various contributions. The use of perfluorocarbon Nafion® as catalyst binder is required to obtain high catalytic activity toward H_2 oxidation and O_2 reduction in the respective electrode layers. However, the interfaces between the mostly hydrocarbon SPEEK electrolyte and the mostly fluorocarbon electrocatalyst layers constitute a significant portion of the total voltage drop across the cell. The presence of PTA apparently serves to alter the surface morphology of SPEEK during casting and/or that of the catalyst layer during spray application, so that the interfacial resistance after wetting up is lessened. This effect is under further study.

Figure 19 shows the cell resistance-compensated voltages as measured using the current interrupt method. All membranes showed very similar IR-free performance in the activation-controlled region (0-100 mA/cm^2). Even with the IR-corrected voltages, the Nafion® outperformed the SPEEK analogues at high current densities (100-700 mA/cm^2). The lower RH not only increased membrane resistance, but also dried out the electrode layer and decreased the effective catalyst utilization. Dry electrodes have been shown to have lower oxygen permeability compared to their fully hydrated analogues.[18] The addition of PTA has given the composite S-15/Cs^+/H^+ membrane more acid sites to which protons can be transmitted through the SPEEK membrane with low degrees of sulfonation. It is thus expected that the resistance of these membranes can be lowered even further if a proton-conducting material can: 1) retain a high level of hydration under low relative humidity conditions, 2) exhibit high proton conductivity and 3) avoid leaching or dissolution while being subjected to long term operation under PEM fuel cell conditions.

Hydrogen fuel cross-over was also measured by linear sweep voltammetry experiments using the limiting current method. The cross-over rate can account for potential losses due to hydrogen diffusing from the anode, through the membrane and into the cathode compartment. If the cross-over rate is high, cell voltage short-circuits and increased membrane degradation will lower cell performance and fuel/oxidant utilization substantially. Figure 20 shows the cross-over measured at 25 °C, prior to and post PEM fuel cell performance testing, for a 50 µm S-0/Cs^+/H^+ membrane with electrodes made from Pt-Co/C in a Nafion® binder.

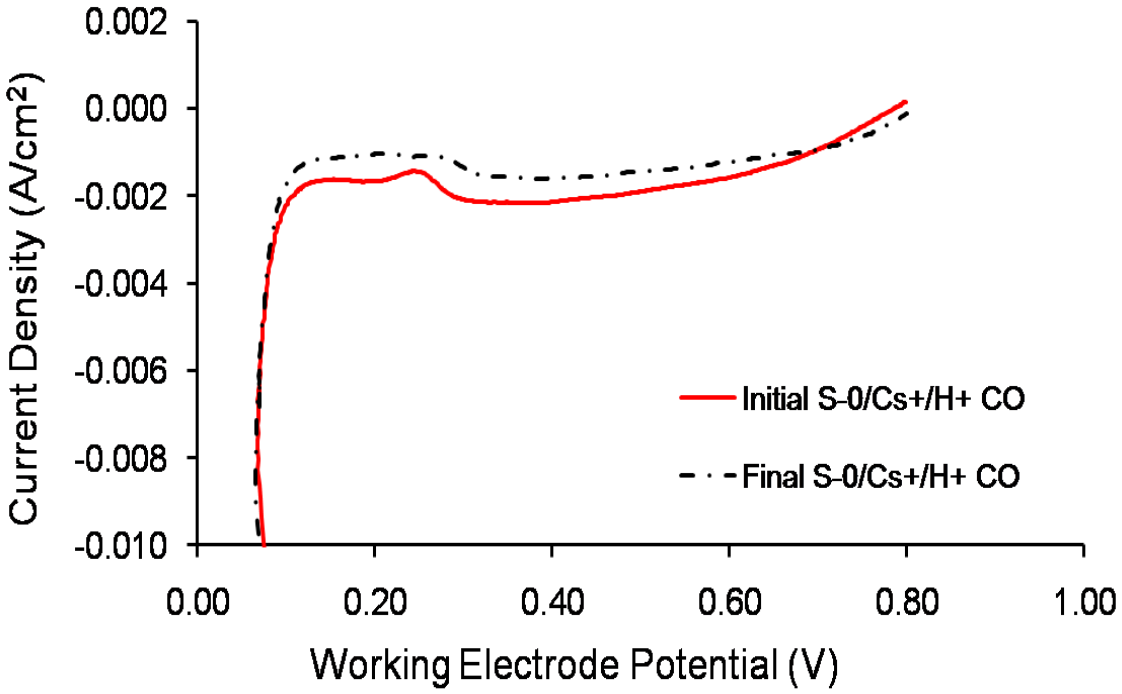

Figure 20. Hydrogen cross-over measured by linear sweep voltammetry of the S-0/Cs^+/H^+ membrane performed at 25 °C (cell, anode and cathode) before and after performance testing at 80 and 100 °C.

The difference in fuel cross-over current before and after fuel cell testing was negligible. This was understood to indicate the absence of direct channels/holes through

the MEA, as well as structural robustness of low DS SPEEK. The negative currents measured were thought to be due to low 10 to 100 ppm levels of oxygen in the ultra-high purity nitrogen gas stream.

Conclusion

While it was shown that PTA could be incorporated into SPEEK membrane and largely stabilized via exposure to Cs salts, the solid acid gave no improvement in membrane conductivity at low water vapor pressure. This was attributed to the finding that PTA, precipitated from DMF/ethanol and exchanged with cesium ion, does not show any significant ability to bind or uptake waters of hydration that would facilitate the conduction of protons. Nevertheless, PTA/SPEEK membranes incorporated into an MEA and tested in a fuel cell gave better performance than did SPEEK itself. This suggests that the stabilized Cs-PTA is able to lower membrane-electrode interfacial resistance at least at in the temperature range of 80 to 100 $^{\circ}$C. Further work is being carried out in order to fully immobilize PTA, with and without Cs^{+} ion stabilization, and better understand its role in the interfacial kinetics of PEM fuel cell operation.

References

1. Deveaux, J., Delimoy, D., Daoust, D., Legras, R., Mercier, P., Strazielle, C. and Nield, E., On the molecular weight determination of a poly(aryl-ether-ether-ketone) (PEEK) *Polymer,* 26, (1985), 1994-2000.
2. Hickner, M. A., Ghassemi, H., Kim, Y. S., Einsla B. R., Mcgrath, J. E, Alternative polymer systems for proton exchange membranes (PEMs), *Chem. Rev.*, 104 (2004), 4587.
3. Brown, G. M., Noe-Sprilet, M. R., Busing, W. R., Levy, H. A., Dodecatungstophosphoric acid hexahydrate, $(H_5O_2^+)_3(PW_{12}O_{40}^{3-})$. The true structure of Keggins 'pentahydrate' from single-crystal X-ray and neutron diffraction data, *Acta Cryst.*, B33, (1977), 1038.
4. Ramani, V., Swier, S., Shaw, M. T., Weiss, R. A., Kunz, H. R., Fenton, J. M., Membranes and MEAs based on sulfonated poly(ether ketone ketone) and heteropolyacids for polymer electrolyte fuel cells, *J. Electrochem. Soc.*, 155, (2008), B532-B537.
5. Ponce, M. L., de A. Prado, L. A. S., Silva, V., Nunes, S. P., Membranes for direct methanol fuel cell based on modified heteropolyacids, *Desalination,* 162, (2004), 383.
6. Rocchiccioli-Deltcheff, C., Fournier, M., Franck, R., Vibrational investigations of polyoxometalates. 2. Evidence for anion-anion interactions in molybdenum (VI) and tungsten (VI) compounds related to the Keggin structure, *Inorg. Chem*., 22, (1983), 207.

7. Kreuer, K. D., Proton conductivity: Materials and applications, *Chem. Mater.*, 8, (1996), 610.

8. Kreuer, K. D., Proton transport in some heteropolyacid hydrates a single crystal PFG-NMR and conductivity study, *Solid Sate Ionics*, 28-30 (1988), 589.

9. England, W. A., Cross, M. G., Hamnett, A., Wiseman, P. J., Goodenough, J. B., *Solid State Ionics*, 1, (1980), 231.

10. Janik, M. and Davis, R. J., Anhydrous and water assisted proton mobility in phosphotungstic acid, *J. Am. Chem. Soc.*, 127, (2005), 5238.

11. Shoukry, A. F., Maraffie, H. M., El-Shatti, L. A., X-Ray photoelectron spectroscopy and electron microscopy of hydralazinium ion-selective electrode membrane's surface, *Electroanalysis*, 18, (2006), 7795.

12. Feng, W., Ding, Y., Liu Y., Lu, R., The photochromic process of polyoxometalate-based nano-composite thin film by in situ AFM and spectroscopy, *Materials Chem. and Phys*., 98, (2006), 347.

13. Liu, L., Chen, Z. X., Liu, S. Z., Zhang, H., Studies on the preparation, characterization and catalytic activity of the nano-solid heteropolyacid $H_3PW_{12}O_{40}/SiO_2$ using the sol-gel method, *Aust. J. Chem.*, 54 (2001), 299.

14. Lingane, J. J., Small, L. A., Polarography of the various oxidation states of tungsten, *J. Am. Chem. Soc.*, 71, (1949), 973.

15. Kulesza, P. J., Faulkner, L. R., Electrocatalysis at a novel electrode coating of non-stoichiometric tungsten(VI,V) oxide aggregates, *J. Am. Chem. Soc*., 110, (1988), 4905.

16. Kaba, M. S., Song, I. K., Barteau, M. A., Investigation of framework and cation substitutions in Keggin-type heteropolyacids probed by scanning tunneling microscopy and tunneling spectroscopy, *J. Vac. Sci. Technol. A*, 15, (1997), 1299.

17. Jiang, R., Kunz, H. R., Fenton, J. M., Investigation of membrane property and fuel cell behaviour with sulfonated poly(etheretherketone) electrolyte: Temperature and relative huidity effects, *J. Power Sources* 150, (2005), 120.

18. Broka, K., Ekdunge, P., Oxygen and hydrogen permeation properties and water uptake of Nafion® 117 membrane and recast film for PEM fuel cell, *J. Appl. Electrochem.* 27, (1997), 117.

CHAPTER 4. HIGHLY SULFONATED CROSS-LINKED SPEEK MEMBRANES

Preparation of High Degree of Sulfonation PEEK

Sulfonation of 450 pf PEEK was successfully done using 96% H2SO4 to achieve SPEEK-96 in 95% yield after purification. Electrophillic aromatic sulfonation of PEEK has second order kinetics, with the reaction taking place at the electron-rich aromatic ring flanked by two ether linkages. The electron-attracting nature of the carbonyl group between the two other aromatic rings in the repeat unit causes the aromatic sites to be unreactive toward sulfonation. This tends to limit the number of sulfonic acid groups per monomer to one per repeating monomer unit, or 100% DS. DS and rate of sulfonation can be controlled by changing the reaction temperature, time, and acid concentration. A high DS is achieved by utilizing long reaction times and preferably strong H2SO4 concentrations. It was reported elsewhere that sulfonation of PEEK with chlorosulfonic acid or fuming sulfuric acid has caused cross-linking and degradation, during respective procedures.1 However, it was assumed that these side reactions were avoided by using H2SO4 as the sulfonation reagent. In a hydrated state, PEEK polymer sulfonated by this method was orange in color, but became a deep red after drying. Determination of SPEEK's DS is most commonly done by titration of the dried polymer. DS measurements using nuclear magnetic resonance (1H NMR) and TGA were not done, as they predict inaccurate DS.2,3 Placing the dried SPEEK in a saturated NaCl solution overnight has the effect of exchanging all sulfonate protons with Na+; with the equivalence point measured using phenolphthalein indicator, as well as

potentiometrically. Soaking times longer than 24 hours did not significantly affect the results. PEEK membranes sulfonated by this method had a DS of 96%, and as mentioned before, will be denoted SPEEK-96. This DS corresponds to an EW and IEC of 381 g/ eq and 2.62 meq/ g respectively.

Cross-linking Mechanism

Friedel-Crafts cross-linking of high sulfonation PEEK polymers was investigated using BDM, an aromatic bis(hydroxymethyl) compound. The idea of utilizing high temperatures (> 150 $^{\circ}$C) for cross-linking of polymers with aromatic backbone structures has been adopted by many.[4,5,6,7,8] Cross-linking by such methods may produce polymer chains with increased chemical, thermal and mechanical properties. It was hypothesized that condensation of the hydroxyl groups on BDM with the aromatic protons on the SPEEK polymer backbone would form characteristically strong covalent bonds, especially for highly conjugated systems.[9]

The synthetic mechanism assumed for cross-linking is shown in Figure 21. The Friedel-Crafts catalyst $ZnCl_2$ acts as a Lewis acid by accepting an electron pair present on a BDM hydroxyl radical, thereby initiating the reaction. The BDM carbocation produced reacts readily with an electron rich aromatic ring on the SPEEK backbone. The sulfonic acid-substituted aromatic rings are not expected to take part in the cross-linking reaction, as sulfonic acid groups are very deactivating towards electrophilic aromatic substitution reactions. Due to their highly electron withdrawing nature, sulfonic acid groups are very deactivating towards electrophillic aromatic reactions. There still remain two non-sulfonated aromatic rings per monomer unit, however, which may react to produce the

insoluble cross-linked SPEEK polymer. The reaction is repeated on another monomer of a SPEEK polymer chain, with subsequent regeneration of the $ZnCl_2$ catalyst and the evolution of water.

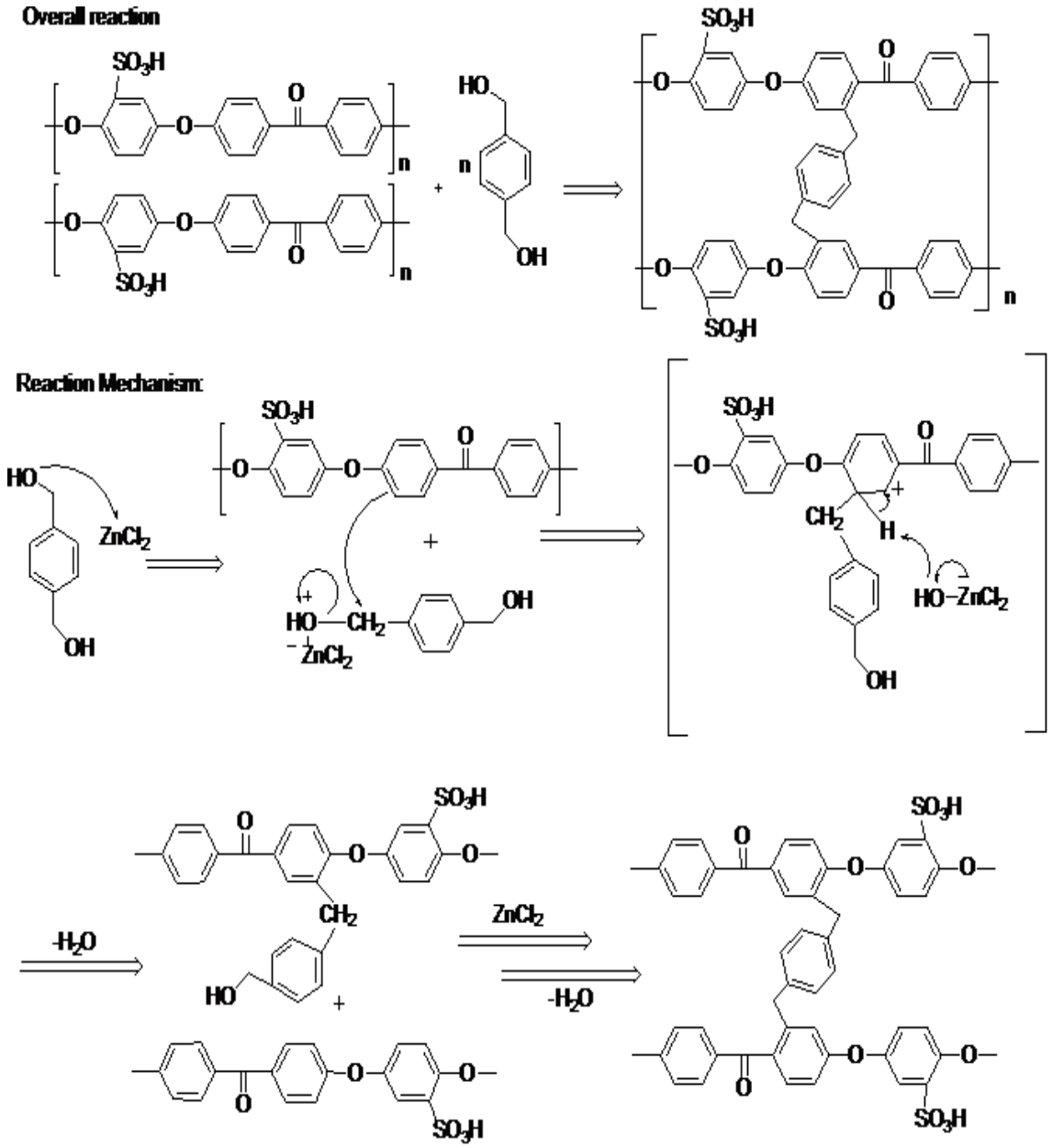

Figure 21. Detailing the mechanism of $ZnCl_2$ catalyzed cross-linking of SPEEK chains with benzenedimethanol.

The main step in the cross-linking procedure is the 200 °C temperature treatment; this affects the solid state reaction. To obtain maximum yield, a large excess of $ZnCl_2$ was added to provide an excess of Friedel-Crafts active catalytic sites. The solubility of $ZnCl_2$ in H_2O and various alcoholic solvents is well known, and as such the as-cross-linked product was washed with DI H_2O until the chloride concentration in solution was deemed to be in the parts per billion range by ion chromatography measurements. Recently Kaliaguine et al. have demonstrated how the membrane-casting solvent may hinder cross-linking of SPEEK polymers with polyatomic alcohols.[10] Solvents such as DMF and DMAc may cause side reactions, block reactants from effectively reacting together, and lower proton mobility by blocking the hydrophilic channels from effectively adsorbing H_2O.[11] All reactants used were also highly soluble in warm H_2O, and hence the latter-mentioned solvent related problems were avoided.

A solid state condensation reaction between the sulfonic acid of SPEEK polymer and the hydroxyl moiety of the alcohol used can form sulfonic acid ester linkages.[12,13,14] These linkages bind the SPEEK polymer chains to the polyatomic alcohol used, effectively lowering the DS of the SPEEK. From this work, it was inferred that a poly-functionalized alcohol may be employed to create an extensive network of cross-links. Polymers produced in this manner have increased mechanical and chemical stability, and lowered swelling in solvents for all cases. However, it is difficult to properly characterize the reaction mechanism/cross-linked product, due to its high chemical stability.

The 200 °C heat treatment resulted in a color change from clear yellow films to dark brown, with a decrease in membrane solubility. This color change, was indicative

of completion of the cross-linking, as membranes heated at lower temperatures were lighter in color, and the products did not show any chemical resistance and/or increased mechanical strength. Evaporation of the BDM, especially at the surface, is highly likely due to its lower 150 $^{\circ}$C boiling point. However, the evaporation process is thought to be mitigated by the SPEEK polymer. That is, hydrogen bonding probably occurs between polar sulfonic acid and hydroxymethyl groups present on the SPEEK and BDM respectively. Determination of the total BDM reacted was achieved by calculating the ratio of peak areas under the SPEEK carbonyl stretch to BDM alkyl stretching bands on the FTIR spectra, before and after heat treating at 200 $^{\circ}$C (X-24-SPEEK-96 shown in Figure 23-2). The ratio correlated to a 50% loss in BDM from the membrane surface after heat treating.

A comparison of EW determinations for SPEEK-96 and cross-linked products containing various BDM amounts is listed in Table 11. The relatively small decrease in IEC was concluded to be due to a Friedel-Crafts mechanism on the SPEEK aromatic chain and not sulfonate-ester cross-linkage formation. The increase in mass by adding the BDM to SPEEK is expected to decrease the IEC, i.e. a lower sulfonic acid group per unit mass ratio. Determination of the cross-link positions and their substitution patterns on the SPEEK backbone is of much interest. Conventional methods such as FTIR, ^{1}H-NMR and ^{13}C-NMR were either inconclusive due to the insolubility of the membranes in any common solvent or lack of any significant change in the peaks. Membrane characterization was accomplished by EW, FTIR, TGA and WU measurements.

SPEEK-96 polymers cross-linked with 6 wt% or less BDM (X-6-SPEEK-96) had low levels of cross-linking and demonstrated high swelling in H_2O and poor mechanical

properties, in comparison with the X-12-SPEEK-96 and X-24-SPEEK-96 membranes. Notwithstanding, the X-6-SPEEK-96 polymer was characterized given its low degree of cross-linking.

Determining the extent to which BDM cross-linking of SPEEK-96 alters the properties in comparison to its pure SPEEK precursor will be explained in the coming sections.

Water Uptake and Solubility Properties

The high saturation point and temperatures necessary for fuel cell durability is known to alter the membrane hydration state and dimensional stability. These two properties were studied by comparing the membranes' WU and IEC, as shown in Table 11**Table 11**.

Table 11. IEC, water uptake and λ_{max} of cross-linked and a non-cross-linked SPEEK-96 membranes

Sample	**IEC (meq/g)**	**Water uptake (%)**			**λ_{max}**
		25 °C	80 °C	100 °C	
SPEEK-96	2.62	700[a]	∞	∞	148
X-6-SPEEK-96	2.56	550	640	638	138
X-12-SPEEK-96	2.53	179	228	214	47
X-24-SPEEK-96	2.40	69	99	96	22

[a]Used to calculate λ_{max} for highly swollen SPEEK-96 membrane

Decreasing WU for cross-linked membranes was in the order X-6-SPEEK-96, X-12-SPEEK-96 and finally X-24-SPEEK-96. Pure SPEEK membranes were highly swollen in H_2O at room temperature, and dissolved at elevated temperature. Membranes

of DS 70% or above are known to swell excessively and lose their mechanical toughness.[15] The SPEEK-96 polymer had an IEC of 2.62 meq/g, which was nominally higher compared to the 2.53 meq/g determined for the X-12-SPEEK-96 membrane. The X-24-SPEEK-96 membrane had 2.4 meq of protons per gram of polymer, only a slight decrease when compared to SPEEK-96, even though the chemical and physical properties imparted to this highly cross-linked SPEEK polymer are substantially different. These rather small decreases in IEC would lead one to infer that the cross-links formed do not remove sulfonic acid functionality via sulfonate ester linkage formation, as was previously reported.[11]

The solubility of the cross-linked polymer was investigated using some common solvents: acetone, DMF, DMAc, and H_2O. SPEEK-96 dissolved readily in room temperature and 60 $^{\circ}$C DMF and DMAc, and boiling water; with the polymer showing high swelling in room temperature H_2O. X-6-SPEEK-96 swelled heavily in boiling DMF, DMAc and H_2O, with a simultaneous reduction in mechanical strength. This was conclusive evidence for low levels of cross-linking in the X-6-SPEEK-96 polymer.

The SPEEK-96 membranes cross-linked with 12% or 24% BDM had higher levels of cross-linkages and showed no loss of weight or mechanical stability while boiling in any of the listed solvents. Heating these membranes in concentrated sulfuric acid caused negligible change in the polymers' mass and physical appearance. Membranes exhibiting properties such as these are known to be good candidates for hydrogen PEM fuel cell applications.[16,17]

FTIR Analysis

FTIR spectra of the neat PEEK, SPEEK-96 and X-SPEEK-96 membranes with varying cross-linker amounts were evaluated for the presence of the cross-linker BDM. Representative transmittance peaks for PEEK and 96% sulfonated PEEK are shown in Figure 22, Figure 23-1 and 23-2, showing increasing percent transmittance (% T) of the alkyl stretches expected from the addition of BDM in X-SPEEK-96 membranes.

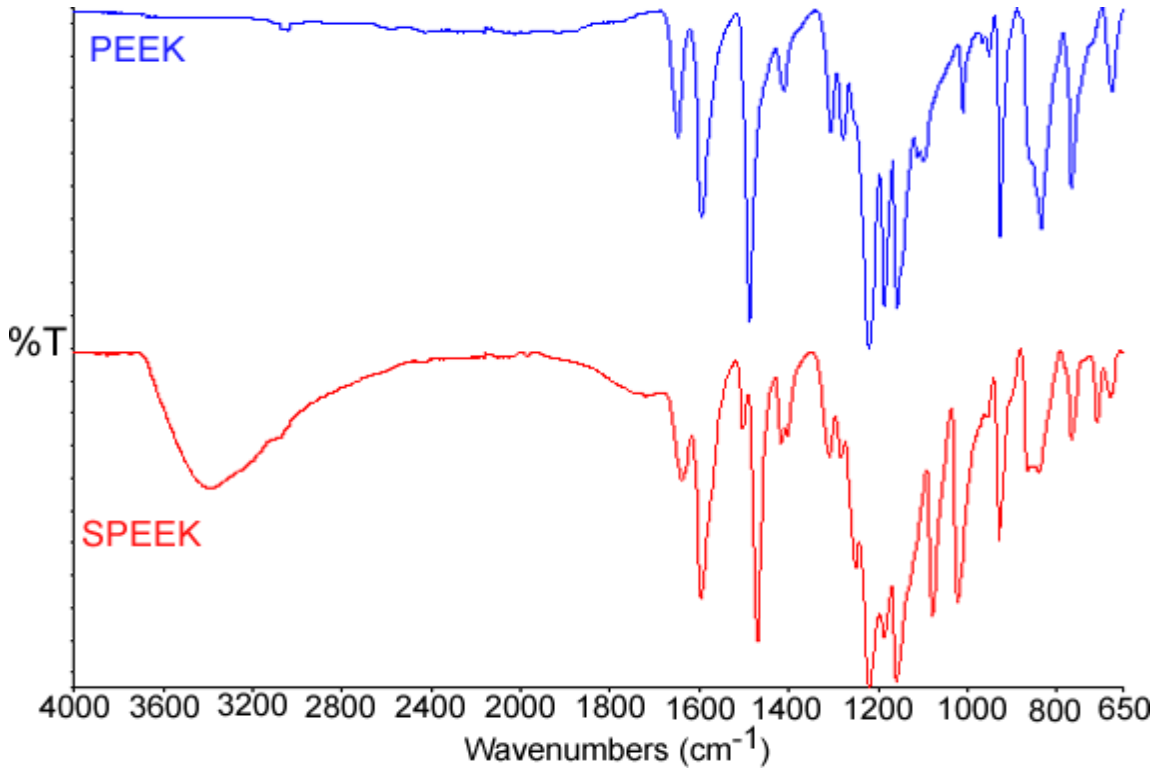

Figure 22. FTIR evidence of electrophilic aromatic sulfonation reaction: PEEK (Blue) and SPEEK-96 (Red).

PEEK shows several distinct IR-active bands at: 1659, 1599, 1290, 1230, 1186, 930 and 865 cm^{-1}, which correspond to symmetrical stretching of carbonyl, in-plane aromatic C=C stretching, asymmetrical stretching of Ph-CO-Ph, asymmetric stretching of diphenyl ether groups, in-plane bending of aromatic hydrogens, symmetric stretching of

Ph-CO-Ph and finally the out of plane bending of aromatic hydrogens, respectively.[18] After sulfonation, bands associated with asymmetric and symmetric stretching of the sulfonic acid groups appear at 1020, 1080 and 1255 cm^{-1}.[19,20]

Comparative ATR-FTIR split-spectra of pure BDM and cross-linked SPEEK-96 membranes containing 0, 6, 12 and 24 wt% of BDM are illustrated in Figure 23. The highlighted alkyl stretches at 2915 and 2850 cm^{-1} indicate the presence of aliphatic/benzylic C-H stretching and bending, and the highlighted peak at 825 cm^{-1}, representative of 1,2,4-trisubstitution on the SPEEK backbone aromatic rings.[21] The peak area ratio of alkyl to carbonyl bands for both 12 and 24 wt% BDM cross-linked SPEEK-96 membranes corresponds well to the BDM mass fraction contained in each. The alkyl stretching bands of the as-cast X-24-SPEEK-96 membrane before 200 $^{\circ}C$ heat treatment were increased in comparison to that of the heat treated X-24-SPEEK-96 (Figure 23-2), while the transmittance peaks which correspond to the X-6-SPEEK-96 and X-12-SPEEK-96 benzylic C-H bands were barely discernible.

From this evidence it was concluded that a small mass fraction of BDM is lost by evaporation during the heat treatment of the X-24-SPEEK-96 polymer. However, the changes in cross-linker content of un-heat-treated and heat-treated 6 and 12% membranes were inconclusive.

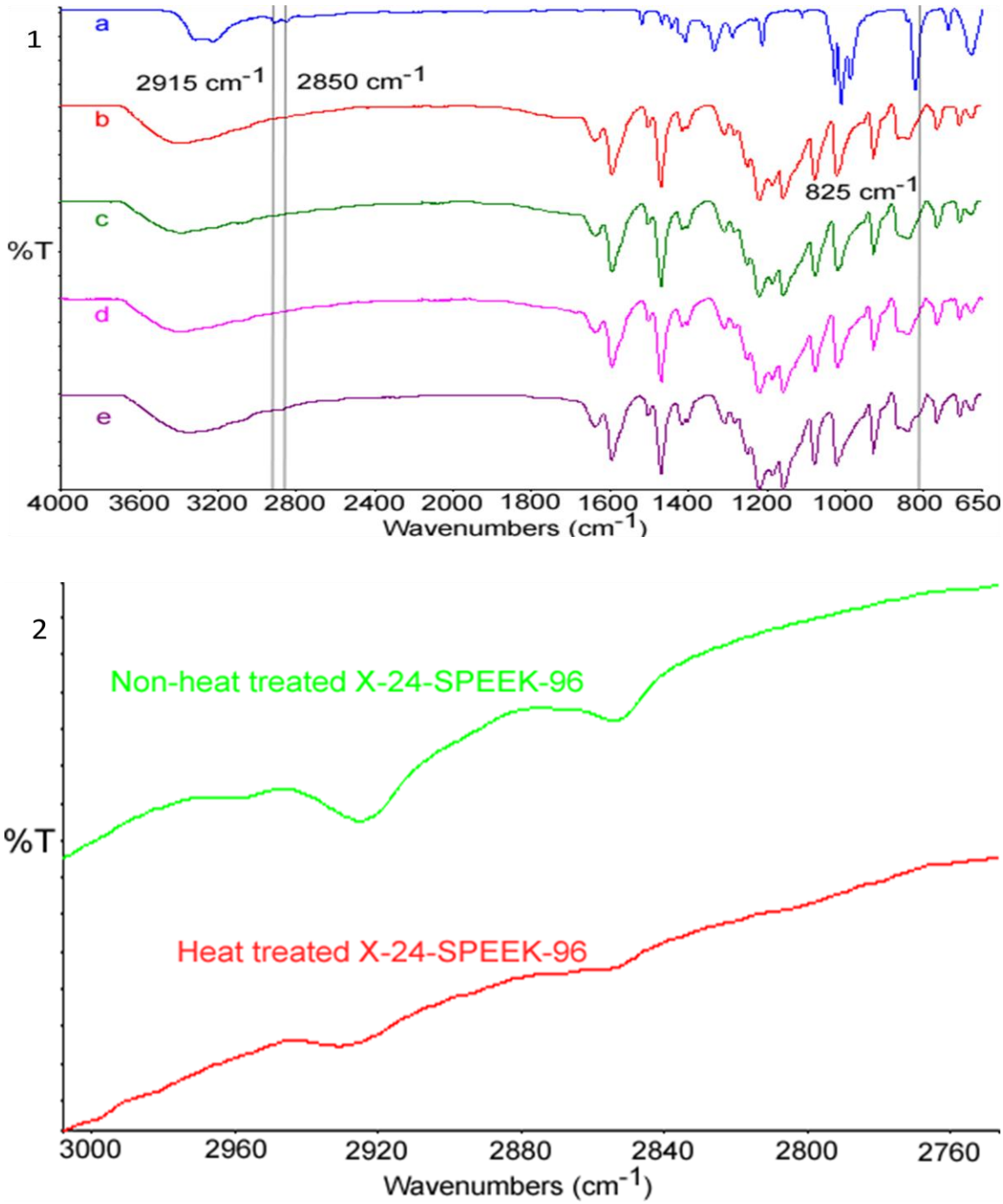

Figure 23 -1. FTIR Evidence of Friedel-Crafts cross-linking a) BDM, b) SPEEK-96, c) X-6-SPEEK-96, d)X-12-SPEEK-96 and e) X-24-SPEEK-96. **Figure 23 -2**. Comparison of peaks related to benzylic C-Hs before and after 200 ^{o}C heat treatment in X-24-SPEEK-96 polymer.

In-plane Membrane Conductivity

Measurement of PEM in-plane resistivity under flowing hydrogen gas has been used as a method of characterization. The inverse of resistivity is conductivity, which can be directly related to sulfonic acid group density, as well as the acid's ability to conduct protons. In-plane conductivity of SPEEK-96, X-12-SPEEK-96 and X-24-SPEEK-96 membranes were evaluated using the four-probe conductivity technique; the results are shown in Figure 24.

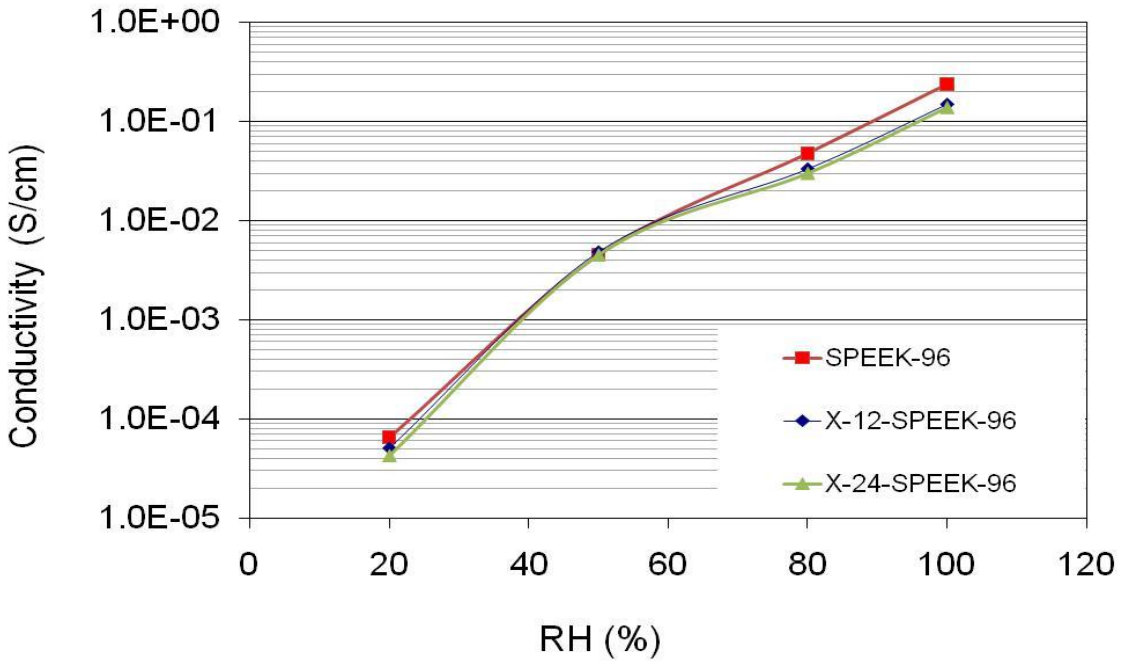

Figure 24. In-plane conductivity of SPEEK-96, X-12-SPEEK-96 and X-24-SPEEK-96.

The proton conductivities of the three materials are quite similar over the sequence of relative humidity ranges tested: 80, 50, 20, 50, 80 and 100%. The SPEEK-96 membrane showed conductivity values slightly greater than that of its cross-linked

counterpart. This can be correlated to the lower EW of the former compared with the latter. At 100% RH, proton conductivity was at 0.2, 0.15 and 0.14 S/cm for SPEEK-96, X-12-SPEEK-96 and X-24-SPEEK-96, respectively. Below the saturation point, the SPEEK-96 and cross-linked SPEEK-96 samples showed similar order of magnitude decreases in proton conductivity. The measured proton conductivities were: 4.89×10^{-2}, 2.23×10^{-3} and 6.56×10^{-5} S/cm for the SPEEK-96 polymer, while the X-12-SPEEK-96 membrane showed 3.10×10^{-2}, 1.87×10^{-3} and 5.06×10^{-5} S/cm for 80, 50 and 20% RH, respectively. The X-24-SPEEK-96 membrane followed a similar trend. The significant loss in conductivity at low RHs for all hydrocarbon membranes is purely dependent on the amount of H_2O beyond the primary and secondary hydration spheres.[22] The effect of the cross-linker in this case is two-fold: it forms cross-links to stabilize the polymer against dissolution, but also increases the hydrophobic non proton-conductive domain. Introducing the nonconductive hydrophobic BDM molecules has the effect of decreasing sulfonic acid density within SPEEK, increasing the energy needed for a proton to 'hop' from one acid site to another. The BDM cross-links between the SPEEK polymer chains lowers the volume compared to the pure polymer for WU within the polymer matrix. This is also reflected in the decreased WU of the X-24-SPEEK-96 polymer comparatively to the X-12-SPEEK-96 and pure SPEEK-96 membranes (Table 11). By increasing the proportion of cross-linker to SPEEK polymer, an insoluble polymer demonstrating a highly hydrophobic nature can be produced. Based on this, it is expected that cross-linking by this method should integrate high dimensional stability in PEEK polymers sulfonated to 90% DS or higher.

It would be advantageous to operate a PEM fuel cell above 100 °C, and so it is desirable that membrane degradation could be mitigated under high temperature conditions.

PEEK and SPEEK Membrane Thermal Properties

Thermogravimetric and Differential Thermal Analyses

Under Helium

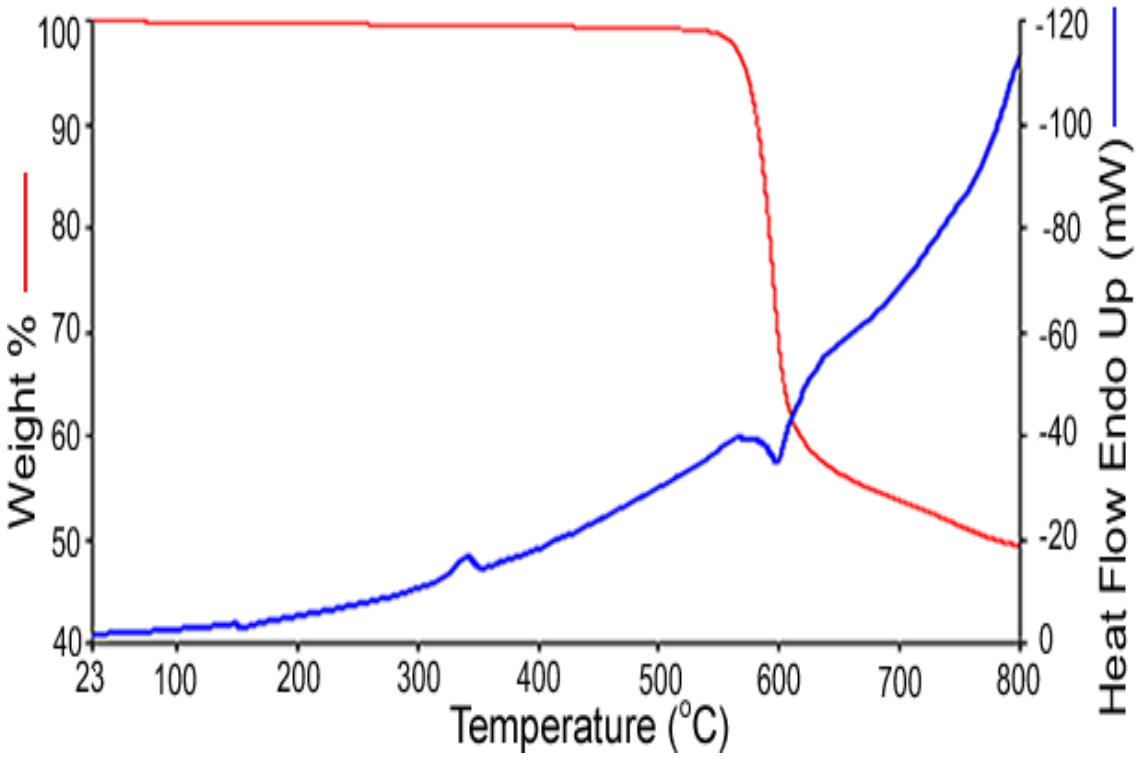

Figure 25. Thermogravimetric analysis of 450pf PEEK under flowing helium measured from 23 to 800 °C at 20 °C/min.

Thermogravimetric analysis of 450pf PEEK powder was done from 23 to 800 °C at 20 °C/min; this is illustrated in Figure 25. The thermogram was similar to that obtained

by Mikhailenko et al., where a T_g value of ~150 °C and a melting temperature of 350 °C were observed.[2] Decomposition of the PEEK began at 500 °C; this property makes the unsulfonated polymer fit for numerous high temperature applications.[23]

Table 12. Summary of thermogravimetric coupled mass spectroscopy experiments.

Sample	23-200 °C		200 to 400 °C		400 to 600 °C	
	Weight loss (%)	Ions present (g/ mol)	Weight loss (%)	Ions present (g/ mol)	Weight loss (%)	Ions present (g/ mol)
SPEEK-96	7	18	18	18, 44, 48, 64	20	18, 44, 48, 64, 94, 168, 170
X-6-SPEEK-96	8	18	19	18, 44, 48, 64	19	18, 44, 94 106*, 168, 170
X-12-SPEEK-96	7	18	19	18, 44, 48, 64	20	18, 44, 94 106*, 168, 170
X-24-SPEEK-96	10	18	18	18, 44, 48, 64	21	18, 44, 94 106*, 168, 170

*evidence of cross-linker 1, 4-dimethyl benzene

Table 12 outlines the thermogravimetric weight losses, with corresponding weight losses occurring for all cross-linked and pure SPEEK-96 membranes. Results for SPEEK-96 are shown in Figure 26(a-c), and were found to be very similar to the work done by Arthanareeswaran et al.[24] Over the temperature range studied, there were four endotherms for SPEEK-96 with three mass losses. The initial 7 wt% mass loss between 23 to 200 °C corresponds to the evolution of H_2O vapor. This was followed by the evolution of CO_2 and sulfur monoxide and dioxide (two endotherms), with a corresponding weight loss of 18% between 200 and 400 °C. The detection of CO_2 has been previously correlated to free-radical decomposition of the polymer backbone.[25] Since sulfonic acid groups may form cluster regions of high acid density, some carbonyl groups may tend towards degradation quicker than others, based on their quantity and

proximity to a given desulfonation site.[26] A final 20% mass loss recorded from 400 to 600 °C was related to the onset of polymer backbone decomposition.

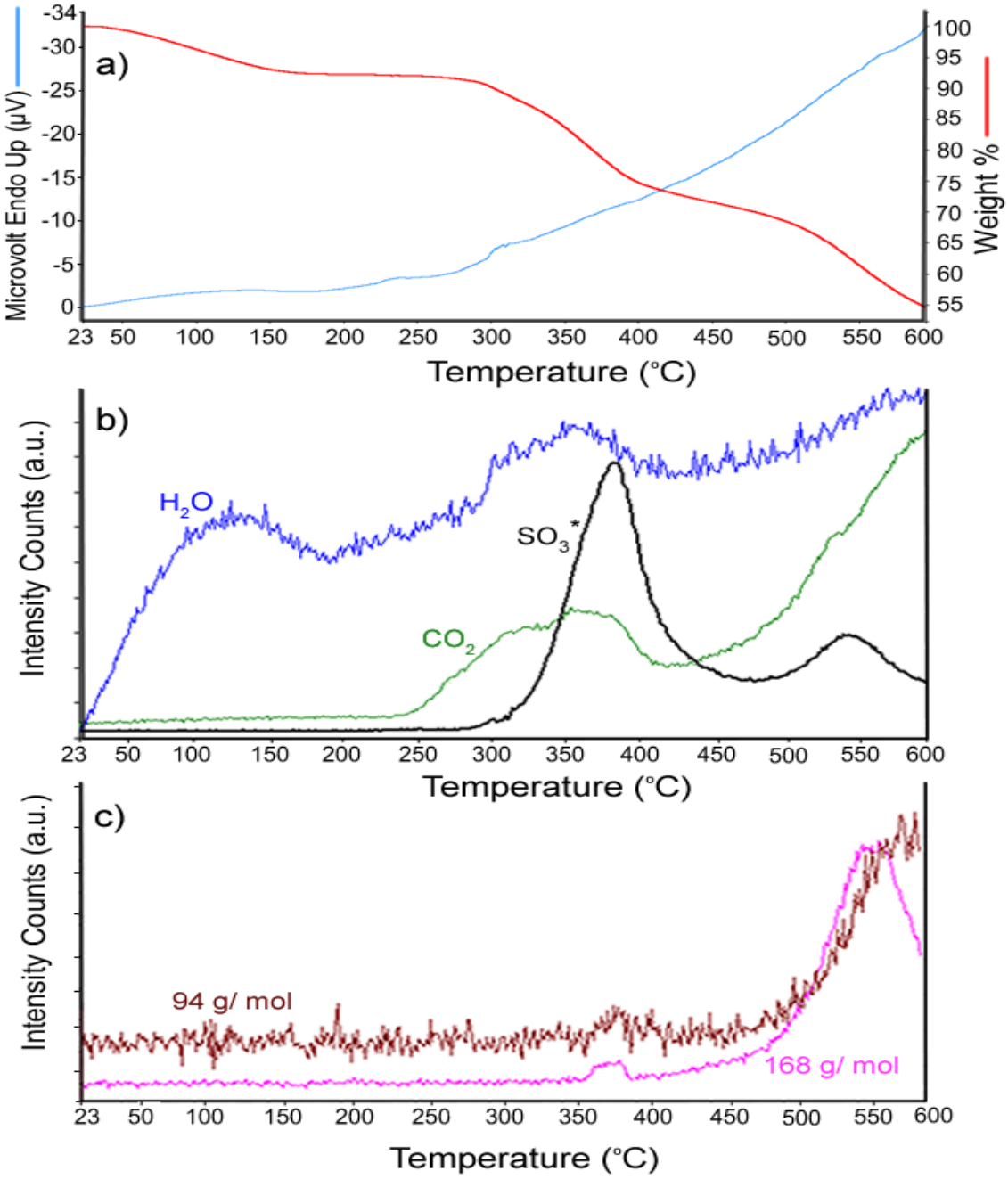

Figure 26. Thermogravimetric analysis of SPEEK-96 showing: a) thermogravimetric profile measured under flowing helium from 23 to 600 °C at 20 °C/min. b) Evolution of CO_2, H_2O and SO_3 (seen as SO_2 and SO^*). c) Detection of phenol (94 g/mol) and dibenzofuran (168 g/mol).

Phenol (94 g/mol), diphenylether (170 g/mol) and dibenzofuran (168 g/mol) were also detected at about 450 °C. Similar results were shown earlier by Kopitzke et al.[15] The fragments isolated by the TGA-MS are also in good agreement with the findings by Karasz and Mustafa.[27,28] Degradation is initialized within the aromatic rings associated with sulfonic acid groups; firstly scission of the sulfonic acid groups occurs, followed by random free-radical cleavage of the polymer chains. The formation of cyclic decomposition products such as dibenzofuran, occur due to a rearrangement on the polymer backbone. Termination of the free-radical degradation was thought to occur by recombination and/ or disproportionation of the polymer chains.

A representative TGA-MS of SPEEK cross-linked with BDM (X-12-SPEEK-96) is plotted in Figure 27(a-c). The cross-linked and non-cross-linked membranes had similar degradation products of H_2O, CO_2, SO, SO_2, phenol, diphenylether, and dibenzofuran over the temperature range studied. From 23 to 200 °C, an initial 7% weight loss due to bound H_2O was recorded. A weight loss of 19% was noted when the temperature was increased from 200 to 400 °C, with the MS recording CO_2, SO_2 and SO emissions. On increasing the temperature from 400 to 600 °C, the cross-linked membranes showed a new *m/z* ion at 106 g/ mol indicative of a 1, 4-dimethylbenzene-type compound.

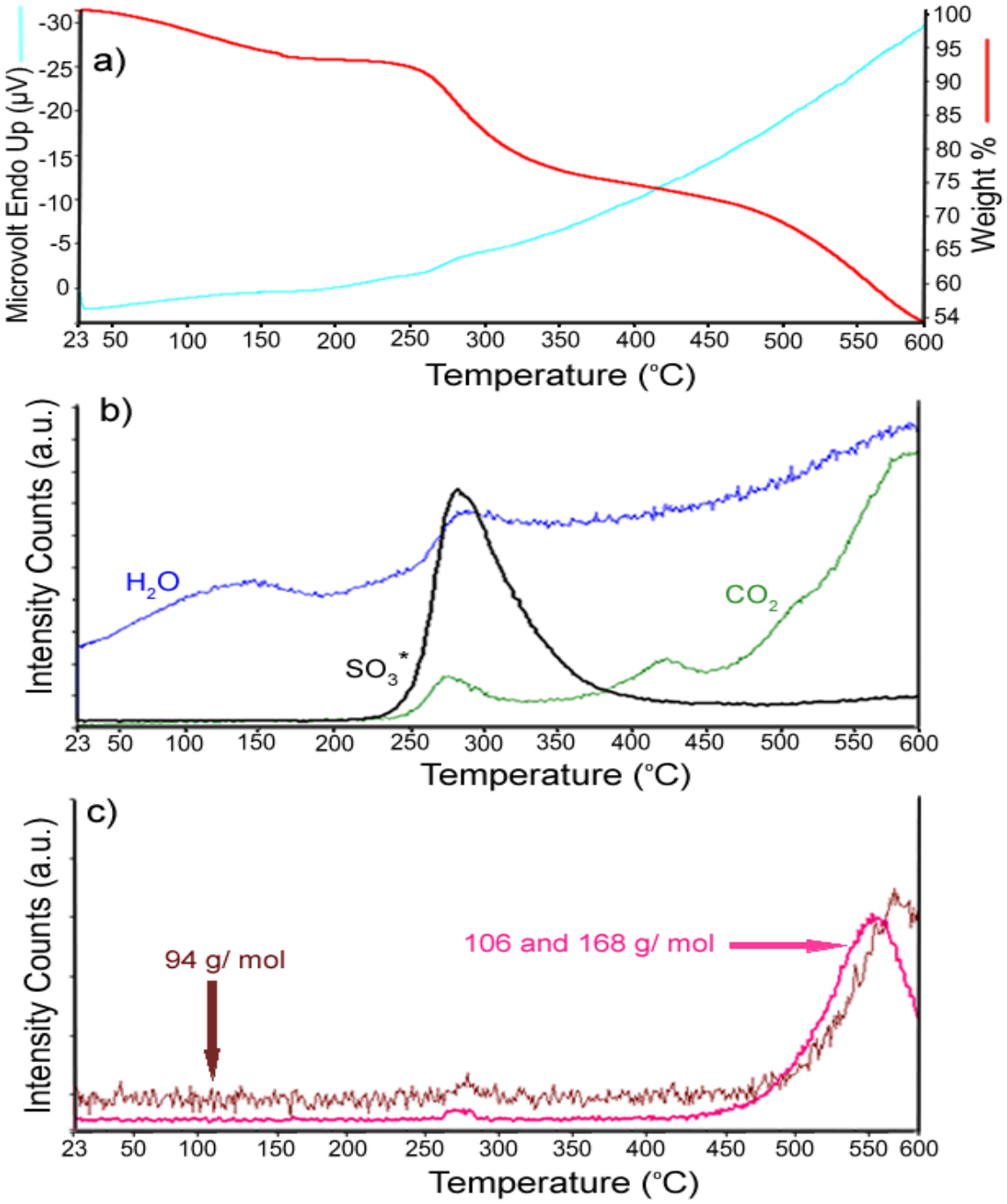

Figure 27. Thermogravimetric analysis of X-12-SPEEK-96 showing: a) thermogravimetric profile measured under flowing helium from 23 to 600 °C at 20 °C/min. b) Evolution of CO_2, H_2O and SO_3 (as SO_2 and SO^*). c) Detection of phenol (94 g/ mol), 1,4-dimethylbenzene (106 g/mol) and dibenzofuran (168 g/ mol).

Although the CO_2 is released at the same temperature, the desulfonation step for the cross-linked polymers occurs about 50 °C lower than for SPEEK-96. This may be due to the cross-linked polymer having a more inert backbone chain, which can effectively stabilize the free-radical ion formed after C-S bond breaking occurs. It is noteworthy that the energy required to break a C-C bond is higher than a C-S covalent bonds, at 348 and 259 kJ/mol respectively, so the detection of CO_2 is expected to occur later above 400 °C. However, the release of CO_2 has been thought to be a function of decomposition of the ketone groups.[27,18] Above 400 °C during the second degradation step shown in Figure 27c), m/z ratios of 168 and 94 g/mol representative of dibenzofuran and phenol were also discovered which when compared, are quite similar to SPEEK-96. However, an ion with an m/z of 106 g/mol was discovered and recognized as 1, 4-dimethylbenzene. This was believed to form the cross-links between the SPEEK chains (Figure 21).

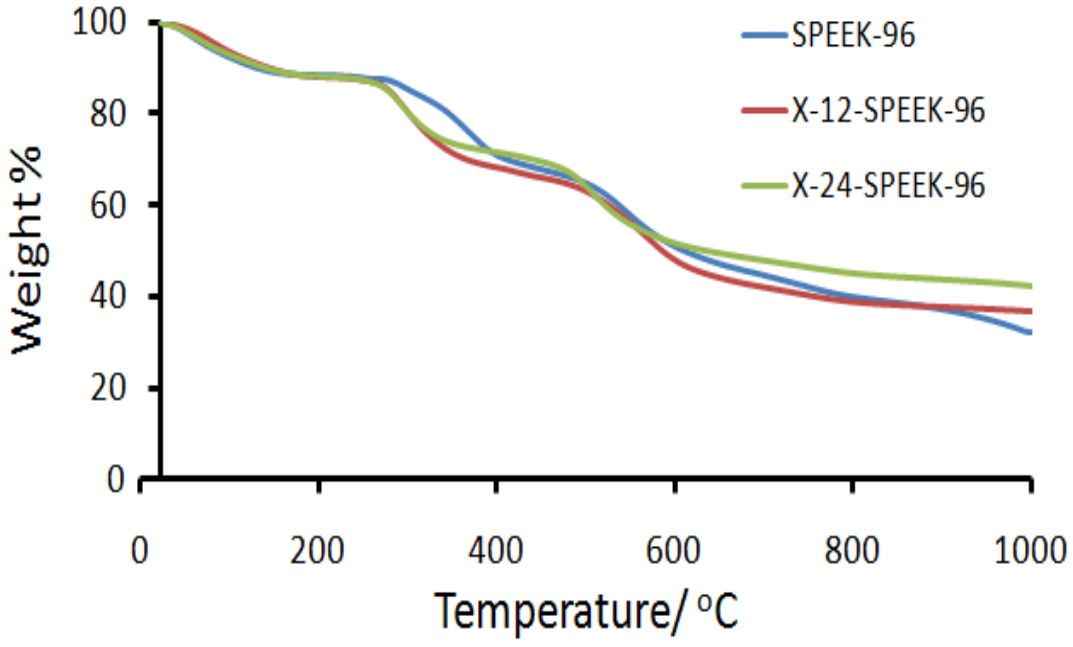

Figure 28. TGA comparison of SPEEK-96 and $ZnCl_2$ catalyzed cross-linked SPEEK-96 membranes under helium atmosphere, from 23 to 1000 °C at 20 °C/ min.

The TGA weight loss below 600 °C of each polymer, especially the cross-linked polymers, did not correlate well with what was expected based on the amount of cross-linker added. These results are shown in Figure 28. This may be due to the polymers being in a higher hydration state compared to the pristine SPEEK-96. The maximum temperature of the experiment was thus increased to 1000 °C to determine the polymer stabilities. Weight percents of 32, 36 and 42% char remained respectively for SPEEK-96, X-12-SPEEK-96 and X-24-SPEEK-96. Based on these results, the char yield is directly indicative of a trend between the amount of BDM additive, and the decomposition of these polymers.

Under Air

TGA of the polymers was also studied under flowing air. Figure 29 illustrates a TGA taken of 450 pf PEEK from 23 to 800 °C. From room temperature to 500 °C there was a 2 % weight loss, possibly due to absorbed water.[29] Under air, the PEEK polymer chain begins decomposing at 500 °C, in comparison with 550 °C under helium atmosphere. Total thermolysis of PEEK occurs at about 715 °C, with 0 wt% residue left, while there was 50% residue for the sample thermolyzed in the inert helium atmosphere (Figure 25).

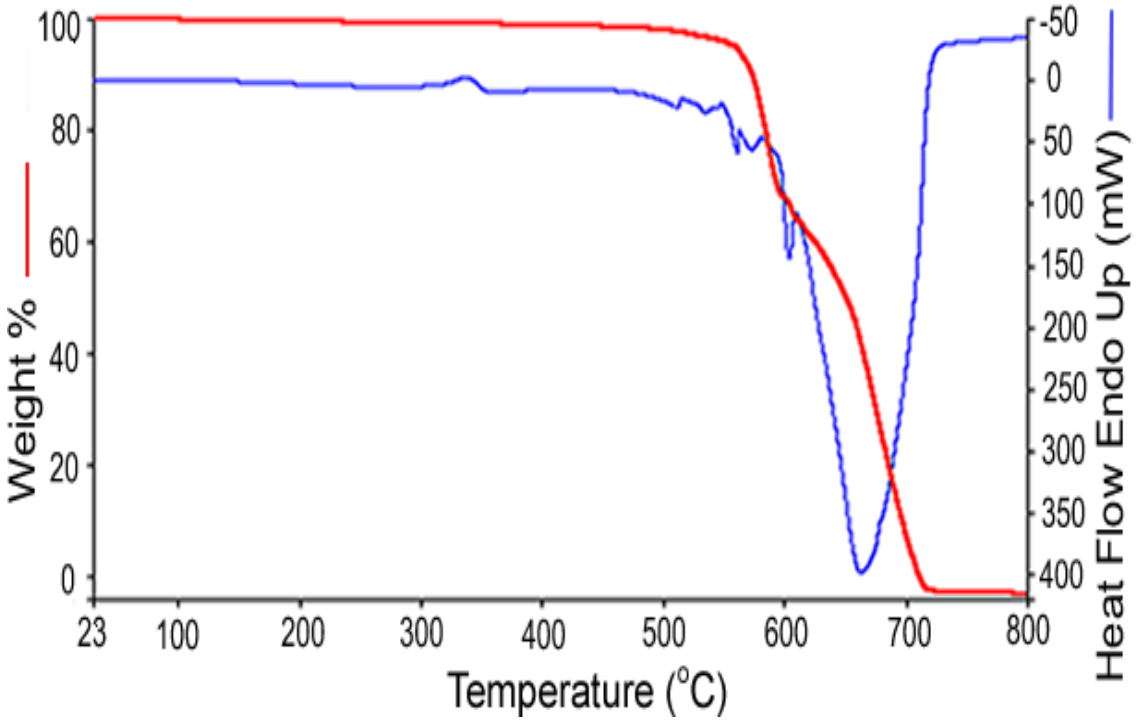

Figure 29. TGA/ DTA 450pf PEEK under flowing air measured from 23 to 800 °C at 20 °C/ min.

The thermal degradation of the sulfonated polymers in air occurs in three steps, similar to the experiments done under helium atmosphere. However, the backbone chain thermolysis temperature (third degradation step) for each tested polymer increased. The results taken from Figure 30, 31 and 32 for SPEEK-96, X-12-SPEEK-96 and X-24-SPEEK-96, show the polymers having char residues of 0, 13 and 25 wt% respectively. Based on these values, it was concluded that with increasing BDM cross-linker mass fractions, there is an increase in the thermo-oxidative stability of the highly sulfonated SPEEK-96 polymer. The fact that the mass loss in the third degradation step is dependent on cross-linker amount shows that the cross-linking is mainly occurring through the backbone of the polymer. Table 13 compiles TGA data obtained under air atmosphere for the sulfonated polymers.

Table 13. TGA weight percents left for cross-linked and non cross-linked SPEEK-96 samples under air

Sample	Weight % Left		
	23 to 200 °C	200 to 400 °C	400 to 600 °C
SPEEK-96	83	65	0
X-12-SPEEK-96	89	72	13
X-24-SPEEK-96	89	71	25

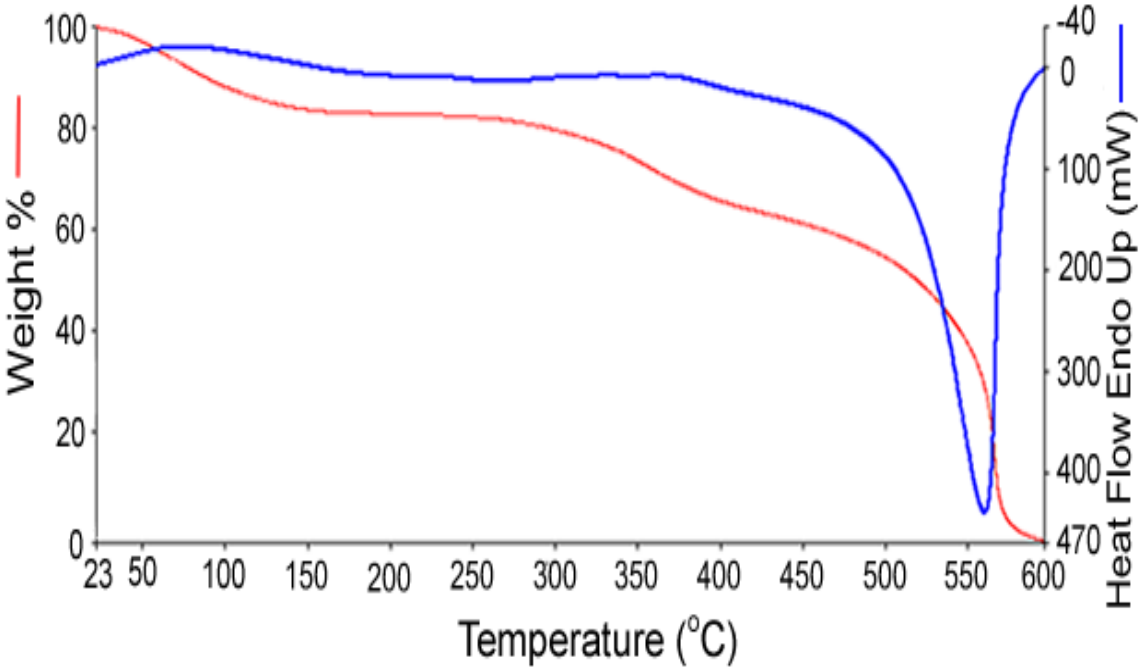

Figure 30. TGA/ DTA SPEEK-96 under flowing air measured from 23 to 600 °C at 20 °C/ min.

The thermal degradation of SPEEK-96 (Figure 30) under air proceeds via a similar three step mechanism, seen when helium atmosphere was utilized. The final step however, showed and an almost two-fold increase in weight loss under the oxidizing atmosphere. The X-12-SPEEK-96 and X-24-SPEEK-96 membranes also had similar air TGA/DTA thermograms, for the first two decomposition steps compared with the

thermogram done under helium. Thermolysis and backbone decomposition of these cross-linked membranes occurred at about 400 °C. It is well known that the presence of oxygen leads to increased thermal combustion at lower temperatures compared to inert atmospheres.[25]

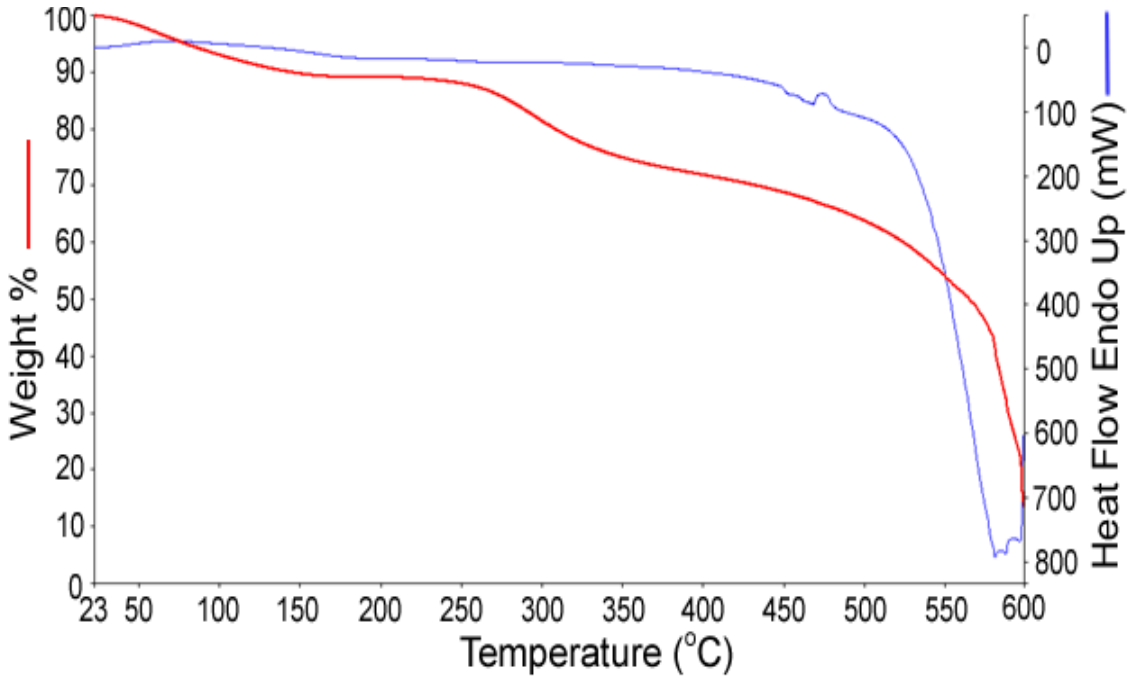

Figure 31. TGA/DTA of X-12-SPEEK-96 measured under flowing air measured from 23 to 600 °C at 20 °C/ min.

Over the temperature range studied, SPEEK-96 and X-SPEEK-96 membranes showed increased weight loss compared to samples placed in helium atmosphere. The mass losses in the temperature range necessary for fuel cell applications was however negligible or related to loss of waters of hydration. Conclusively, the use of these cross-linked membranes in a thermo-oxidative environment, such as for 100 °C temperature fuel cell applications would not be unfounded based on their thermal stabilities.

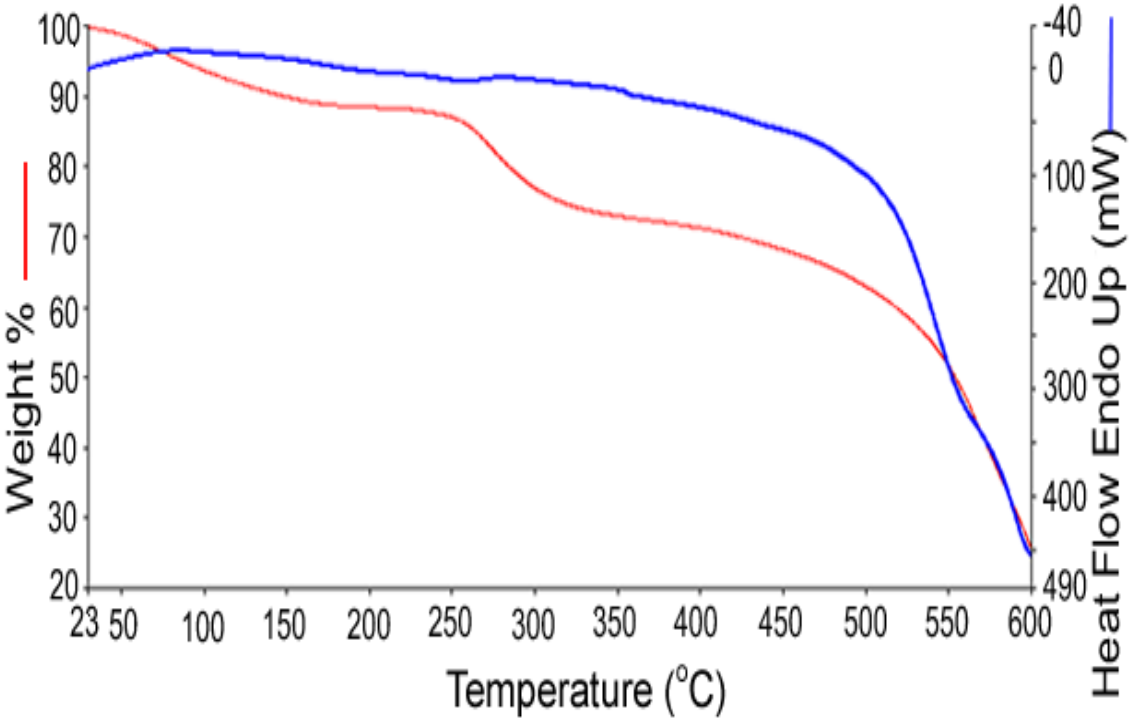

Figure 32. TGA/ DTA of X-24-SPEEK-96 polymer measured under flowing air measured from 23 to 600 °C at 20 °C/ min.

In hopes to get a better understanding of low temperature effects, such as glass transition temperature (T_g) and melting point temperatures differential scanning calorimetry was employed.

Differential Scanning Calorimetric Analysis

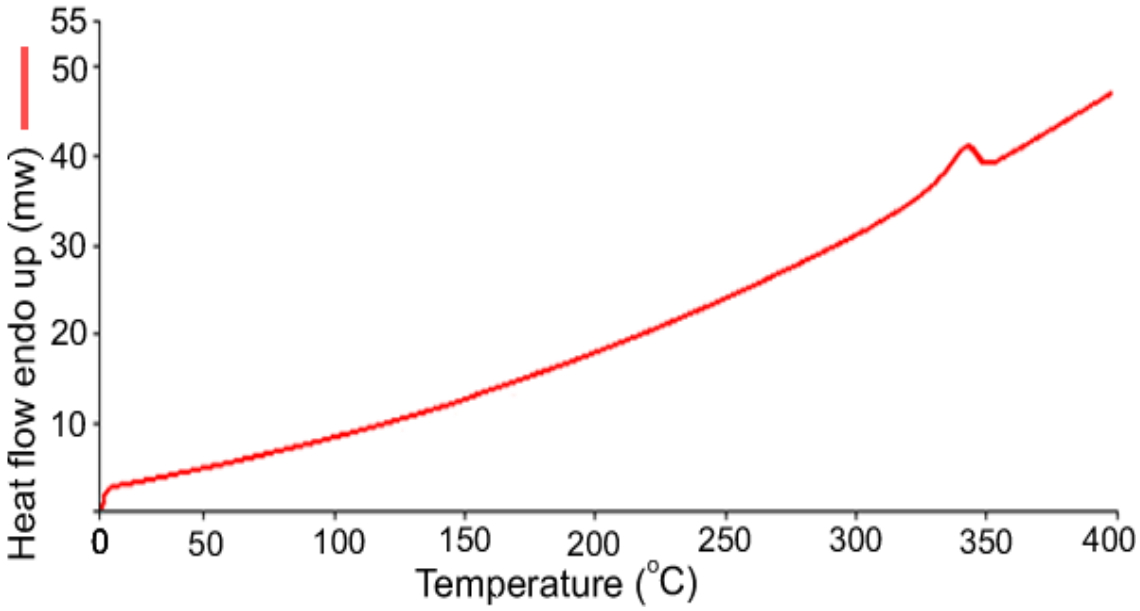

Figure 33. DSC of 450 pf PEEK taken from 0 to 400 at 10 °C/min

The values of the T_g and melting point of 450pf PEEK were determined by DSC to be 155 and 348 °C. It is well known that the PEEK polymers' crystallinity decreases with increasing DS, and thus the thermal behavior of the polymer is expected to change significantly.[28] The sulfonated PEEK polymers begin thermal degradation at about 300 °C, and as such all DSC experiments involving sulfonated PEEK were kept below this temperature.

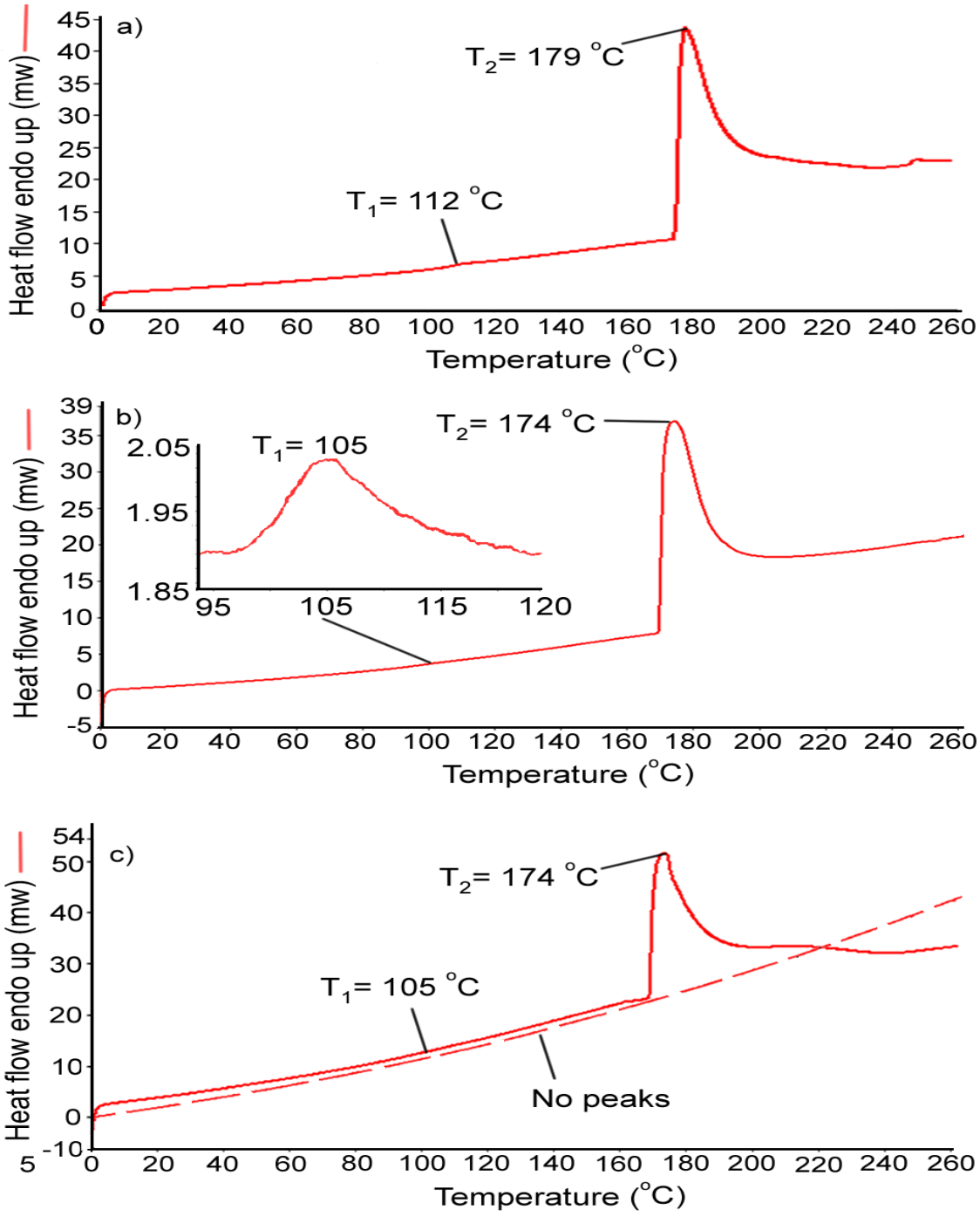

Figure 34. DSC temperature sweep of a) SPEEK-96 and b) X-12-SPEEK-96 obtained by drying at 140 °C for 15 minutes, cooling to 0 °C and finally ramping the temperature at 10 °C/min to 260 °C. c) Obtained after drying X-12-SPEEK-96 at 175 °C, cooling to 0 °C and increasing the temperature to 260 °C (broken line), and after soaking in water for a few hours, drying the rehydrated X-12-SPEEK-96 at 140 °C for 15 minutes, cooling to 0 °C and finally ramping the temperature at 10 °C/min to 260 °C (solid line).

Representative DSC plots were performed by initially drying SPEEK-96 polymer at 140 °C for 10 minutes, cooling to 0 °C and finally increasing the temperature to 260 °C. The results are shown in Figure 34a). The onset of an initial small transition occurs at 98 °C, peaking at 112 °C and ending at 122 °C. The endothermic transition was taken as the pure polymer's T_g, due to its reproducibility on temperature cycling below 160 °C. The following thermal transition at 179 °C was initially thought to be a secondary T_g for SPEEK-96, but the peak was not reproducible on cycling the temperature. Reviewing the TGA-MS spectrum for SPEEK-96 (Figure 26), the release of water bound to the sulfonic acids occurs in this temperature range. The polymer became brittle and deep red in color after drying at these temperatures, but became pliable and orange once returned to a hydrated state. Decomposition of the SPEEK-96 polymers began to occur at 249 °C, although others have concluded it to be a T_g.[2,28] Referring to the TGA-MS plot from Figure 26b), the onset temperature of this first degradation (CO_2 release) step of SPEEK-96 can be correlated to this temperature. The choice of casting solvent and polymer thermal history are known to affect the physicochemical properties of these sulfonic acid polymers. An earlier patent has claimed cross-linking to occur just by curing SPEEK at 120 °C, so care must be taken when processing these polymers for specific fuel cell application.[30]

A representative DSC of X-12-SPEEK-96 was done utilizing the same method as before; with the resulting thermogram being shown in Figure 34b). The first endotherm in the spectrum at 105 °C was the T_g of the X-12-SPEEK-96 polymer. The T_g for the cross-linked membrane is slightly lower than that of the pure SPEEK-96 membrane, with a difference of about 7 °C. Also quite similar to pure SPEEK-96, a peak at 174 °C was

indicative of a transition in the polymer occurring due to the loss of bound H_2O. The X-24-SPEEK-96 membrane however, did not show a discernible T_g, but had the T_2 transition occurring at 172 $^{\circ}$C.

After oven-drying the X-12-SPEEK-96 at 175 $^{\circ}$C, the thermogram obtained for the cross-linked membranes is featureless. But after exposing to DI water for a couple hours, drying the polymer in the DSC for 15 minutes at 140 $^{\circ}$C and finally ramping the temperature to 260 $^{\circ}$C, the thermogram recorded in Figure 34c) for the rehydrated X-12-SPEEK-96 was quite similar to the initial thermograms taken on the DSC (Figure 34a). Similar results were also obtained for SPEEK-96 and X-24-SPEEK-96. From these results, it is expected that exposing either high DS PEEK or its Friedel-Crafts cross-linked analogues to temperatures above 180 $^{\circ}$C, but below about 250 $^{\circ}$C, will keep polymer thermal degradation to a minimum.

SPEEK membranes cast from H_2O were shown previously to begin decomposition between 250 to 300 $^{\circ}$C, while membranes cast from DMF or DMAc began decomposing at temperatures above 180 $^{\circ}$C. Decomposition has been shown to vary widely based on casting solvent and sulfonated polymer thermal history. [2,11,20] The solvent choice has been shown to significantly alter properties such as PEM proton conductivity, ductility and nanoscopic structure.[31,32]

Stress-Strain Testing

All polymeric systems are known to encompass different physical, chemical and mechanical properties. These depend mainly on 1) macromolecular makeup, 2) inter-chain bonding and packing, and 3) chemical and thermomechanical history. [33] Tensile

strength of the SPEEK membranes was recorded while pulling the membrane at a constant cross-head speed of 254 mm/min. Results from this test are shown in Figure 35. The results from the water-cast SPEEK-96 membranes were similar to those of high DS SPEEK cast from organic solvents.[34] The SPEEK-96 membrane exhibited a sharp yield point at 28 MPa, followed by breaking at 65% strain. However, the cross-linked membranes exhibited brittle mechanical behaviors, with low strains at break (5.5 and 6%), and increased tensile stresses of 39 and 46 MPa for X-12-SPEEK-96 and X-24-SPEEK-96.

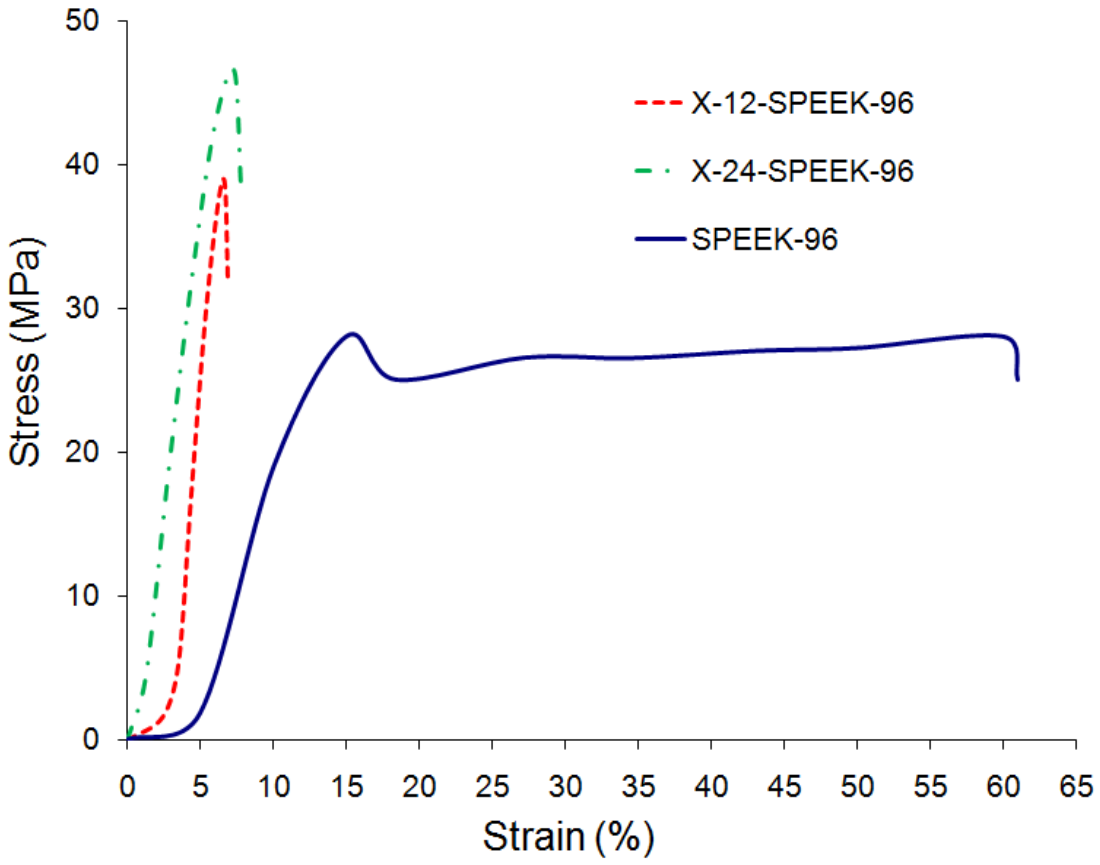

Figure 35. Stress-strain curves of SPEEK-96, X-12-SPEEK-96 and X-24-SPEEK-96 membranes tested at 70% RH and 23 °C. Increasing BDM wt% increases stress at break.

Electrochemical Performance

The mechanical and chemical stability of the cross-linked SPEEK-96 membranes was found to be satisfactory for manufacturing of CCMs. As such, these membranes were sprayed with Pt/C electrocatalyst ink and were hot pressed to give uniform electrode surfaces. The cross-linked SPEEK-96 CCM's electrochemical performance was tested under fuel cell operating conditions, and its worthiness as a replacement candidate for Nafion® was evaluated, with the latter being the standard.[35]

In work done earlier by this research group, it was found that low DS SPEEK membranes and composites made with stabilized phosphotungstic acid are suitable for fuel cell operation.[36] Although these membranes demonstrated both low respective fuel cross-over and degradation, high resistances caused sharp losses in voltages at medium current densities. It was concluded that low DS SPEEK does not have the sulfonic acid group density to maintain the high levels of hydration necessary for good protonic conductivity (>0.1 S/ cm). Cells were initially performance tested at 80 °C with the anode and cathode gases being humidified at 80 °C and 73 °C respectively (100% and 75% RH) (80/80/73). Following this, performance testing at 100 °C was done with anode and cathode gases humidified to 90 °C (69% RH) (100/90/90). Electrochemical characterization was performed by LSV experiments before and after at 25 cell/25 anode/25 cathode.

Performance of a SPEEK-96 membrane was also done, but failed as air was introduced to the cathode compartment. Visual inspections along with LSV experiments were done, and both gave conclusive evidence of a significant decrease in membrane physical structure and high hydrogen fuel cross-over, respectively.

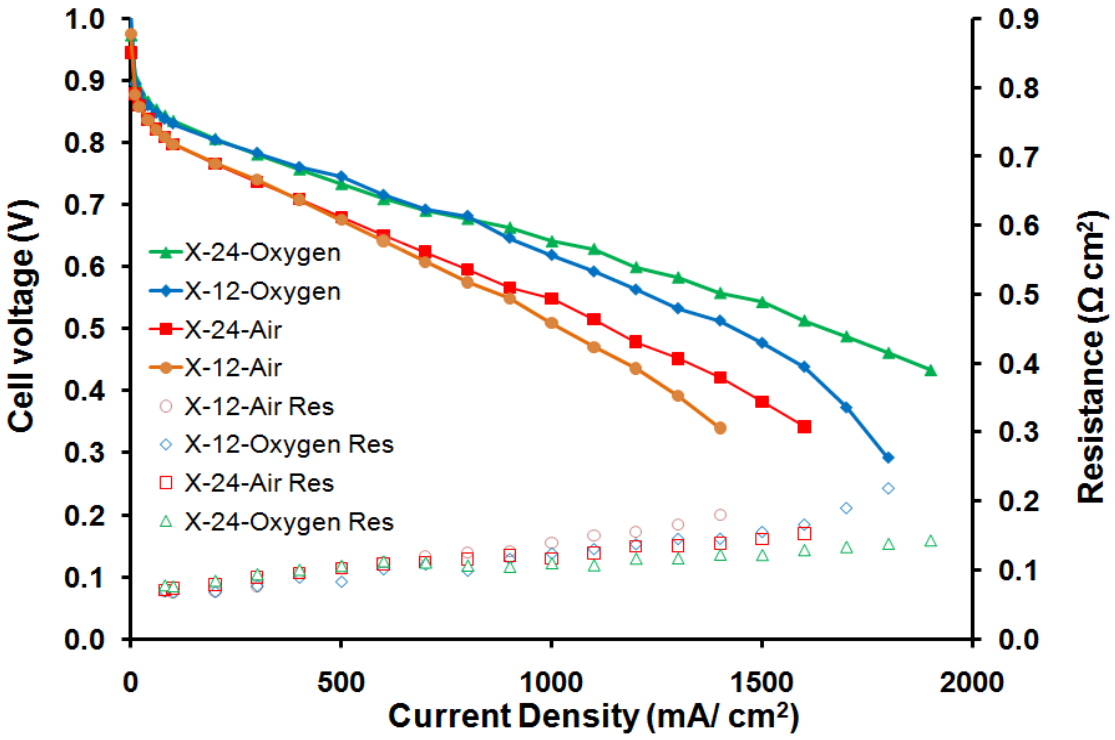

Figure 36. Fuel cell performance curves for X-12-SPEEK-96 and X-24-SPEEK-96 CCMs measured at 80 °C cell temperature, 80 °C anode and 73 °C cathode fuel temperatures. H_2 gas was the only fuel used on the anode, while utilizing air (air), followed by O_2 (oxygen) on the cathode. The change in membrane resistance for each membrane was also plotted.

Figure 36 shows the polarization curve taken for X-12-SPEEK-96 CCM and X-24-SPEEK-96 performed under air and then oxygen atmospheres at 80/80/73. The membranes performed essentially the same on the respective fuels until about 800 mA/cm^2. Above this current density, the X-24-SPEEK-96 performed better, with lower resistance than the X-12-SPEEK-96. This difference in the resistance at higher current density may be due to better transport of water in the X-24-SPEEK-96 membrane. Cell resistance is known to increase drastically with current density; this is caused by the water distribution in the membrane, a function of both the back transport of water to the anode and electro-osmotic drag transporting water toward the cathode.[37,38] At 100/90/90

(Figure 37), the higher temperature and lower relative humidity conditions caused the resistance of both cells to double compared to performance taken at 80/80/73, over all current densities tested (Figure 36).

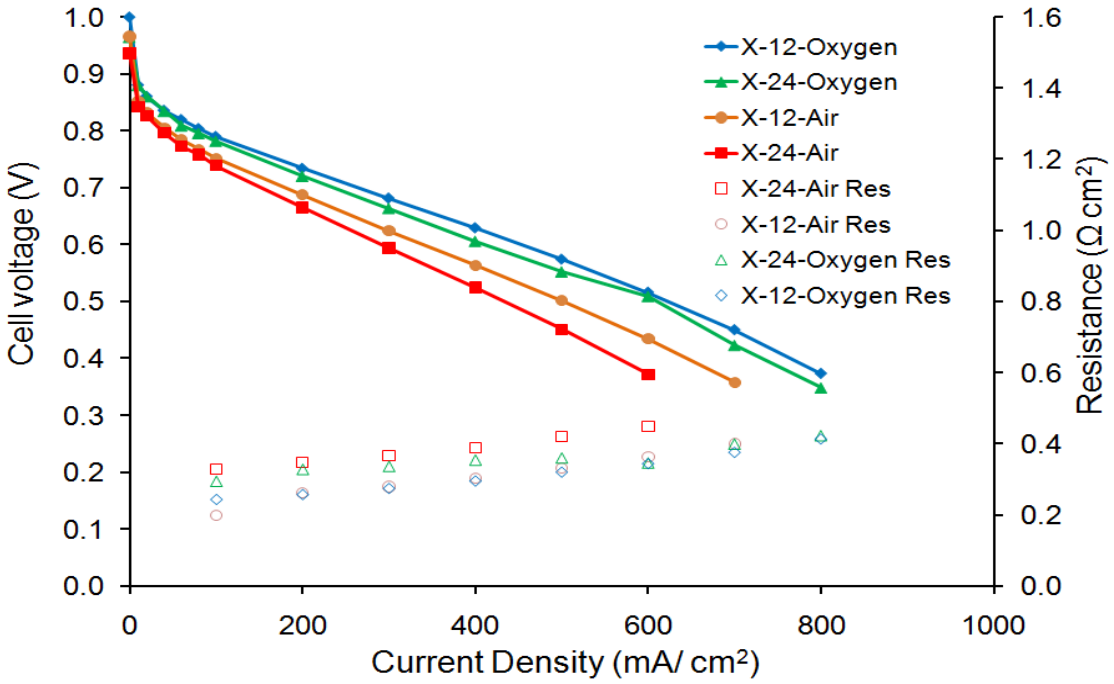

Figure 37. Fuel cell performance of X-12-SPEEK-96 and X-24-SPEEK-96 CCMs measured at 100 °C cell temperature, 90 °C anode and 90 °C cathode fuel temperatures. H_2 gas was the only fuel used on the anode, while air and oxygen was utilized on the cathode.

These conditions, however, were better suited for the X-12-SPEEK-96 membrane. Its performance was slightly better on oxygen, but notably superior on air in comparison to the X-24-SPEEK-96 membrane. At these low current densities, the ohmic membrane resistance causes decreased cell performance. The X-24-SPEEK-96 PEM does not uptake waters of hydration as well as the X-12-SPEEK-96 membrane; evidence for this was recorded in Table 11. This phenomenon follows from decreased membrane

conductivity as a function of lower relative humidity. It follows that proton diffusion will be increased many orders of magnitude through a conducting medium in a fully hydrated state.[39] High levels of swelling as a result of the hydration can lead to structural changes, such as bond breaking, and finally degradation.[26] SPEEK polymer allows strong proton conduction and very low permeability to fuels when compared to Nafion®. These are essential membrane properties for high efficiency and long term cell durability.[40] Fuel cell performance is known to decrease at lower RH, due to a combined effect of lower proton conductivity of dry membrane and catalyst layer, as well as the poor oxygen permeability of dry electrodes.[41]

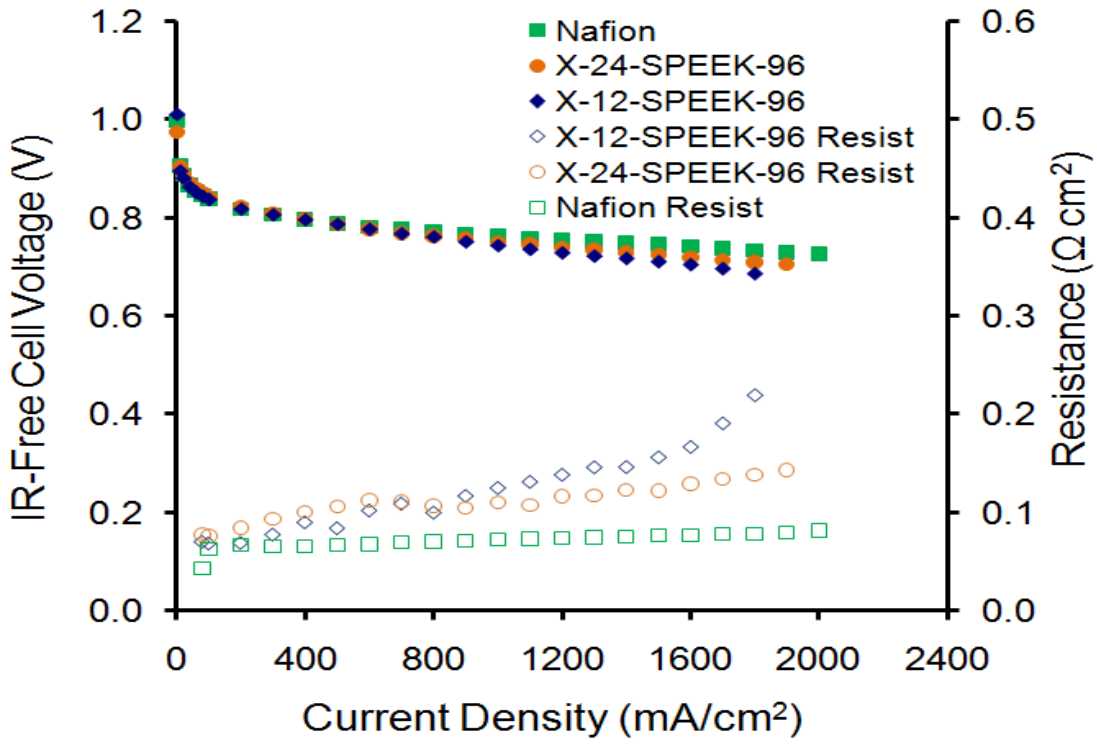

Figure 38. IR-free voltage PEM fuel cell performance of various SPEEK CCMs performed at 80 °C in a H_2/O_2 cell, with anode and cathode gases humidified to 100% and 75% RH respectively.

Figure 38 and Figure 39 illustrate IR-free cell voltages obtained by the current interrupt method for Nafion®, X-12-SPEEK-96 and X-24-SPEEK-96 at both testing conditions. The cross-linked SPEEK-96 membranes had comparable performance to Nafion 211 MEA with similar electrocatalyst loading. The differences between these IR free voltage curves were not totally understood, but it was noted that they may due to incompatibilities between the Nafion® binder in the electrocatalyst and the SPEEK hydrocarbon PEM.[26]

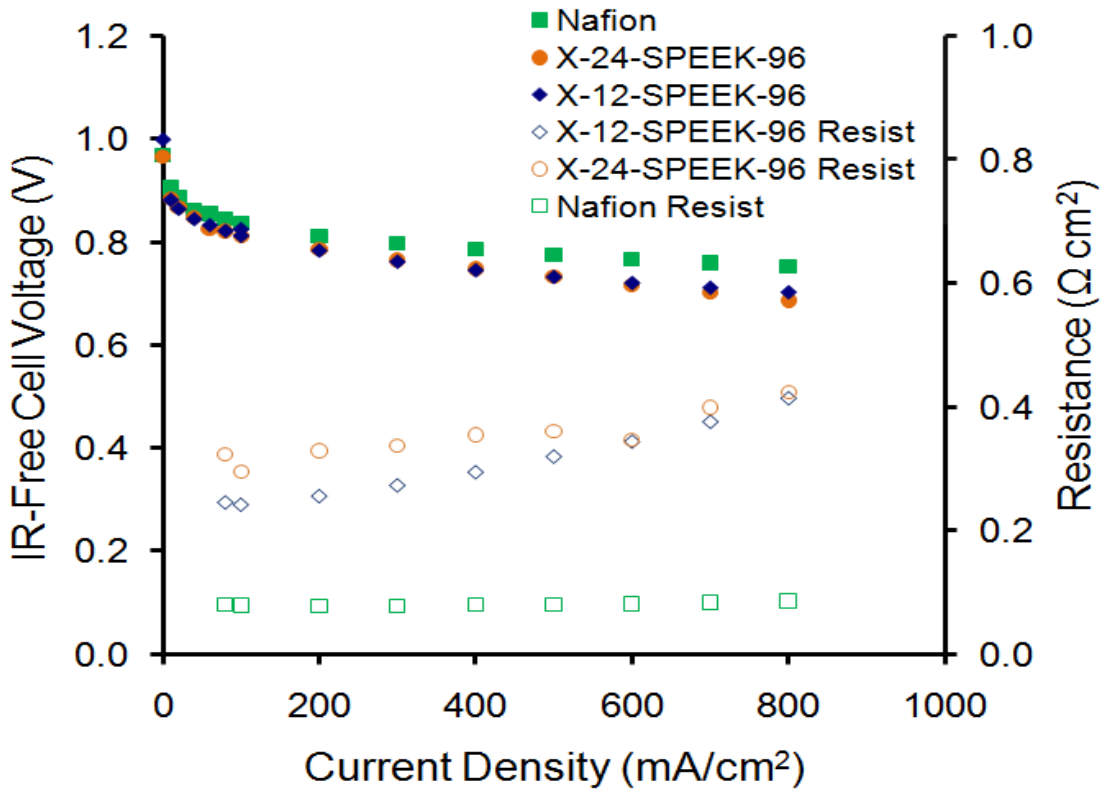

Figure 39. IR-free voltage PEM fuel cell performance of various CCMs performed at 100 °C in a H_2/O_2 cell, with anode and cathode gases humidified to 69% RH

Before and after conducting each performance experiment, LSV was used to determine fuel cross-over currents. Tests for cross-over currents before the performance

tests at 80/80/73 and 100/90/90 showed negligible hydrogen gas cross-over. Figure 40 illustrates the results of a LSV experiment on an X-24-SPEEK-96 CCM. The change in cross-over of hydrogen gas before and after testing was deemed negligible. The LSV had a limiting current comparable with a Nafion 211 and the X-12-SPEEK-96 membranes. From Faraday's Law, this means that the flux of hydrogen gas from anode to cathode compartment is low. Thus while free radical-driven decomposition of SPEEK CCMs has been noted by others, there were no durability issues encountered in the performance of our testing protocols.[42]

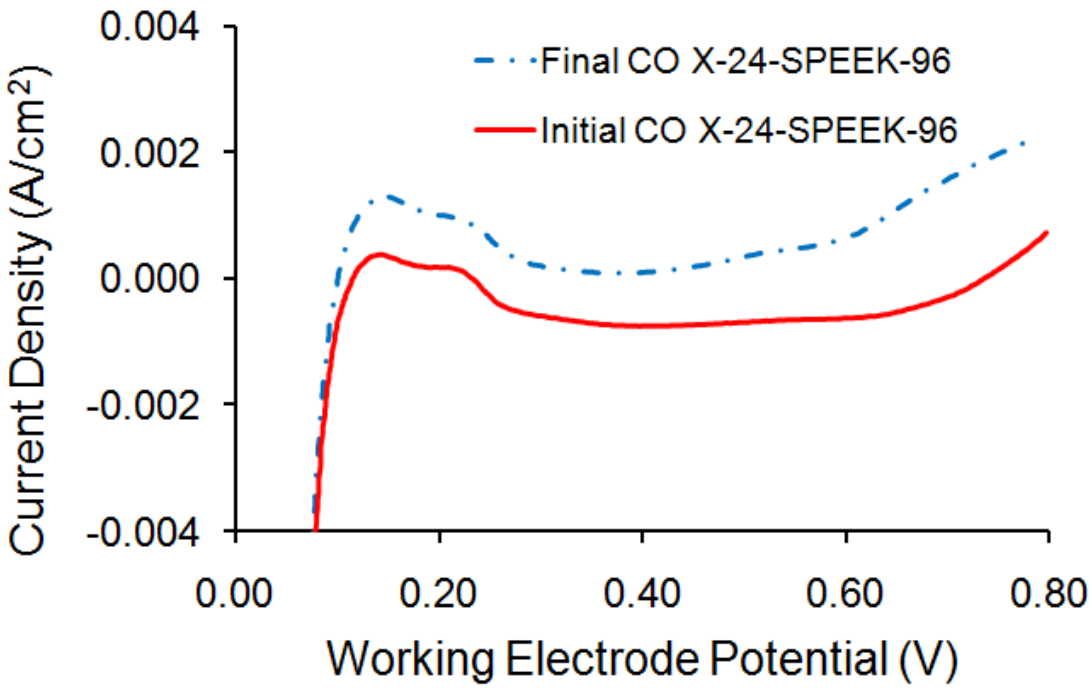

Figure 40. Linear sweep voltammetry experiment demonstrating the low hydrogen gas cross-over flux before and after performance testing X-24-SPEEK-96 at 80 and 100 °C.

Conclusion

We have shown that PEEK can be sulfonated to high degree of sulfonation, rendering it water soluble, and then subsequently cross-linked via a Friedel-Crafts method to produce a highly chemically resistant proton exchange membrane. Although the thermal resistance of the cross-linked polymer did not show much improvement over the plain SPEEK sulfonate, mechanical strength and dimensional stability were substantially improved, while maintaining the protonic conductivities required for long term operation in high temperature fuel cell applications.

References

1. Bishop, M. T., Karasz, F. E., Russo, P. S., Langley, K. H., Solubility properties of a poly(aryl ether ether ketone) in strong acids, *Macromolecules*, 18, (1985), 86.
2. Xing, P., Robertson, G. P., Guiver, M., Mikhailenko, S. D., Wang, K., Kaliaguine, S., Synthesis and characterization of sulfonated poly(etheretherketone) for proton exchange membranes, *J. Membr. Sci*,. 229, (2004), 95-106.
3. Zaidi, S. M. J., Mikhailenko, S. D., Robertson, G. P., Guiver, M. D., Kaliaguine, S., Proton conducting composite membranes from polyether ether ketone and heteropolyacids for fuel cell applications, J. Membr. Sci. 173 (2000) 17-34.
4. Grassie, N., Gilks, J., Thermal analysis of polystyrenes cross-linked by p-di(chloromethyl)benzene, *J. Polym. Sci., Part A: Polym. Chem.*, 11, (1973), 1985-1994.
5. Wilkie, C. A., Yao, H., Zhu, J., McKinney, M., Cross-linking of polystyrene by Friedel-Crafts chemistry: Multifunctional additives, *J. Vinyl and Additive Technology*, 6, (2000), 205-210.
6. Rabek, J. F., Lucki, J., Cross-linking of polystyrene under Friedel-Crafts conditions in dichloroethane and carbon tetrachloride solvents through the formation of strongly colored polymer-$AlCl_3$-Solvent complexes, *J. Polym. Sci., Part A: Polym. Chem.*, 26, (1988), 2537-2551.
7. Brauman, S. K., Friedel-Crafts reagents as charring agents in impact polystyrene, *J. Polym. Sci., Part A: Polym. Chem.*, 17, (1979), 1129-1144.

8. Coughlan, B., Carroll, W. M., Nunan, J., Alkylation reactions over ion-exchanged molecular sieve zeolite catalyst: Part 1.-Alkylation of toluene with methanol: consideration of the effects of reaction parameters on catalyst deactivation and the extent of poly-substitution. *J. Chem. Soc., Faraday Trans.*, 1, 79, (1983), 281-296.

9. Carey, F. A., Sundberg, R. J., *Advanced Organic Chemistry - Part A: Structure and Mechanisms*, Fifth ed., Springer, New York, (2007).

10. Mikhailenko, S. D., Wang, K. P., Kaliaguine, S., Xing, P., Robertson, G., Guiver, M. D., Proton conducting membranes based on cross-linked sulfonated poly(etheretherketone), *J. Membr. Sci.*, 233, (2004), 93-99.

11. Robertson, G. P., Mikhailenko, S. D., Wang, K., Xing, P., Guiver, M. D., Kaliaguine, S., Casting solvent interactions with sulfonated poly(ether ether ketone) during proton exchange memrbane fabrication, *J. Membr. Sci.*, 219, (2003), 113-121.

12. Mikhailenko, S. D., Robertson, G. P., Guiver, M. D., Kaliaguine, S., Properties of PEMs based on cross-linked sulfonated poly(etheretherketone), *J. Membr. Sci.*, 285, (2006), 306-316.

13. Deb, P. C., Rajput, L. D., Hande, V. R., Sasane, S., Kumar, A., Modification of sulfonated poly(etheretherketone) with phenolic resin, *Polym. Adv. Technol,*. 18, (2007), 419-426.

14. Hande, V. R., Rao, S., Rath, S. K., Thakur, A., Patri, M., Cross-linking of sulfonated poly(etheretherketone) using aromatic bis(hydroxymethyl) compound, *J. Membr. Sci.*, 322, (2008), 67-73.

15. Kopitzke, R. W., Linkous, C. A., Anderson, H. R., Nelson, G. L., Conductivity and water uptake of aromatic based proton exchange membrane electrolytes, *J. Electrochem. Soc.*, 147, (2000), 1677-1681.

16. Appleby, A. J., Recent developments and applications of the polymer fuel cell, *Phil. Trans. R. Soc. Lond. A*, 354, (1996), 1681-1693.

17. Savadogo, O., Emerging membranes for electrochemical systems: (I) solid polymer electrolyte membranes for fuel cell systems, *J. New Mater. Electrochem. Syst.*, 1, (1998), 47-66.

18. Marani, D., Di Vona, M. L., Traversa, E, Licoccia, S., Beurroies, I., Llewellyn, P. L., Knauth, P., Thermal stability of hybrid proton conducting polyaryletherketones, *J. Phys. Chem. B*, 110, (2006), 15817.

19. Gil, M., Ji, X., Li, X., Na, H., Hampsey, J. E., Lu, Y., Direct Synthesis of sulfonated aromatic poly(etheretherketone) proton exchange membranes for fuel cell applications, *J. Membr. Sci.*, 234, (2004) 75.

20. Othman, M. D. H., Ismail, A. F., Mustafa, A., Physico-chemical study of sulfonated poly(etheretherketone) membranes for direct methanol fuel cell application, *Malaysian Polym. J.* 2, (2007), 10-28.

21. Silverstein, R. M., Webster, F. X., Kiemble, D. J., Spectrometric Identification of Organic Compounds, Seventh ed., John Wiley & Sons, New Jersey, (2005).

22. Kreuer, K. D., On the development of proton conducting materials for technological applications, *Solid State Ionics*, 97, (1997).

23. Mark, H. F., Kroschwitz, J. I., Polyetheretherketones, *Encyclopedia of polymer science and engineering*, 12, (1985), 313-320.

24. Arthanareeswaran, G., Srinivasan, K., Mahendran, R., Mohan, D., Rajendran, M. Mohan, V., Studies on cellulose acetate and sulfonated poly(ether ether ketone) blend ultrafiltration membrane, *Eur. Polym. J.*, 40, (2004), 751-762.

25. Kopitzke, R. W., Linkous, C. A., Nelson, G. L., Thermal stability of high temperature polymers and their sulfonated derivatives under inert and saturated vapour conditions, *Polym. Degr. and Stab.*, 67, (2000), 335-344.

26. Kreuer, K. D., On the development of proton conducting membranes for hydrogen and methanol fuel cells, *J. Membr. Sci.* 185, (2001), 29-39.

27. Luo, Y., Ruizhen, H., Jin, X., Karasz, F. E., Thermal degradation of sulfonated poly(aryl ether ether ketone), *J. Anal. and Appl. Pyr.* 34, (1995), 229-242.

28. Jaafar, J., Ismail, A. F., Mustafa, A., Physicochemical study of poly(ether ether ketone) electrolyte membranes sulfonated with mixtures of fuming sulfuric acid and sulfuric acid for direct methanol fuel cell applications, *Mat. Sci. Eng.*, A 460, (2007), 475-484.

29. Fried, J. R., Poly(ether ether ketone), Polymer Data Handbook, 2nd Ed., Oxford University Press, Inc., New York, New York. Editor James E. Mark. (1999)

30. Yen, S. P. S., Narayanan, S. R., Halpert, G., Graham, E., Yavrouian, A., Polymer material for electrolyte membranes in fuel cells, US Patent 5,795,496 (1998).

31. Paik, Y., Chae, S. A., Han, O. H., Hwang, S. Y., Ha, H. T., Influence of water and degree of sulfonation on the structure and dynamics of SPEEK studied by solid state ^{13}C and $^{1}HNMR$, *Polymer*, 50, (2009), 2664-2673.

32. Ye, G., Mills, C. M., Goward, G. R., Influences of casting solvents on proton dynamics within sulfonated poly ether ether ketones (S-PEEKs) studied using high-resolution solid-state NMR, *J. Membr. Sci.*, 319, (2008), 238-243.

33. Meijer, H. E. H., Govaert, L. E., Mechanical performance of polymer systems: The relation between structure and properties, *Prog. Polym. Sci.*, 30, (2005), 915-938.

34. Reyna-Valencia, A., Kaliaguine, S., Bousmina, M., Tensile mechanical properties of sulfonated poly(ether ether ketone) (SPEEK) and BPO_4/SPEEK membranes, *J. App. Polym. Sci.*, 98 ,(2005), 2380-2393.

35. Kerres, J. A., Development of ionomer membranes for fuel cells, *J. Membr. Sci.*, 185, (2001), 3-27.

36. Rhoden, S. L. N. H. , Linkous, C. A., Mohajeri, N., Díaz, D. J., Brooker, P., Slattery D. K., Fenton, J. M., Composite polymer electrolyte membranes based on stabilized phosphotungstic acid and sulfonated poly(etheretherketone) for fuel cell applications, *J. Electrochem. Soc*., 157, (2010), B1092-B1102.

37. Zawodzinski Jr., T. A., Derouin, C., Radzinski, S., Sherman, R. J., Smith, V. T., Springer, T. E., Gottesfield, S., Water uptake by and transport through Nafion® 117 membranes, *J. Electrochem. Soc.*, 140, (1993), 1041-1047.

38. Büchi, F. N., Scherer, G. G., Investigation of the transversal water profile in Nafion membranes in polymer electrolyte fuel cells, *J. Electrochem Soc.*, 148, (2001), A183-A188.

39. Kreuer, K. D., Fast proton conductivity: A phenomenon between the solid and liquid state? *Solid State Ionics*, 94, (1997), 55-62.

40. Sambandam, S., Ramani, V., SPEEK/functionalized silica composite membranes for polymer electrolyte fuel cells, *J. Power Sources.* 170, (2007), 259-267.

41. Broka, K., Ekdunge, P., Oxygen and hydrogen permeation properties and water uptake of Nafion® 117 membrane and recast film for PEM fuel cell, *J. Appl. Electrochem.*, 27, (1997), 117-123.

42. Mikhailenko, S. D., Celso, F., Kaliaguine, S., Properties of SPEEK based membranes modified with a free radical scavenger, *J. Membr. Sci.*, 345, (2009), 315-322.

CHAPTER 5. SPEEK AND TUNGSTIC ACID HYDRATE COMPOSITES

Synthesis and Characterization of Tungsten Oxide Hydrates and SPEEK Composite Blends

The addition of hydrated inorganic proton conductors such as PTA.nH_2O and hydrated tungsten oxide ($WO_3 \cdot xH_2O$), also called tungstic acid, to sulfonic acid ionomer membranes in order to improve their conductivities are well known.[1,2] The waters of hydration intrinsic to these inorganic solid acids have shown increased proton conductivity compared to their anhydrous equivalents. Different techniques such as sputtering, electrodeposition, chemical vapor deposition and sol-gel syntheses have been employed for making WO_3.[3] These techniques allow differing states of morphology and hydration levels, and hence may facilitate varying degrees of enhanced ion transport.

Stoichiometric amounts of water can be precipitated with WO_3 in solutions, depending on the pH, temperature and pressure to which the solid acid is exposed.[4,5,6,7] A cheap and efficient way to produce the dihydrate ($WO_3 \cdot 2H_2O$), is via a wet chemistry/ sol-gel process.[8,9] Structural characterization of these films was done, and their morphology and crystallinity found to be dependent on the temperature at which the films were annealed, as well as precursors used. The dihydrate, $WO_3 \cdot 2H_2O$, loses interlayer water if held at 90 $^{\circ}$C to form the monohydrate (x=1), and on increasing the temperature a second weight loss attributed to coordinated water is also lost, affording the anhydrous WO_3.[7] This was corroborated using thermogravimetric analysis, and is explained in a later subsection

$$WO_4^{-2} + 2H^+ \xrightarrow{H_2O} H_2WO_4 \xrightarrow{H_2O} WO_3 \cdot xH_2O \quad (14)$$

Equation 14 shows the formation of $WO_3 \cdot xH_2O$ obtained after passing Na_2WO_4 through an acid cation exchange column. The low pH (<1) in the column bed forces the H_2WO_4 to precipitate, yielding $WO_3 \cdot xH_2O$ and water. It should be noted that shortly after $WO_3 \cdot xH_2O$ elutes from the column, the viscosity of the solution increases slowly. After two hours the solution goes from colorless to a bright yellow precipitate. The secondary acid-catalyzed step is a condensation polymerization reaction. This reaction occurs when two H_2WO_4 molecules come into contact, with two hydroxyl ligands combining to eliminate water, while simultaneously forming an oxo-linkage between the two tungsten centers. The scheme of this reaction and cluster formation is shown in Figure 41.[10] It was noted by the authors that the oxo-linkages between the tungsten centers can be hydrolyzed, producing the original reactants.

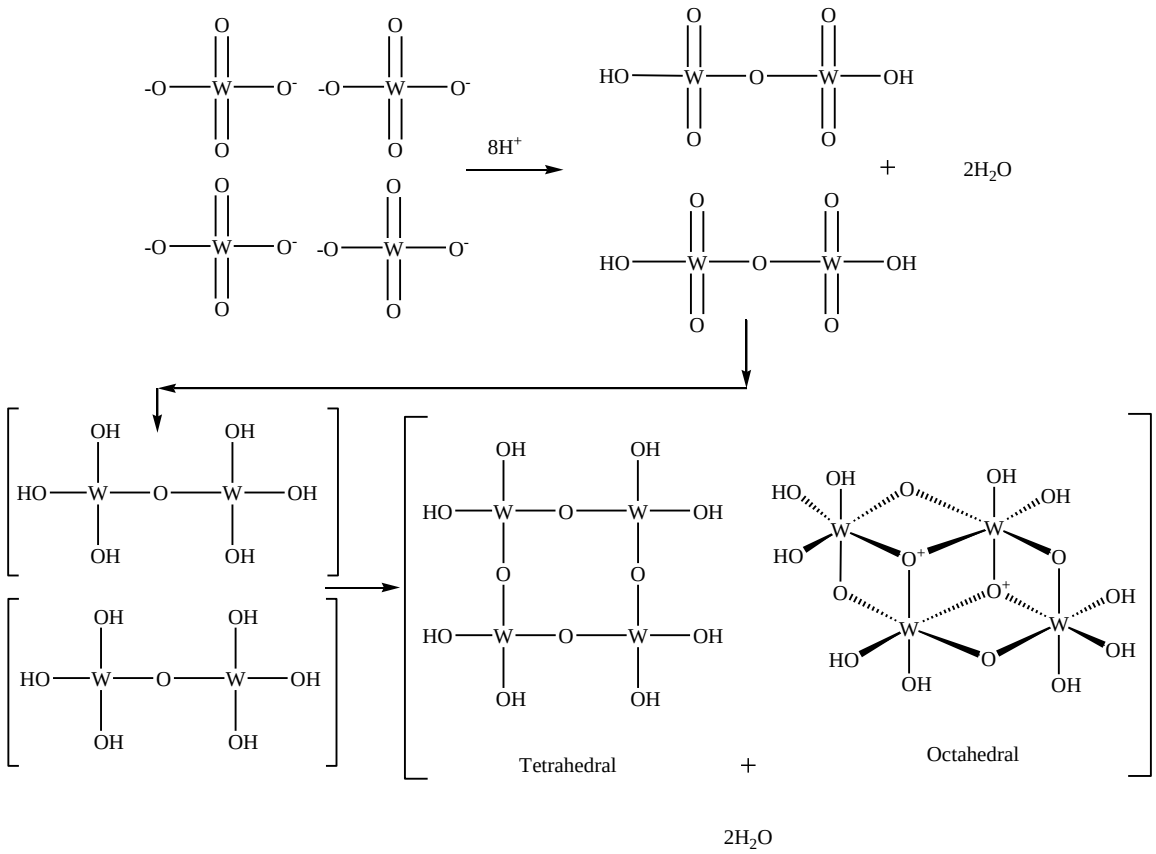

Figure 41. Redraw from 10 showing sol-gel condensation polymerization of tungstates in acidified solutions

Thermal Analysis of $WO_3 \cdot xH_2O$ and SPEEK Membrane Cross-linked with WO_3

The possible morphological and crystalline states of $WO_3 \cdot xH_2O$ were investigated via thermogravimetry. Figure 42 shows the thermogravimetric curve of $WO_3 \cdot 2H_2O$ powder. Following the blue thermogram curve, the presence of two different bound water molecules can be confirmed by the two endotherms. The first weight loss, related to loss of interlayer water, begins at about 70 °C and finishes at about 100 °C. The loss of

coordinated water begins at about 140 °C with further out-gassing at higher temperatures.[7]

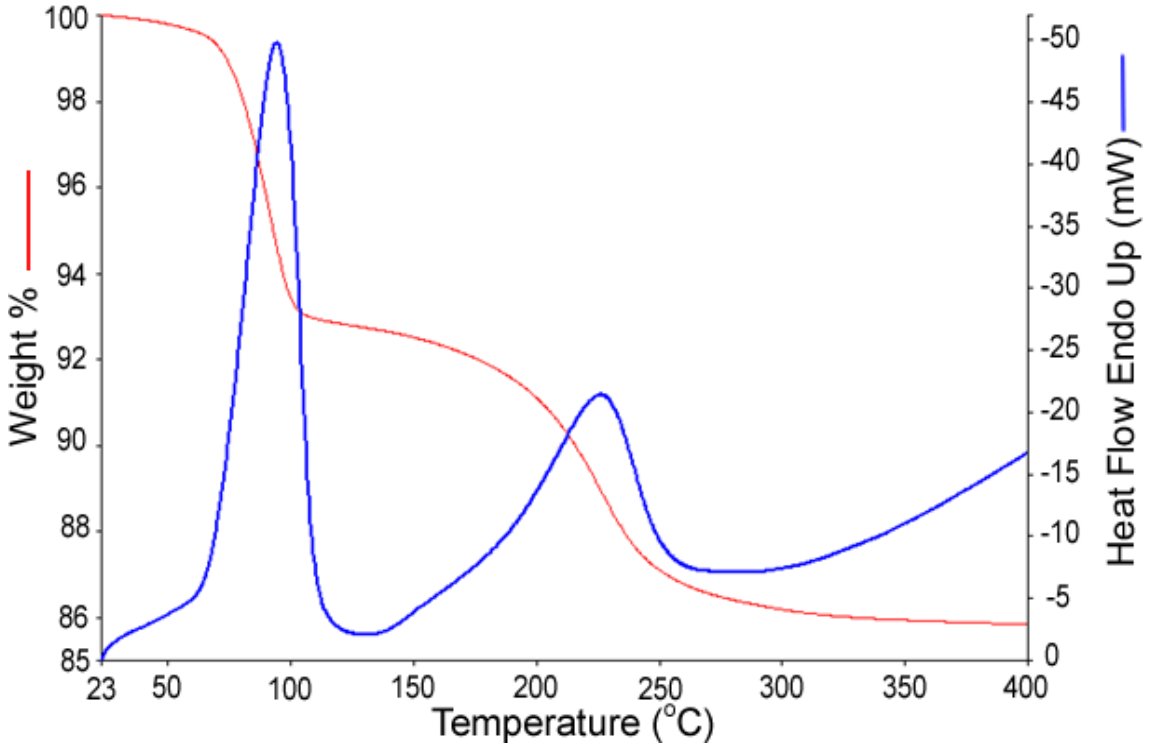

Figure 42. Thermogram of $WO_3 \cdot 2H_2O$ powder, obtained while heating under helium from 23 to 400 °C at 20 °C/min.

Good connectivity between acid sites, both sulfonic groups and inorganic solid acid, is essential for improved proton conduction in PEM materials. When in the dihydrate or monohydrate form, tungsten oxide has demonstrated high proton conductivities.[7] Based on this conclusion, blends of the hydrated tungsten oxide particles with SPEEK-96 were cast from aqueous solutions, with hopes of obtaining improved proton conductivities. Membranes were cast preferentially from H_2O to avoid strong sulfonic acid/ solvent interactions, hence the need for a subsequent acid bath or high temperature drying to break up the latter-mentioned interactions can be avoided.[11] It

follows that using high temperatures would also remove the waters of hydration from the tungsten oxide species, making their doping into the SPEEK membranes ineffective.

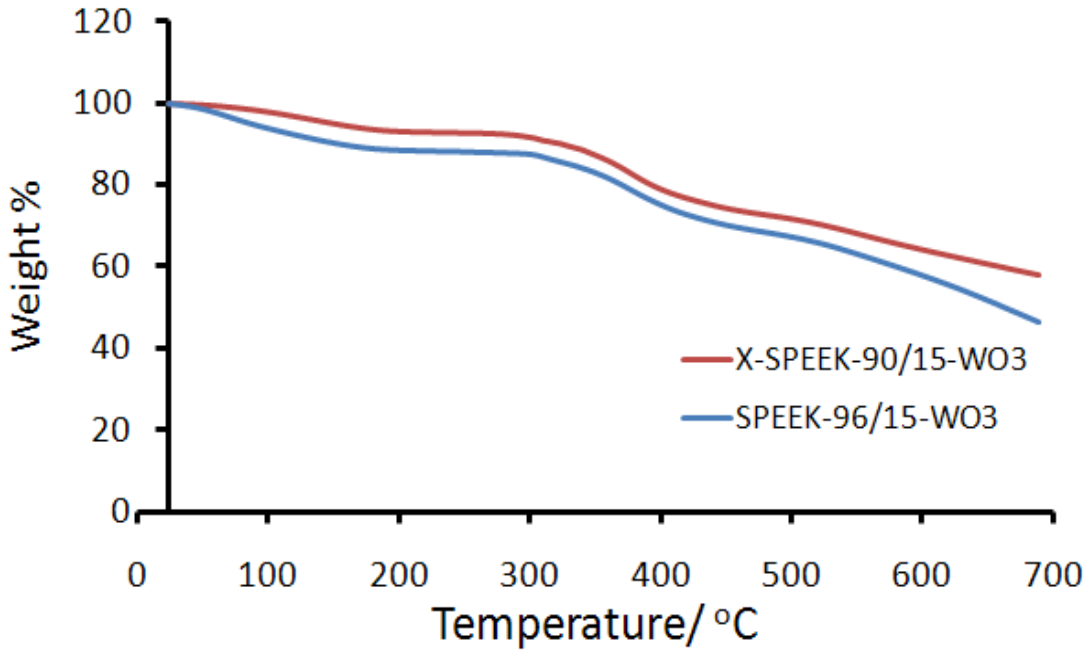

Figure 43. TG/DTA thermogram for SPEEK-96/15-$WO_3 \cdot xH_2O$ and a SPEEK-90 membrane cross-linked at 200 °C with $WO_3 \cdot xH_2O$. The temperature was scanned from 0 to 700 °C under inert helium atmosphere at 20 °C/min.

Figure 43 shows the thermal degradation of a SPEEK-96 membrane cast with $WO_3 \cdot xH_2O$ (blue curve), and a cross-linked SPEEK-90 membrane with 15 wt% solid acid (red curve). From 0 to 200 °C, the SPEEK-96/15-WO_3 membrane lost 17% compared to 10% from the X-SPEEK-90/15-WO_3. This was interpreted to be due to less water content in the cross-linked membrane's $WO_3 \cdot xH_2O$, which had prior exposure to 200 °C, possibly driving off all bound and intercalated water molecules (x=2). Above this temperature, the cross-linked material showed better thermal stability at 700 °C, with a residue of 53% compared to 46% for the un-cross-linked material.

Conductivity Analysis of SPEEK-96, SPEEK-96/WO_3 and SPEEK-90/15-WO_3 Cross-linked Composite Membranes

Conductivity testing was conducted at 80 $^{\circ}$C to determine if the waters of hydration present in the $WO_3 \cdot xH_2O$ increase proton conductivity of the composite SPEEK membranes.[12] Mecheri showed earlier that adding the dihydrate material to SPEEK sulfonated to 70% DS had increased conductivity and attributed this to the sulfonic acids on the SPEEK interacting "synergistically" with the waters of hydration on the $WO_3 \cdot xH_2O$.

Also, SPEEK-96/15-WO_3 membrane showed over one order of magnitude better proton conductivity at 20% relative humidity, compared to a SPEEK-96, an X-SPEEK-90/15-WO_3 and an 80% DS SPEEK membrane containing 15 wt% stabilized PTA. At 100% RH, the pristine SPEEK-96 material had better conductivity than all other membranes at 0.25 S/cm; SPEEK-96 showed 148 H_2O/SO_3H, and the higher water-uptake at these saturated conditions may be the main factor. The X-SPEEK-90/15-WO_3 performed almost equally to the pure SPEEK-96 at low relative humidities, but the former membrane's proton conductivity was considerably lower at high relative humidity. Heat treatment of these membranes may have forced water from the $WO_3 \cdot xH_2O$ and hence does not help the water-assisted vehicle mechanism of proton conduction. Similarly, as the Cs^+-stabilized PTA was concluded (Chapter 3) to have minimal water uptake, the SPEEK-80/15-PTA membrane having low proton conductivity is somewhat expected. Although the DS of the SPEEK-80 and SPEEK-90 membranes was lower than the 96% sulfonated membrane, the difference in their proton conductivity was not thought to be due to their respective sulfonic acid density. Adequate sustained proton

conductivities of PEMs can be achieved by the addition of insoluble strong acids to assist the Grotthus mechanism of "proton hopping", and/or hygroscopic materials, which help the water-assisted vehicle mechanism proton between acid sites.[13]

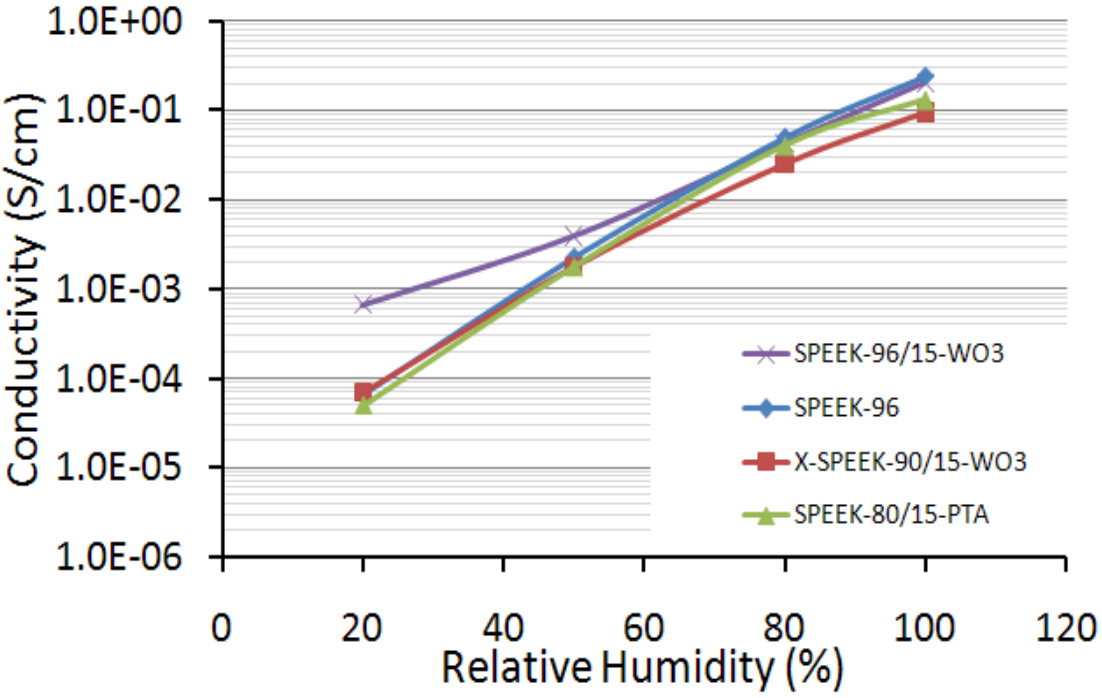

Figure 44. 80 °C conductivity comparison between high degree sulfonation PEEK membranes with different treatments and solid acids

After testing of the SPEEK-96/15-WO_3 membranes, it was discovered that they adopted a distinct blue color. After allowing the membranes to equilibrate for a few days at 25 °C and 70% RH, this blue color disappeared. This electrochromic phenomenon which causes interchangeable coloring of the tungsten oxide (bleached) to tungsten bronze (various colors) is well known.[14,15,16] The electrochromic properties of tungsten oxide are based on the reversible reaction:

$$WO_3 + \alpha e^- + \alpha M^+ \leftrightarrow M_\alpha WO_3 \qquad (15)$$

If an electrochromic material is in contact with an electrode, applying the appropriate voltage results in intercalation/deintercalation of cations M^+ (M^+=H^+, Li^+, Na^+, K^+ or Cs^+) which is accompanied by a respective color change. WO_3 is transparent, whereas $M_\alpha WO_3$ absorbs various wavelengths of light, depending on the nature of the cation M^+ and the α value.[17,18] In the case of our conductivity study, $M^+ = H^+$, as the test is done under flowing hydrogen atmosphere, affording a blue tungsten bronze. During oxidation, protons and electrons are expelled from the oxide, which simultaneously bleaches the solid acid to its original color.

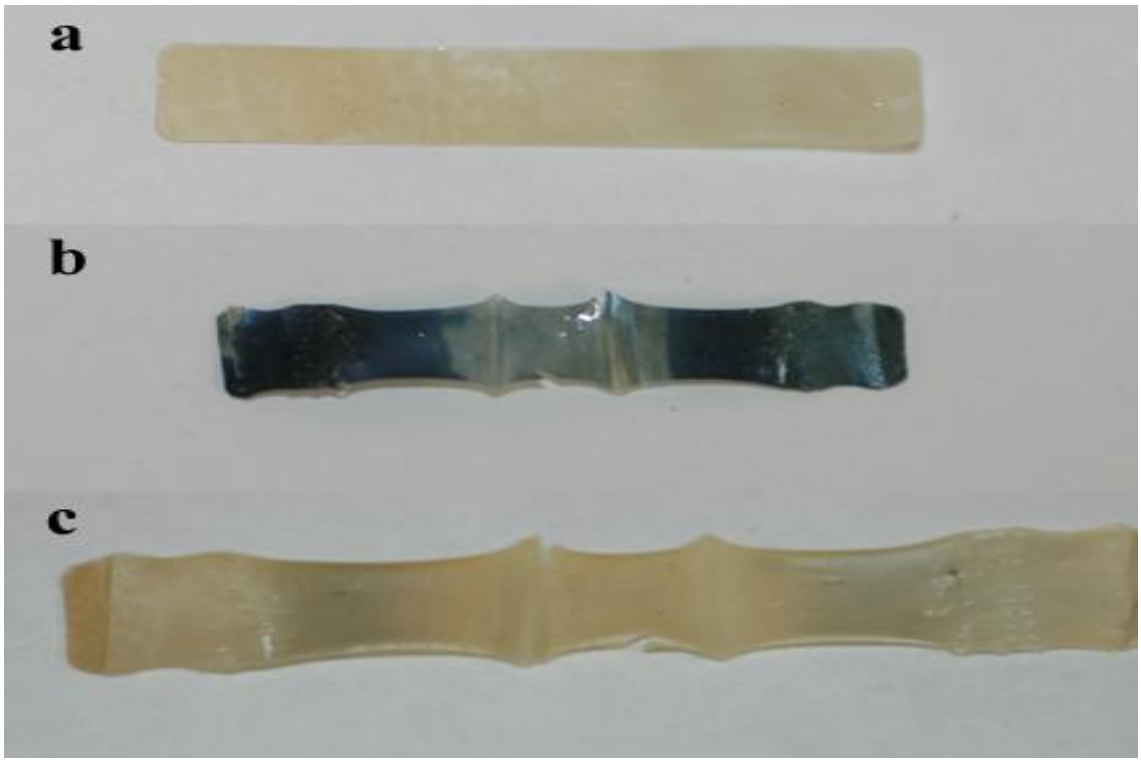

Figure 45. SPEEK-96/15-WO_3: a) At 25 °C and 70% RH before conductivity testing; b) After conductivity testing at 80 °C and 80% RH conditions for 5 hours; c) Equilibrated for four days at 25 °C and 70% RH after conductivity testing

Kuelsza, and more recently Iglesia has explained the simultaneous reduction of W(VI) to lower tungsten oxides are possible in highly reducing environments[14,19]:

$$WO_3 + 2ye^- + 2yH^+ \leftrightarrow WO_{3-y} + yH_2O \quad (16)$$

where ($0 < y < 1$).

The tungsten-oxygen based structures, as well as their hydration state while present in the SPEEK-96/15-WO_3 and X-SPEEK-90/15-WO_3 membranes will be investigated using XRD and FTIR techniques.

XRD Analysis of SPEEK-96, SPEEK-96/WO_3 and Cross-linked Composite Membranes

X-Ray Diffraction (XRD) is a powerful technique used to determine the structure of various compounds or complex matrices. X-rays are swept along the surface of the material at varying angles, and based on the diffraction pattern the molecular structure and particle size can be deduced from various standards of the compound being scanned.[20]

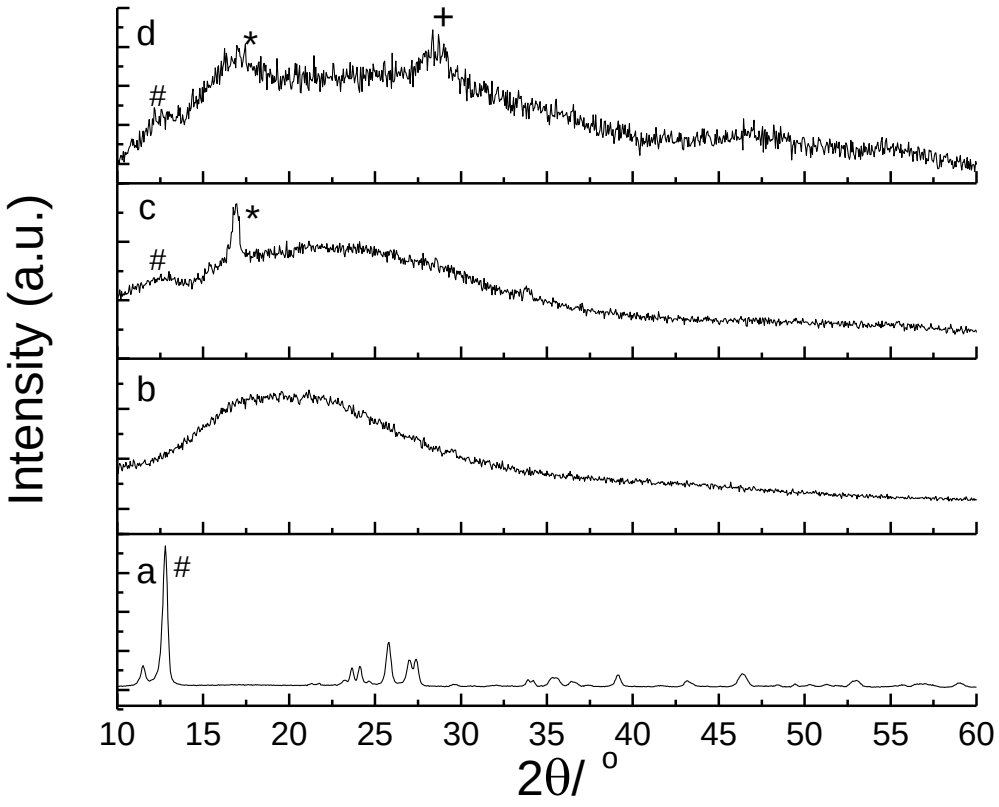

Figure 46. XRD pattern for: a) $WO_3 \cdot 2H_2O$ as prepared; b) pristine SPEEK-96 membrane; c) SPEEK-96/15-$WO_3 \cdot xH_2O$ and d) SPEEK-96/30-$WO_3 \cdot xH_2O$.

On inspecting the XRD pattern for the pure SPEEK-96 membrane (Figure 46b), it can be concluded that the structure is mostly amorphous based on the curve generated. Sulfonation of PEEK is known to reduce the crystallinity of the polymer significantly.[21] Figure 46a) is the diffraction pattern of the as prepared $WO_3 \cdot 2H_2O$ solid acid. In c and d, amorphous peaks related to the dihydrate material are shown by #, with the presence of the $1/3H_2O$ and monohydrate presence confirmed by + and the *, respectively.[6,22]

Precipitation of tungsten oxides in various acidic media (Figure 41), can lead to condensation reactions forming polyoxoanions (or dimers/ trimers etc), so it is no surprise that by adding $WO_3 \cdot xH_2O$ the hydration state changes. [23]

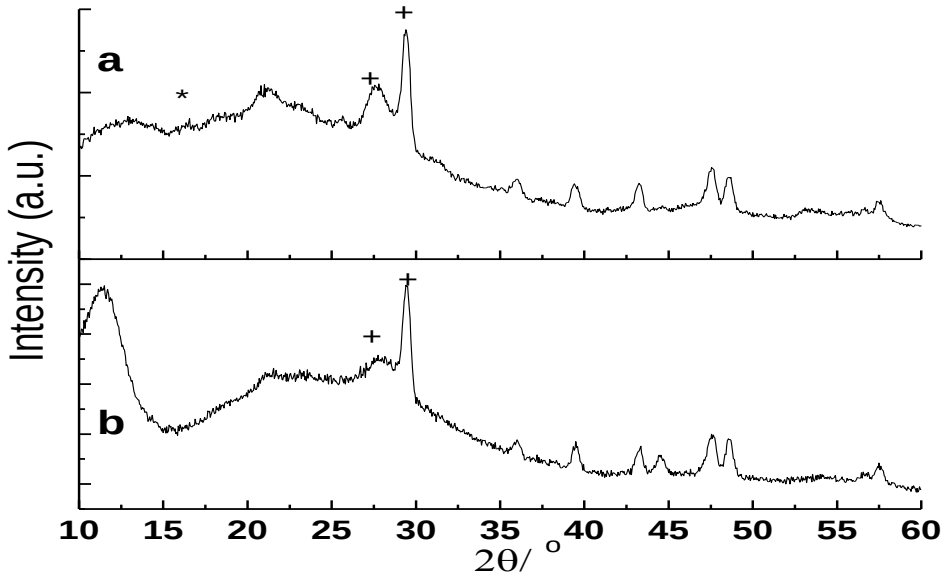

Figure 47. XRD pattern for cross-linked SPEEK-90 with various wt% WO_3 membranes: a) 15wt% WO_3 heat treated, b) 15wt% WO_3 non- heat treated. Heat treatment to effect cross-linking was done at 200 °C for 10 minutes.

Cross-linking of highly sulfonated SPEEK membranes with benzenedimethanol utilizing $WO_3 \cdot xH_2O$ as catalyst was also investigated by XRD. The 200 °C thermal treatment was expected to change the hydration state of the $WO_3 \cdot xH_2O$ in the cross-linked SPEEK membranes. The diffraction patterns for a non-thermally treated and a thermally treated SPEEK-90/15-WO_3 membrane are shown in Figure 47. The non-heat-treated membrane (Figure 47a)) showed a diffraction peak at $2\theta = 12.5^\circ$ for $WO_3 \cdot 2H_2O$, with the intensity of the peak decreasing upon membrane heat treatment (Figure 47b)). Peaks of the monohydrate and the $1/3H_2O$ were also present in both membranes. In conclusion, the XRD spectra show some underlying chemistry occurs during the

membrane casting of high degree sulfonation PEEK and the tungstic acid hydrate, and then dehydration occurs during subsequent heat treatment.

FTIR Spectroscopic Analysis

Figure 48 shows the FTIR of $WO_3 \cdot 2H_2O$ as prepared (red curve) and after annealing the $WO_3 \cdot 2H_2O$ sample at 200 $^{\circ}C$ for 10 minutes. Following the red curve for the dihydrate, the peaks at 3150, 3370 and 3530 cm^{-1}, which are high-lighted, are due to the waters of hydration present in $WO_3 \cdot 2H_2O$. Stretches at 1008 and 950 cm^{-1} are due to W=O linkages, with the stretches at 680 and 730 cm^{-1} being due to the O-W-O present.[24,25]. The FTIR spectra of the heat treated dihydrate shows features very similar to $WO_3 \cdot 1/3H_2O$: stretches at 3220, 1620 and 1413 $cm^{-1}$are representative of water present; W=O and O-W-O stretches are at 990, and 830 and 710 cm^{-1} respectively. The sharp stretch at 800 cm^{-1} was thought to be related to a O-W-O stretch in monoclinic phase of WO_3.[24]

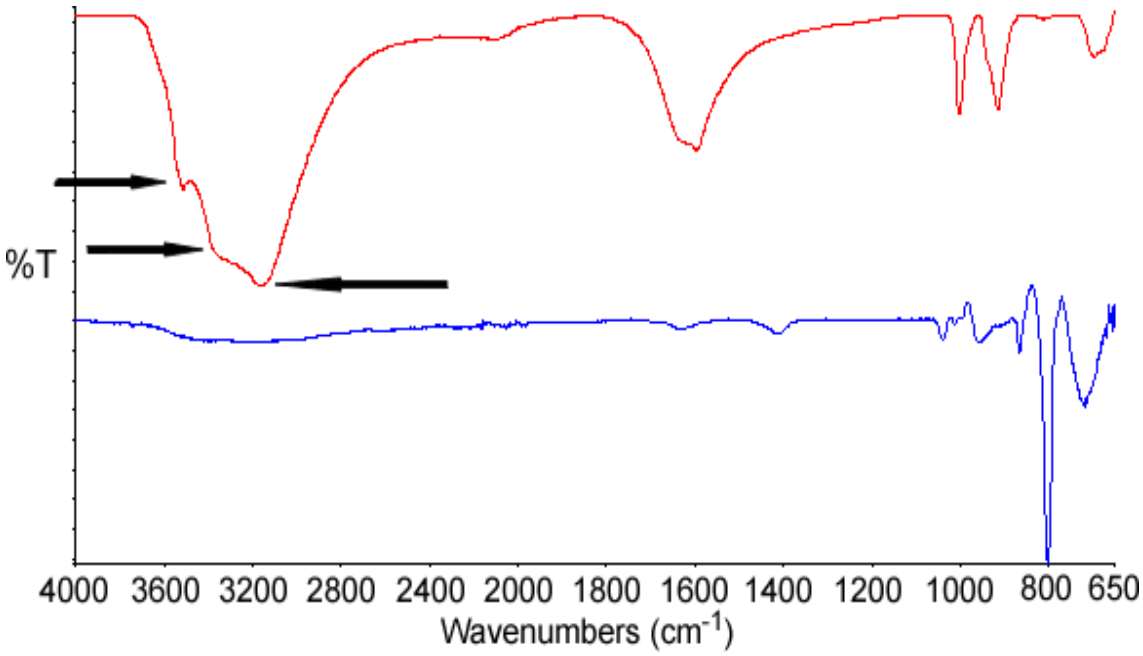

Figure 48. FTIR of $WO_3 \cdot 2H_2O$ as prepared (red) and $WO_3 \cdot 2H_2O$, heat treated at 200 °C for 10 minutes (blue). The arrows indicate the presence of bound water.

The presence of water in the tungsten oxide hydrates has been characterized definitively. As to how the dihydrate reacts when a voltage is applied will be studied further by cyclic voltammetry. Previous work concluded that the formation of tungsten bronzes is thought to be accelerated by the presence of waters of hydration.[14]

Cyclic Voltammetry of WO_3

The utility of cyclic voltammetry is mostly dependent on the analyte being studied. The analyte has to be redox-active within the experimental potential window. A sweep of the voltage between a maximum and a minimum, achieves change in the current-voltage graph, which can characterize materials by their redox properties. The

electrochemical redox property of colloidal $WO_3 \cdot xH_2O$, as prepared in aqueous solution was studied.

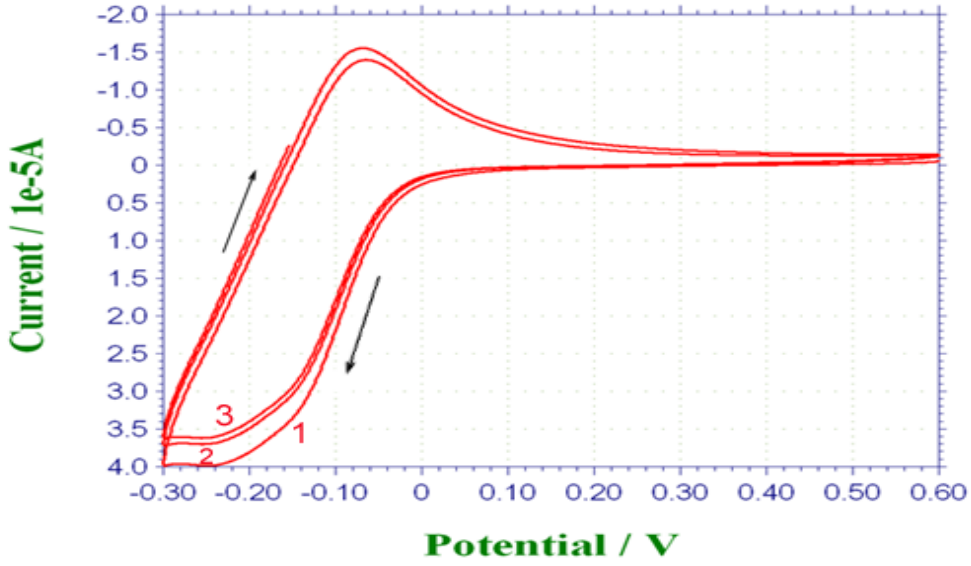

Figure 49. Cyclic voltammogram of colloidal $WO_3 \cdot xH_2O$ as prepared in an aqueous solution of pH < 1. A scan rate of 30 mV/s was used to scan from 0.6 to -0.3 V. The initial 3 scans are shown.

Figure 49 illustrates the voltammogram of a 40 mM $WO_3 \cdot xH_2O$ was made by passing a solution of 40 mM Na_2WO_4, through the acid exchanged Rexyn 101 H column. The solution was then analyzed immediately using a CH1202A Electrochemical Analyzer Instrument. Platinum counter and working electrodes were employed. The arrows are indicative of the direction which the voltage was scanned. Starting from 0.6 V, the voltage was scanned at 30 mV/s (initially decreasing) with a subsequent increase in current. This corresponds to de-intercalation, where electrons and H^+ ions present in the WO_3 matrix, being inserted into the Pt electrode and electrolyte solution, cause bleaching of the WO_3. As soon as the current changes from positive to negative values, intercalation (coloration) starts. The coloration of the solid acid was not directly observed, probably due to low concentration, but the results were very similar to work

done previously.[26,27] Over the lifetime of the scans, a rapid decrease in the observed peak current densities on cycling, is indicative of their unsuitability for use in PEMFC applications. The constant decrease will eventually cause shorting in the fuel cell.

Performance Testing of X-SPEEK-90/15-WO_3 Composite Membranes

All non-cross-linked SPEEK-96/15-WO_3 membranes failed during the first 2 days of testing. On the first day, the membrane was brought to the correct hydration level under H_2/N_2 atmosphere. On the second day, H_2/air is applied to anode and cathode respectively. Water is formed in the cathode at this point, causing the water-soluble, high sulfonation SPEEK polymer to dissolve.

To achieve better chemical stability and still be able to explore the effects of $WO_3 \cdot xH_2O$ on SPEEK PEMFC performance, a 90% DS SPEEK membrane was mixed with 12% benzenedimethanol and 16wt% $WO_3 \cdot 2H_2O$ as prepared and cast on a glass plate. After the membrane was air dried, the membrane was heat treated to a 10 minute 200 $^{\circ}$C heat treatment to effect cross-linking. The membrane was submerged in 0.5 M H_2SO_4 acid for 30 minutes, and was then washed until a neutral wash was obtained (X-SPEEK/15-WO_3) . The fuel cell performance of the Pt/C coated X-SPEEK-90/15-WO_3 membrane was recorded at 80/80/73 (cell/anode/cathode) and 100/90/90 testing conditions. The I/V polarization curves generated for the 80 $^{\circ}$C test is shown in Figure 50.

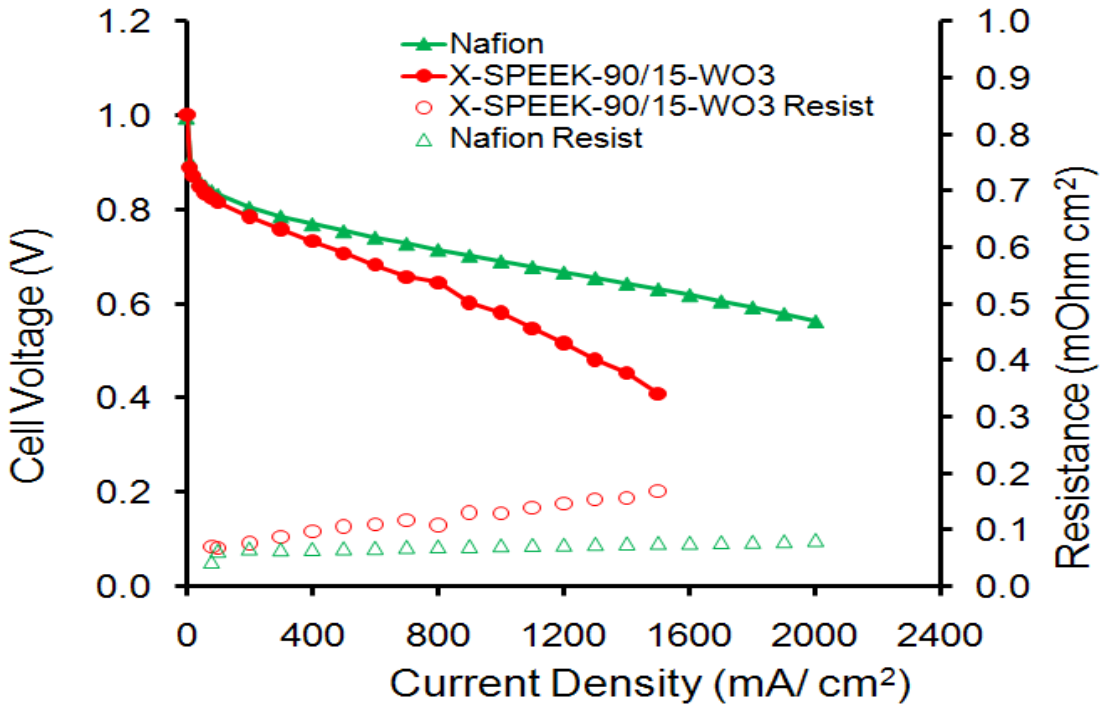

Figure 50. Fuel cell performance curves for X-SPEEK-90/15-WO_3 and Nafion 211 CCMs measured at 80 °C cell temperature, 80 °C anode and 73 °C cathode fuel temperatures. H_2 gas was the only fuel used on the anode, while utilizing O_2 (oxygen) on the cathode. The change in membrane resistance for each membrane was also plotted.

At OCV, the SPEEK based membrane showed enhanced kinetics compared to a Nafion 211 membrane. At 400, 800 and 1200 mA/cm^2, the Nafion® membrane demonstrated 0.770, 0.715 and 0.667 V while the WO_3 cross-linked SPEEK membrane held voltages of 0.733, 0.644 and 0.516.

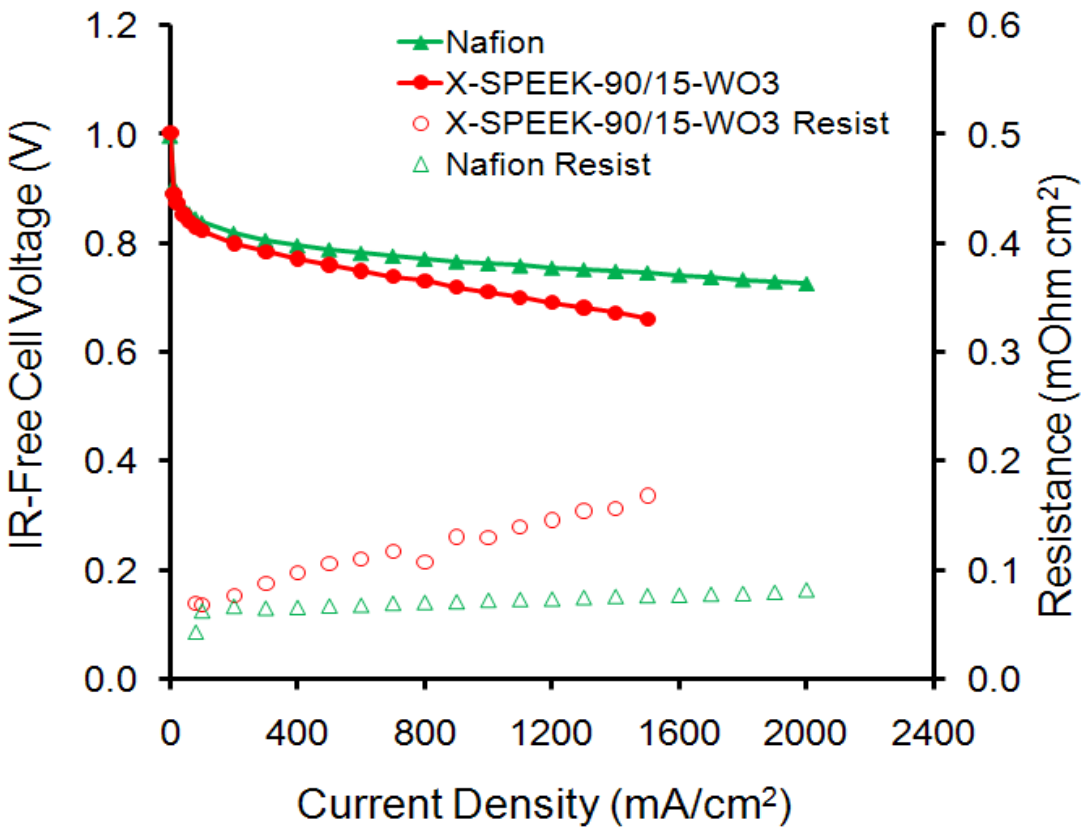

Figure 51. IR-free fuel cell performance curves for X-SPEEK-90/15-WO_3 and Nafion 211 CCMs, measured at 80 °C cell temperature, 80 °C anode and 73 °C cathode fuel temperatures. H_2 gas was the only fuel used on the anode, while utilizing O_2 (oxygen) on the cathode. The change in membrane resistance for each membrane was also plotted.

The ohmic resistance of the SPEEK membrane increased steadily from 100 mA/cm^2 upwards to 1500 mA/cm^2, at which point it doubled. At this point the cell voltage fell below 0.3V, stopping the 80 °C test. IR-free voltages are plotted in Figure 51. Even if sources related to polarization of the cell are removed, the Nafion® membrane still out performs the X-SPEEK-90/15-WO_3 membrane. The effect of the $WO_3 \cdot xH_2O$ doped into the SPEEK was not as thought; addition of the hydrated solid acid was expected to decrease membrane resistance in the ohmic region by: 1) providing acid sites for proton conduction; and 2) increasing the membrane water content. Unfortunately the

90% DS SPEEK membranes cross-linked with WO_3 could not be compared to a similar SPEEK membrane. This would help determine the advantages/ disadvantages in properties which the solid acid gave the hydrocarbon membrane overall.

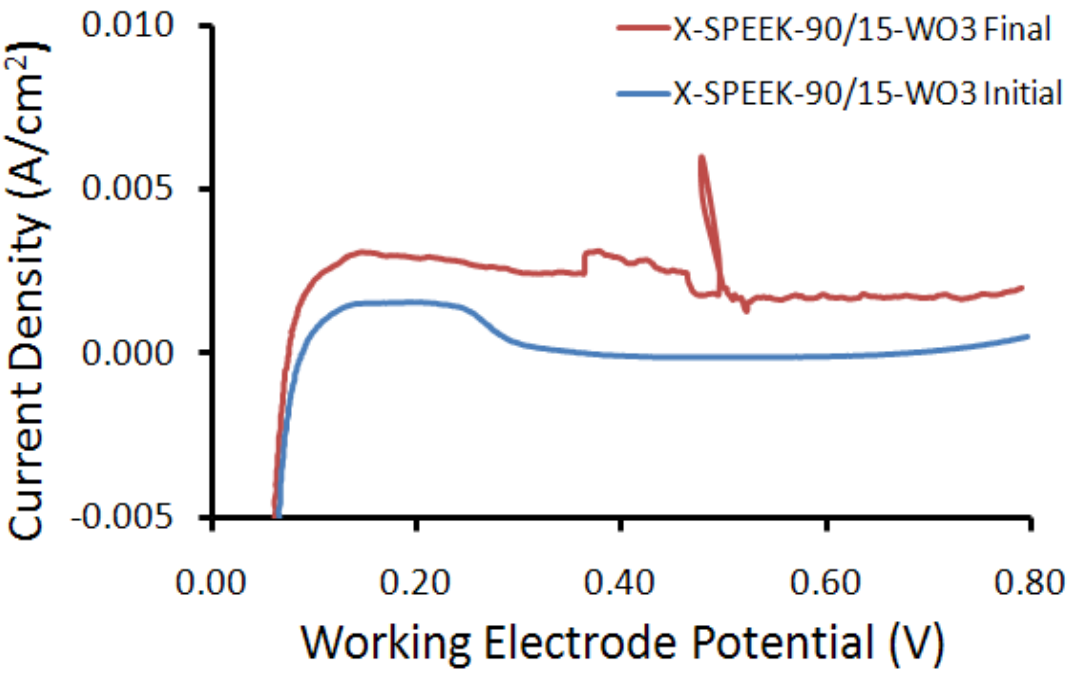

Figure 52. Linear sweep voltammetry demonstrating low hydrogen gas cross-over flux before and after performance testing X-SPEEK-90/15-WO_3 at 80 $^{\circ}$C.

Before and after conducting each performance experiment, LSV was used to determine fuel cross-over currents. Figure 52 illustrates the results of the LSV experiment conducted on an X-SPEEK-90/15-WO_3 Pt/C CCM. Cross-over currents due to fuel cross-over before and after the performance test at 80/80/73 showed negligible hydrogen gas cross-over. However, there was some unexpected electrochemical activity between 0.35 and 0.58 V, which was not understood. This may be due to the formation of the tungsten bronzes in the PEM while the working electrode voltage was swept.

These membranes did not dissolve or have premature failure during the testing protocols, so there may be merit in doping and cross-linking membranes with hydrates of WO_3.

Conclusion

WO_3 and its hydrates have been shown as good prospects for addition to fuel cell membranes. Their unique redox chemistry has made their utility in a plethora of applications widespread. $WO_3 \cdot 2H_2O$ precipitated into a high degree of sulfonation SPEEK membrane has shown over two orders of magnitude improvement in proton conductivity at low relative humidity compared to the pristine material. These membranes do not gain any chemical or mechanical stability with the addition of the solid acid, so PEMFC applications based on these hybrid membranes would b limited.

The solid acid did, however, catalyze cross-linking of high DS SPEEK in the presence of benzenedimethanol, with the membranes produced, showing robust chemical and mechanical properties. The proton conductivity was, however, significantly lowered, possibly due to the loss of solid acid waters of hydration during its 200 $^{\circ}$C heat treatment. These hybrid hydrocarbon/solid acid composite membranes need further characterization to determine the applications to which they will be rightly suited.

References

1. Shao, Z. G., Xu, H., Li, M., Hsing, I. M., Hybrid Nafion–inorganic oxides membrane doped with heteropolyacids for high temperature operation of proton exchange membrane fuel cell, *Solid State Ionics*, 177, (2006), 779-783.
2. Mecheri, B., D'Epifiano, A., Di Vona, M. L., Traversa, E., Licoccia, S., Miyayama, M., Sufonated Poly ether ether ketone-based composite membranes doped with a tungsten-based inorganic proton conductor for fuel cell applications, *J. Electrochem. Soc*., 153, (2006), A463-A467.
3. Abramova, V. V., Sinitskii, A. S., Goodilin, E. A., Tretyakov, Y. D., Preparation and properties of electrochromic coatings based on nanoparticle tungsten oxide, *Mendeleev. Commun.* 15, (2005), 178-180.
4. Chemseddine, A., Bloeck, U., How isopolyanions self-assemble and condense into a 2D tungsten oxide crystal: HRTEM imaging of atomic arrangement in an intermediate new hexagonal phase, *J. Solid State Chem.*, (181, (2008), 2731-2736.
5. Cotton, F. A., Wilkinson, G., Murillo, C. A., Bochmann, M. Advanced Organic Chemistry, 6th ed., Wiley Interscience, (1999).
6. Hibino, M., Nakajima, H., Kudo, T., Mizuno, N., Proton conductive amorphous thin films of tungsten oxide clusters with acidic ligands, *Solid State Ionics*, 100, (1997), 211-216.
7. Li, Y. M., Hibino, M., Miyayania, M., Kudo, T., Proton conductivity of tungsten trioxide hydrates at intermediate temperature, *Solid State Ionics*, 134, (2000), 271-279.

8. Santato, C., Odziemkowski, M., Ulmann, M., Augustynski, J., Crystallographically oriented mesoporous WO_3 films: Synthesis, characterization and applications, *J. Am. Chem. Soc*. 123, (2001), 10639-10649.

9. Solarska, R., Alexander, B. D., Augustynski, J., Electrochromic and structural characteristics of mesoporous WO_3 films prepared by a sol-gel method, *J. Solid State Electrochem.* 8, (2004), 748-756.

10. Breedon, M., Spizzirri, P., Taylor, M., Plessis, J. D., McCulloch, Zhu, J., Yu, L., Hu, Z., Rix, C., Wlodarski, W., Kalantar-zadeh, K., Synthesis of nanostructured tungsten oxide thin films: a simple controllable, inexpensive, aqueous sol-gel method, *Crystal Growth and Design*, 10, (2010), 430-439.

11. Robertson, G. P., Mikhailenko, S. D., Wang, K., Xing, P., Guiver, M. D., Kaliaguine, S., Casting solvent interactions with sulfonated poly(ether ether ketone) during proton exchange membrane fabrication, *J. Membr. Sci.*, 219, (2003), 113-121.

12. Mecheri, B., D'Epifiano, A., Di Vona, M. L., Traversa, E., Licoccia, S., Miyayama, M., Sufonated Poly ether ether ketone-based composite membranes doped with a tungsten-based inorganic proton conductor for fuel cell applications, *J. Electrochem. Soc*., 153, (2006), A463-A467.

13. Kreuer, K. D., Paddison, S. J., Spohr, E., Schuster, M., Transport in proton conductors for fuel cell applications: Simulations, elementary reactions, and phenomenology, *Chem. Rev.*, 104, (2004), 4637-4676.

14. Kuelsza, P. J., Faulkner, L. R., Electrocatalysis at a novel electrode coating of nonstoichiometric tungsten(VI,V) oxide aggregates, *J. Am. Chem. Soc.* 110, (1988), 4905-4913.

15. Pauporte, T., A simplified method for WO_3 electrodeposition, *J. Electrochem. Soc.* 149, 11, (2002), C539-C545.

16. Bock, C., MacDougall, B., The electrochemical oxidation of organics using tungsten oxide based electrodes, *Electrochimica Acta.* 47, (2002), 3361-3373.

17. Abramova, V. V., Sinitskii, A. S., Laptinskaya, Veresov, A. G., Goodilin, E. A., Tretyakov, Y. D., Nanoporous electrochromic coatings based on tungsten oxide, *Doklady Chem. part 1*. 407, (2006), 31-34.

18. Granqvist, C. G., Handbook of Inorganic Electrochromic Materials, Elsevier, NY, NY. (1995).

19. Barton, D. G., Shtein, M., Wilson, R. D., Soled, S. L., Iglesia, E., Structure and electrode properties of solid acids based on tungsten oxide nanostructures, *J. Phys. Chem. B.* 103, (1999), 630-640.

20. Hyde, T., Crystallite size analysis of supported platinum catalysts by XRD, *Platinum Metals Rev.* 52, (2008), 129-130.

21. Bishop, M. T., Karasz, F. E., Russo, P. S., Langley, K. H., Solubility properties of a poly(aryl ether ether ketone) in strong acids, *Macromolecules*, 18, (1985), 86.

22. Balázsi, Cs., Zayim, E., Preparation and characterization of $WO_3.1/3/H_2O$ thin films, Mat. Sci. Forum, 537-538, (2007), 113-120.

23. Solarska, R., Alexander, B. D., Augustynski, J., Electrochromic and structural characteristics of mesoporous WO3 films prepared by a sol-gel method, *J. Solid State Electrochem.* 8, (2004), 748-756.

24. Daniel, M. F., Desbat, B., Lassegues, J. C., Gerand, B., Figlarz, M. Infrared and raman study of WO_3 tungsten trioxides and WO_3,xH_2O tungsten trioxide hydrates, *J. Solid State Chem.* 67, (1987), 235-247.

25. Balázsi, Cs., Development of tungsten oxide hydrate phases during precipitation-washing-ripening process, *Mater. Struct.* 6, (1999), 135-139.

26. Deepa, M., Srivastava, A. K., Shrma, S. N., govind, Shivaprasad, S. M., Microstructural and electrochromic properties of tungsten oxide thin films produced by surfactant mediated electrodeposition, *App. Surf. Sci.* 254, (2008), 2342-2352.

27. Agnihotry, S. A., Sharma, R., Kar, M., Saxena, T. K., Towards electrochromic stability in sol-gel-derived tungsten oxide films: cyclic voltammetric and spectrophotometric investigations. *Solar En. Mat. Solar Cells*, 90, (2006), 15-24.